Adaptation mechanisms of the myocardium: adverse effects of hypercholesterolemia and cardioprotection with skeletal muscle electrical stimulation

PhD thesis

Márton Richárd Szabó

Supervisors:

Tamás Csont MD, PhD and Csaba Csonka MD, PhD

Doctoral School of Multidisciplinary Medical Sciences

Metabolic Diseases and Cell Signaling Research Group
Department of Biochemistry
Albert Szent-Györgyi Medical School
University of Szeged

2023

Table of contents

1 List of publications

Full papers directly related to the subject of the thesis

I. Szabó, M. R., Gáspár, R.; Pipicz, M.; Zsindely, N.; Diószegi, P.; Sárközy, M.; Bodai, L.; Csont, T., Hypercholesterolemia Interferes with Induction of miR-125b-1-3p in Preconditioned Hearts. *International Journal of Molecular Sciences* **2020,** 21, (11):3744. [D1, IF: 5.924]

II. Szabó, M. R., Pipicz, M.; Sárközy, M.; Bruszel, B.; Szabó, Z.; Csont, T., Diet-Induced Hypercholesterolemia Leads to Cardiac Dysfunction and Alterations in the Myocardial Proteome. *International Journal of Molecular Sciences* **2022,** 23, (13):7387. [D1, IF: 5.6]

III. Szabó, M. R., Csont T; Csonka C., The effect of electrical stimulation of skeletal muscle on cardioprotection and muscle-derived myokine levels in rats: a pilot study *Physiology International* **2023,** 110, (2):135-149 [Q3, IF:1.4]

Cumulative impact factors of papers directly related to the subject of the thesis: 12.924

Other publications

I. Faragó A., Zsindely N., Farkas A., Neller A., Siági F., Szabó M. R., Csont T., Bodai L., Acetylation State of Lysine 14 of Histone H3.3 Affects Mutant Huntingtin Induced Pathogenesis *International Journal of Molecular Sciences* **2022,** 23(23):15173 [D1, IF: 5.6]

II. Mitra, A.; Sarkar, A.; Szabó, M. R.; Borics, A., Correlated Motions of Conserved Polar Motifs Lay out a Plausible Mechanism of G Protein-Coupled Receptor Activation. *Biomolecules* **2021,** 11, (5). [Q2, IF: 6.064]

III. Gopisetty, M. K.; Adamecz, D. I.; Nagy, F. I.; Baji, Á.; Lathira, V.; Szabó, M. R.; Gáspár, R.; Csont, T.; Frank, É.; Kiricsi, M., Androstano-arylpyrimidines: Novel small molecule inhibitors of MDR1 for sensitizing multidrug-resistant breast cancer cells. *European journal of pharmaceutical sciences: official journal of the European Federation for Pharmaceutical Sciences* **2021,** 156, 105587. [Q1, IF: 5.112]

IV. Sárközy, M.; Márványkövi, F. M.; Szűcs, G.; Kovács, Z. Z. A.; Szabó, M. R.; Gáspár, R.; Siska, A.; Kővári, B.; Cserni, G.; Földesi, I.; Csont, T., Ischemic preconditioning protects the heart against ischemia-reperfusion injury in chronic kidney disease in both males and females. *Biology of sex differences* **2021,** 12, (1), 49. [D1, IF: 8.811]

V. Szabó, M. R.; Pipicz, M.; Csont, T.; Csonka, C., Modulatory Effect of Myokines on Reactive Oxygen Species in Ischemia/Reperfusion. *International Journal of Molecular Sciences* **2020,** 21, (24). [D1, IF: 5.924]

VI. Demján, V.; Kiss, T.; Siska, A.; Szabó, M. R.; Sárközy, M.; Földesi, I.; Csupor, D.; Csont, T., Effect of Stellaria media Tea on Lipid Profile in Rats. *Evidence-based complementary and alternative medicine: eCAM* **2020,** 2020, 5109328-5109328. [Q1, IF: 2.629]

VII. Adamska-Bartłomiejczyk, A.; Janecka, A.; Szabó, M. R.; Cerlesi, M. C.; Calo, G.; Kluczyk, A.; Tömböly, C.; Borics, A., Cyclic mu-opioid receptor ligands containing multiple N-methylated amino acid residues. *Bioorganic & Medicinal Chemistry Letters* **2017,** 27, (8), 1644-1648. [Q2, IF: 2.442]

VIII. Váradi, A.; Marrone, G. F.; Palmer, T. C.; Narayan, A.; Szabó, M. R.; Le Rouzic, V.; Grinnell, S. G.; Subrath, J. J.; Warner, E.; Kalra, S.; Hunkele, A.; Pagirsky, J.; Eans, S. O.; Medina, J. M.; Xu, J.; Pan, Y.-X.; Borics, A.; Pasternak, G. W.; McLaughlin, J. P.; Majumdar, S., Mitragynine/Corynantheidine Pseudoindoxyls As Opioid Analgesics with Mu Agonism and Delta Antagonism, Which Do Not Recruit β-Arrestin-2. *Journal of Medicinal Chemistry* **2016,** 59, (18), 8381-8397. [D1, IF: 6.259]

IX. Kotormán, M.; Simon, M. L.; Borics, A.; Szabó, M. R.; Szabó, K.; Szögi, T.; Fülöp, L., Amyloid-like Fibril Formation by Trypsin in Aqueous Ethanol. Inhibition of Fibrillation by PEG. *Protein and peptide letters* **2015,** 22, (12), 1104-10. [Q2, IF: 1.069]

Total cumulative impact factors: 56.834

2 Abbreviations

AKT	protein kinase B
AMI	acute myocardial infarction
BP	biological process
CC	cellular component
cGMP-PKG	cyclic guanosine monophosphate – protein kinase G
CK-MB	cardiac specific creatine kinase isoform
CVD	cardiovascular diseases
DCN	decorin
EMS	electrical muscle stimulation
ERK1/2	extracellular signal-regulated kinase 1/2
FDR	false discovery rate
*Fndc*5	fibronectin type III domain-containing protein 5
FSTL1	follistatin-like 1
GO	gene ontology
GSEA	Gene Set Enrichment Analysis
I/R	ischemia/reperfusion
Igf1	insulin-like growth factor 1
IHD	ischemic heart diseases
IL	interleukin
IPre	ischemic preconditioning
IS	infarct size
KEGG	Kyoto Encyclopedia of Genes and Genomes
LC-MS	liquid chromatography-mass spectrometry
MF	molecular function
miR	micro-ribonucleic acid
mRNA	messenger ribonucleic acid
NRF2	nuclear factor erythroid 2-related factor 2
RISK	reperfusion injury salvage kinase
SAFE	survivor activating factor enhancement
SDS	sodium dodecyl sulfate
STAT3	signal transducer and activator of transcription 3

3 Summary

Background: Ischemic heart diseases including acute myocardial infarction are the leading cause of death. Hypercholesterolemia is a well-known risk factor for the development of coronary atherosclerosis and subsequent ischemic heart diseases. Beyond its impact on the vasculature, direct cardiac consequences are also responsible for the adverse effects of high blood cholesterol levels including elevated oxidative and nitrosative stress, cardiac dysfunction, and disturbed ischemic adaptation. All these adverse cardiac effects are assumed to alter protein networks and regulatory molecules, nevertheless, the exact mechanisms are yet to be fully understood. Regular physical activity is considered a gold standard against the detrimental consequences of coronary heart diseases, however, performing regular exercise is often limited due to unwillingness or other health reasons. For those, electrical stimulation of the skeletal muscle (EMS) might provide an alternative technique to gain some of the benefits of exercise. Although, the potential cardiac conditioning ability of EMS is ambiguous.

Aims: In the present thesis, we aimed to investigate the global proteome changes in the left ventricle of hypercholesterolemic rats to clarify the underlying protein expression changes associated with the direct cardiac effects. Moreover, we aimed to examine the relationship between the blunted infarct size limiting effect of classic ischemic preconditioning (IPre) in the settings of hypercholesterolemia and expression level of miR-125b-1-3p, a microRNA previously implicated with cardioprotection. Furthermore, we tested the potential cardioprotective effect of short-term EMS treatment and its impact on skeletal muscle-derived myokines in normocholesterolemic animals.

Experimental setup: Male Wistar rats were fed with a laboratory rodent chow supplemented with 2% cholesterol and 0.25% sodium-cholate hydrate for eight weeks to induce hypercholesterolemia. Proteomic characterization of left ventricular samples from normo- and hypercholesterolemic animals was performed with liquid chromatography-mass spectrometry analysis. The significantly altered proteins from the proteomic data were subjected to gene ontology and protein interaction analyses. Moreover, gene set enrichment analysis was carried out through the unfiltered proteome data.

In a separate set of experiments, hearts of normo- and hypercholesterolemic animals were isolated and perfused according to Langendorff and were subjected to 35 min global ischemia and 120 min reperfusion with or without IPre. Total RNA was isolated from left ventricles and next-generation sequencing was performed to investigate cardiac miR-125b-1-3p expression.

Low-frequency EMS treatment was applied on the gastrocnemius muscle of male, normocholesterolemic rats for three days (one treatment/day). After 24hr of the last EMS treatment, hearts were isolated and perfused ex vivo using 30 min global ischemia and 120 min reperfusion protocol. At the end of reperfusion, cardiac-specific creatine kinase (CK-MB) and lactate dehydrogenase (LDH) enzyme release and myocardial infarct size were determined. Subsequently, skeletal muscle-driven myokine expression and release were also assessed. Phosphorylation of cardioprotective signaling pathway members AKT, ERK1/2, and STAT3 proteins was also measured from left ventricular samples.

Key results: Elevated circulating cholesterol level was accompanied by mild diastolic dysfunction in cholesterol-fed animals. Proteomic characterization of left ventricular samples revealed an altered level of 45 proteins due to hypercholesterolemia. Based on our gene ontology and protein interaction analysis results, hypercholesterolemia was associated with disturbed expression of cytoskeletal and contractile proteins. Additionally, concordant downregulated expression patterns in proteins related to the arrangement of contractile and cytoskeletal systems, and in protein subunits of the mitochondrial respiratory chain system were identified in the unfiltered proteome dataset.

IPre significantly reduced infarct size and was associated with the upregulated levels of miR-125b-1-3p in the hearts of normocholesterolemic rats. In contrast, IPre was ineffective in the hearts of hypercholesterolemic animals and failed to increase significantly miR-125b-1-3p levels.

EMS attenuated cardiac LDH and CK-MB enzyme release without significant infarct size reduction in the heart of normocholesterolemic rats. The applied EMS treatment considerably altered the myokine content of the stimulated gastrocnemius muscle. However, phosphorylation of cardiac AKT, ERK1/2, and STAT3 remained unaffected compared to the untreated control group.

Conclusion: Based on the results of the present thesis disturbed expression of proteins associated with the contractile apparatus as well as with the mitochondrial respiratory chain due to hypercholesterolemia may play a role in the cardiac diastolic dysfunction in cholesterol-fed animals. Moreover, hypercholesterolemia attenuated the upregulation of miR-125b-1-3p by ischemic preconditioning, which seems to be associated with the loss of cardioprotection. Despite the lack of significant infarct size reduction, the EMS treatment seems to influence the course of cellular damage due to I/R in normocholesterolemia. Our results suggest that EMS may have a protective effect on the myocardium, however, further optimization of the protocol is required.

4 Introduction

4.1 Epidemiological burden of ischemic heart diseases

According to the latest comprehensive reports of the European Society of Cardiology cardiovascular diseases (CVD) are the leading cause of mortality in Europe despite sustained declines in mortality recently (Figure 1) [1, 2]. The risk of CVD is greater with increasing age, however, overall one-third of premature deaths are due to diseases of the heart and circulatory system [1]. Ischemic heart diseases (IHD) contribute significantly to the high mortality rate of cardiovascular diseases (Figure 1). IHD is a group of disorders characterized by reduced oxygen and nutrient supply to the heart muscle, followed by functional and structural deterioration of the myocardium.

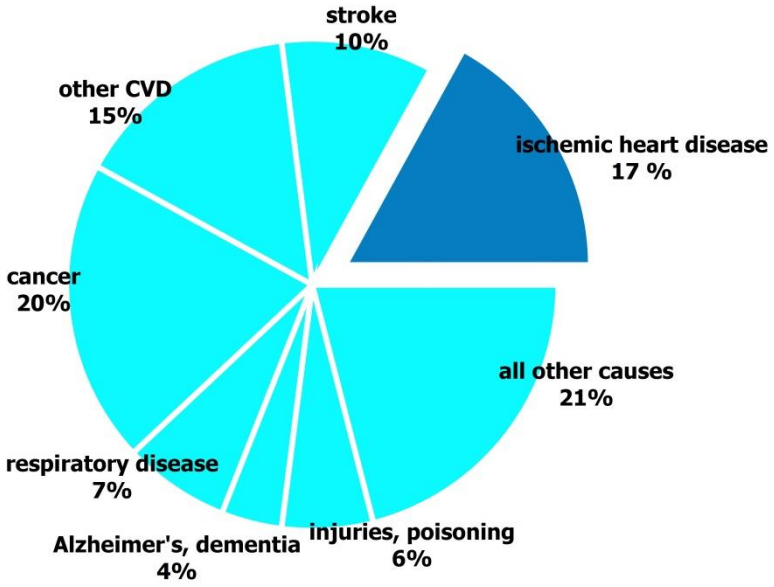

Figure 1. The major cause of death across the European Society of Cardiology member countries. The table shows merged data from both sexes and all-ages. Adopted from [1].

4.2 The concept of ischemia/reperfusion injury

Acute obstruction of a coronary artery, i.e. acute myocardial infarction is the most severe manifestation of IHD [3]. The reduced blood flow to the myocardium results in cardiac arrhythmias, contractile impairment, and irreversible myocardial cell damage depending on the duration of existing ischemia. In-time readmission of blood flow of the affected area, termed reperfusion therapy, is mandatory to salvage the ischemic myocardium. Paradoxically, prompt and full restoration of oxygen and nutrient supply contributes to further structural damage and contractile impairments; therefore, the sum of the resulting cellular and functional myocardial damage is called ischemia/reperfusion (I/R) injury [4]. The infarct size (IS) resulting from I/R is the major determinant of survival and long-term

prognosis of evolving heart failure in patients having a myocardial infarction. Consequently, testing interventions or pharmaceuticals with the special aim to minimize I/R injury is of great clinical importance [5].

4.3 Cardiac adaptation to ischemic injury

Despite being susceptible to I/R injury, the heart has been shown to possess a remarkable ability to withstand the detrimental effects of ischemic injury. These adaptation mechanisms can be triggered by different cardioprotective strategies and interventions. One of the most powerful strategies to trigger endogenous cardioprotective mechanisms is ischemic conditioning when brief, repetitive cycles of I/R are applied to the myocardium. When these episodes are performed before the sustained lethal ischemia, it is called ischemic preconditioning (IPre), whereas ischemic postconditioning (IPost) refers to the application of the conditioning phenomenon at the beginning of the reperfusion [6]. Additionally, alternative approaches that mimic the ischemic conditioning mechanism without direct impact on the myocardium have been also developed. These techniques include temporary cessation of blood flow of distant organs or tissue, termed remote ischemic conditioning (RIPC), or the use of certain pharmacological agents. In the present thesis, we focused on classical IPre and an alternative way to induce RIPC in the heart.

4.3.1 Molecular mechanisms of ischemic preconditioning

IPre was first described by Murry and colleagues [7] and the protective effect against myocardial infarction was confirmed using numerous species in several experimental models [8]. IPre can be considered a biphasic process, with distinct mechanisms for each phase. The classical, early stage of IPre, manifested within minutes after preconditioning stimuli, is termed the first window of preconditioning while the late or second window appears after 12-24 hours of conditioning, further increasing the resistance against myocardial injury [6]. Although several signaling pathways have been implicated in IPre, the exact mechanisms are still not entirely clear. The early phase of the IPre signaling process can be divided into the pre-ischemic trigger phase and the early post-ischemic mediator and effector phases. Production of trigger molecules e.g., adenosine, opioids, bradykinin, nitric oxide, etc. induced by preconditioning has been shown to activate various receptors which recruit downstream effector proteins of the signaling cascades associated with cardioprotection [8]. These mechanisms involve the activation of key proteins of the Reperfusion Induced Salvage Kinase (RISK), the Survivor Activating Factor Enhancement (SAFE), and the cyclic

guanosine monophosphate – protein kinase G (cGMP-PKG) pathways, respectively [9]. Activation of these signaling pathways is believed to ultimately converge on mitochondria, possibly through the prevention of the opening of the mitochondrial permeability transition pore thus averting mitochondrial rupture and subsequent cellular death [10]. The activation of protein components of the RISK and SAFE pathways are considered effector molecules of the cardioprotective pathways; however, the effectors *per se* are not sufficient for the permanent survival of ischemic tissue. The beneficial effects of IPre are associated with long-lasting adaptive responses like changes in metabolism, activation, inhibition, or degradation of numerous proteins, or modulation of protein-coding gene expression suggesting multiple-stage regulatory machinery which finally results in cellular survival.

4.3.2 The role of microRNAs in ischemic preconditioning

The non-coding microRNAs (miR) as post-transcriptional modulators completely fit into this phenomenon. Mature miRs are short, evolutionally conserved, single-stranded RNA molecules [11]. The general concept of miR-mediated post-transcriptional regulation is based on binding to the 3' untranslated region of target transcripts, triggering either mRNA degradation or translation repression upon recruitment into effector complexes (Figure 2). Several studies demonstrated that miRs play an important role in the pathophysiology of myocardial infarction [12] and have emerged as regulators of preconditioning possibly through the modulation of reactive oxygen species production [13-16].

Recently members of the miR-125b family were also implicated in the pathomechanism of IHD [17, 18] with a special emphasis on miR-125b-1-3p (previously named as miR-125b*), the passenger or antisense strand of miR-125b-1 stem-loop precursor. That part of the precursor miRNAs is considered to be degraded during miRNA maturation (Figure 2), however, recent data suggest that passenger strands also have biological functions [19, 20]. So far, only a few studies demonstrated associations between cardioprotection and miR-125b-1-3p expression levels. Upregulated expression was observed in ex vivo perfused rat hearts in response to IPre, while cultured cardiomyocytes transfected with miR-125b-1-3p mimics showed a significant survival rate upon simulated I/R injury [21]. Additionally, myocardial infarction was lower in precursor miR-125b-1 (encoding both 125b-1-3p and -5p strands) overexpressing transgenic mice, possibly due to inhibition of apoptotic signaling [22]. Furthermore, pretreatment with mesenchymal stem cells-derived exosomes containing the sense strand of miR-125b conferred cardioprotection in different experimental setups [23, 24]. Although pieces of evidence suggest a protective role for miR125b-1-3p in

the ischemic heart, little is known about whether these beneficial effects are also manifested in the presence of risk factors predisposing to myocardial infarction.

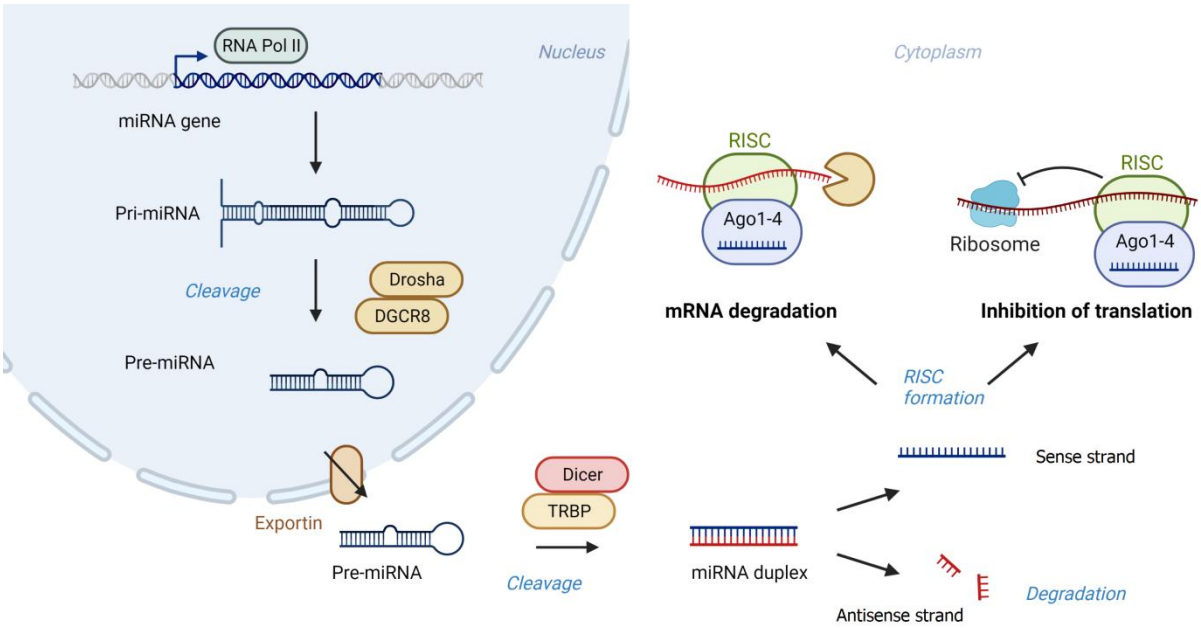

Figure 2. Schematic view of miRNA processing and biological activity. The image is adapted from "miRNA processing in the brain" by BioRender.com (2023). RNA Pol II: RNA polymerase type II; DGCR8: DiGeorge syndrome critical region 8; Ago: Argonaute; TRBP: transactivating response RNA-binding protein; RISC: RNA-indued silencing complex.

4.4 Hypercholesterolemia as a major risk factor for ischemic heart diseases

IHDs are a complex group of diseases that are associated with certain well-known risk factors and comorbidities like high blood pressure, aging, sedentary lifestyle, and metabolic diseases (e.g.: hyperlipidemia, diabetes, insulin resistance), respectively. Among the many risk factors increased blood cholesterol, termed hypercholesterolemia, has a significant role in the development of IHD. Cholesterol is packed into and transferred by lipoproteins, mainly low-density lipoprotein (LDL) which transfers cholesterol from the liver to the peripheral tissues, whereas high-density lipoprotein (HDL) is responsible for reverse cholesterol transport. Elevated circulating cholesterol, especially non-HDL cholesterol, is associated with endothelial dysfunction and subsequent atherosclerosis of the blood vessels. The general hypothesis of atherosclerosis emphasizes the central role of oxidized LDL-cholesterol particles in the promotion of plaque formation, subsequent inflammation, and endothelial dysfunction. According to the latest epidemiological studies of the European Society of Cardiology [1, 2] and the American Heart Association [25] nearly 30% of the adult population have moderately high total cholesterol levels (> 5.2 mmol/L), with more than 10 % having

total cholesterol higher than 6.2 mmol/L. Both modern dietary patterns as well genetic factors influence susceptibility to hypercholesterolemia [26, 27]. However, despite the high prevalence of hypercholesterolemia recent data demonstrated that only 50% of the population received LDL-cholesterol-lowering treatment [25, 28].

4.4.1 Direct effects of hypercholesterolemia on the myocardium

Cholesterol is an essential component of all animal cell membranes and is a precursor of steroid hormones, bile acid, and vitamin D synthesis. Nevertheless, the accumulation of intracellular cholesterol disturbs the homeostasis of a wide variety of cells and tissues [29, 30]. Independently from its proatherogenic effect, high blood cholesterol level exerts direct adverse effects on the heart as well. Previous studies demonstrated that many of these alterations are associated with enhanced formation of reactive oxygen species, decreased nitric oxide bioavailability, and impaired mitochondrial function in the myocardium [31-33]. Consequently, the redox imbalance compromised functional properties of the myocardium is a hallmark of the settings of hypercholesterolemia [34, 35]. Interestingly, cholesterol itself seems to contribute to redox imbalance. The non-enzymatic oxidation of the accumulated intracellular cholesterol to oxysterols, such as 7-ketocholesterol, leads to the augmentation of oxidative and nitrosative stress [36, 37]. Elevated tissue oxysterol level-driven oxidative stress might aggravate contractile impairment of the hypercholesterolemic myocardium [38, 39]. These data might suggest that the major contributor to the direct myocardial effects of hypercholesterolemia is not necessarily the circulating rather than tissue cholesterol.

4.4.2 Hypercholesterolemia induces cardiac dysfunction

The direct impact of increased plasma cholesterol on cardiac function is supported by human and experimental animal investigations [40]. For instance, the development of cardiac dysfunction is a characteristic outcome of a cholesterol-enriched diet [31, 41]. Echocardiographic characterization of patients with primary hypercholesterolemia or familiar hypercholesterolemia without a history of cardiovascular disease disclosed subclinical myocardial abnormalities and contractility impairment [34, 42]. Likewise, diminished cardiac function was also observed in hypercholesterolemic animals *in vivo* [43, 44]. In addition, high cholesterol diet seems to negatively influence the excitation-contraction coupling of cardiac muscle [45], including altered expression of sarcoplasmic reticulum $Ca2^{+}$-ATPase, ryanodine receptor, and Na^{+}/Ca^{2+} exchanger, respectively [35, 46]. Consequently, hypercholesterolemia

might have detrimental effects on additional structural and accessory proteins with a crucial role in normal cardiac function.

4.4.3 Disturbed ischemic stress adaptation in the settings of hypercholesterolemia

Besides cardiac dysfunction, existing hypercholesterolemia suppresses the beneficial effects of cardioprotective approaches and disturbs cardiac stress adaption mechanisms [40, 47]. Previous studies revealed that hypercholesterolemia impairs the cardioprotective effect of IPre [48-50], IPost [51, 52], and RIPC [53], respectively. Regarding the diminished IPre, hypercholesterolemia-induced elevated oxidative/nitrosative stress [40, 54] and decreased nitric oxide availability [55, 56] are considered as one of the main underlying mechanisms of the blunted cardioprotective effect. Moreover, activation of matrix metalloproteinases [57], altered gene expression of antioxidant proteins [58], and modified regulation of apoptosis and autophagy signaling [59, 60] are also implicated with the deleterious effects of hypercholesterolemia on the myocardium. Signal transduction pathways become activated by ischemic conditioning maneuvers converging on a common endpoint, namely, the mitochondria [61]. However, deteriorated mitochondrial function is a hallmark of the hypercholesterolemic myocardium [62, 63] which further worsen the susceptibility to ischemic cell death. Although the adverse cardiac effects of hypercholesterolemia are well known, the precise underlying molecular mechanisms and involved pathways are still not fully understood. Nonetheless, testing alternative conditioning approaches might provide the basis for the elaboration of applicable methods that can restore the endogenous adaptive mechanisms of the hypercholesterolaemic heart.

4.5 An alternative approach for cardioprotection – electromyostimulation (EMS)

Apart from the ischemic conditioning techniques, direct cardioprotection can be elicited remotely through distant organs and tissues. It is well-established that physical activity has potent protective effects against the development of CVD. The therapeutic potential of exercise is manifested in lowering blood pressure, favorably modifying plasma lipoprotein profile, and long-term enhancement cardiac contractile function [64]. Apart from the benefits of exercise, the enormous adaptation capacity of the skeletal muscle can trigger cardiac conditioning, subsequently protecting against the detrimental effects of I/R injury and having favorable outcomes in cardiac rehabilitation. However, performing regular exercise is often limited due to various health reasons. For those, electrical muscle stimulation or electromyostimulation (EMS), the rhythmical muscle activation triggered with electrical

impulses, might provide an alternative way to partially gain the benefits of exercise [65, 66]. EMS is a widely used method in sport- and rehabilitation therapy and is a far more attractive clinical application for subjects unable to perform regular exercise. Nevertheless, improvements in exercise capacity and quality of life are established outcomes of EMS treatment [67-69]. To date, little is known whether these beneficial effects of EMS can trigger cardiac preconditioning and protection against I/R injury. Previous studies suggested the importance of peripheral nerves and cardiac opioid receptor agonism upon transcutaneous electrical nerve stimulation [70, 71]. Nevertheless, the potential beneficial effect of electrical nerve stimulation is examined immediately after the end of the treatment protocol, and although the early phase of conditioning can elicit a robust response, it might have a significant relevance as a continuous preventive method. Moreover, EMS could exceed the limited clinical translational possibilities of the classic ischemic conditioning method while at the same time, it can include the majority of the favorable outcome of regular exercise as suggested by recent clinical trials [72, 73].

4.5.1 The role of myokines in the skeletal muscle-mediated cardioprotection

Based on the advantageous systemic effects of EMS, one may speculate that electrical stimuli-triggered muscle contraction might induce similar signaling mechanisms as regular exercise. Both humoral and neural factors are implicated in the favorable effects of physical activity on the general health of the individual [74]. Recently, skeletal muscle-derived myokines are emerged as the molecular mediators of the systemic beneficial effects of exercise through endocrine signaling pathways. The term myokine or exerkine is collectively used for a wide variety of cytokines and proteins, which are predominantly produced and released by contracting skeletal muscles [75, 76]. Myokines exert an autocrine function to regulate muscle mass and energy homeostasis, as well as a paracrine/endocrine regulatory function on distant organs and tissues [77]. Beyond the effect on the skeletal muscles, myokines are associated with exercise-mediated cardioprotection [78]. Additionally, the release of several muscle-derived myokines has been observed in settings of remote ischemic preconditioning further emphasizing their beneficial role against myocardial I/R injury [79]. Concerning cardioprotection, the most investigated myokines include interleukin-6 (IL-6), irisin, follistatin-like 1 (FSTL1), and myonectin, respectively, [80-82], but several other exercise-mediated myokines are also seemed to confer protection against I/R injury [83]. However, little is known whether muscle contractions evoked by electrical stimuli can trigger the expression and secretion of different myokines.

5 Aims

The present thesis aimed to investigate different aspects of cardiac adaptation mechanisms against I/R injury. In our work, we focused on the detrimental effects of hypercholesterolemia on the heart as well as whether electrical stimuli-triggered skeletal muscle contraction evoked cardiac preconditioning in normocholesterolemia. The specific aims of the thesis are the followings:

1. The recent advances in the field of 'omics' techniques provide a great and effective tool for high throughput screening and molecular profiling of different conditions and diseases. Therefore we aimed to utilize proteomics and subsequent bioinformatic analyses to characterize the global left ventricle proteome in the settings of hypercholesterolemia. Additionally, we were also interested in identifying enriched pathways and protein interaction networks concerning the adverse cardiac effects of hypercholesterolemia.

2. Cardioprotection conferred by IPre is lost in diet-induced hypercholesterolemia, however, limited literature data is available focusing on the precise molecular background and the possible amelioration strategies against the deleterious myocardial effects of hypercholesterolemia. Hence we aimed to address whether is there any association between the blunted cardioprotection of IPre in the settings of hypercholesterolemia and IPre-induced upregulation of miR-125b-1-3p in the heart.

3. The development of alternative conditioning approaches to confer cardioprotection in the presence of different comorbidities has great importance. Taking together the promising therapeutic potential of EMS, we also applied a pilot experimental setup in normocholesterolemic rats to test the remote preconditioning manner of short-term EMS treatment. Moreover, the investigation of skeletal muscle-derived myokine expression and secretion, as the possible mediators of EMS-associated cardioprotection, was also in the scope of the present thesis.

6 Materials and Methods

6.1 Animals

Male Wistar rats, weighing between 300-350 g were used in this study. The animals were kept in pairs in individually ventilated cages in a temperature-controlled room with 12 h:12 h light/dark cycles. Laboratory chow and water were supplied ad libitum throughout the study. All experiments conformed to the Guide for the Care and Use of Laboratory Animals published by the US National Institutes of Health (NIH publication No. 85-23, revised 1996) and were approved by the Animal Research Ethics Committee of Csongrád County (XV.1181/2013, XV.2153/2022) and the local animal ethics committee of the University of Szeged.

6.2 Effect of hypercholesterolemia on the left ventricular proteome

6.2.1 Experimental setup

Male Wistar rats (250–300 g) were fed with 2% (w/w) cholesterol and 0.25% (w/w) sodium-cholate enriched laboratory chow for eight weeks. The control animals were fed with standard rat chow. At the end of the diet period, hearts were isolated from anesthetized animals (sodium pentobarbital, 50 mg/kg i.p., Produlab Pharma b.v., Raamsdonksveer, The Netherlands) and placed into ice-cold Krebs-Henseleit buffer. Isolated hearts were then cannulated and perfused with oxygenated Krebs–Henseleit buffer at 37 °C. After 5 minutes of perfusion, left ventricular tissue samples were rapidly frozen in liquid nitrogen and stored at -80 °C until proteomics and subsequent bioinformatics analyses.

6.2.2 Transthoracic echocardiography

Cardiac morphology and function were assessed by transthoracic echocardiography with a Vivid IQ ultrasound system (General Electric Medical Systems, USA) using a phased array 5.0-11 MHz transducer (GE 12S-RS probe). Rats were anesthetized with 2% isoflurane during the experiment (Forane, AESICA, Queenborough Limited Kent, UK). Systolic and diastolic wall thicknesses were obtained from a parasternal short-axis view at the level of the papillary muscles (anterior and inferior walls) and a long-axis view at the level of the mitral valve (septal and posterior walls). The left ventricular diameters were measured by means of M-mode echocardiography from long-axis and short-axis views between the endocardial borders. Functional parameters, including the ejection fraction and fractional shortening, were

calculated on M-mode images in the long-axis view. Diastolic function was assessed using pulse-wave Doppler across the mitral valve and tissue Doppler on the septal mitral annulus from the apical four-chamber view. Early (E) and atrial (A) flow velocities, as well as septal mitral annulus velocity (e'), indicate diastolic function. Data from three consecutive heart cycles were analyzed (EchoPac Dimension software, General Electric Medical Systems, USA).

6.2.3 Blood lipid measurement

After eight weeks feeding period with cholesterol-enriched diet freshly collected blood samples from the thoracic aorta were collected into EDTA-containing blood collection tubes and separated with centrifugation. The upper, cell-free phase was used to determine total cholesterol and triglyceride concentrations using a colorimetric detection method (Diagnosticum, Budapest, Hungary) with a microplate reader (BMG Labtech, Ortenberg, Germany).

6.2.4 Proteomics analysis by liquid chromatography-mass spectrometry

Frozen left ventricular tissue samples were homogenized in 2% sodium dodecyl sulfate (SDS) and 0.1 M dithiothreitol (DTT) containing lysate buffer and were precipitated with a methanol/chloroform mixture. The homogenates were further reduced and denatured with 0.1 M ammonium bicarbonate (pH = 8.0) buffer supplemented with 0.1% RapiGest surfactant (Waters, MA, USA) and 100 mM DTT solutions. Subsequently, 200 mM iodoacetamide solution was added to alkylate the proteins. The samples were digested with trypsin and pooled to build a spectral library for quantitative liquid chromatography–mass spectrometry (LC-MS) analysis. The separation of the digested samples was carried out on a nanoAcquity Ultra Performance Liquid Chromatograph (Waters, MA, USA). The LC was coupled to a high-resolution Q Exactive Plus quadrupole-orbitrap hybrid mass spectrometer (Thermo Scientific, MA, USA). The measurements of the digested samples were performed in gas-phase fractionated data-independent acquisition mode to build a spectral library.

The quantitative analysis was performed in Encyclopedia v0.9. [84] using the default settings. For the building of the chromatogram library, a spectral library predicted by Prosit [85]. Statistical evaluations were carried out using Perseus [86]. Cutoff values of $p<0.05$ of Welch's t-test as well as 1.2< and <0.83 fold change was used as criteria for significant changes.

6.2.5 Pathway enrichment analysis

Pathway enrichment analysis was performed with the web-based g:Profiler public server using the g:GOSt tool (https://biit.cs.ut.ee/gprofiler) [87]. Functional enrichment profiling was carried out defining *Rattus norvegicus* as a queried organism, using g:SCS multiple testing correction method and $p<0.05$ as the threshold value. For visualization of the results, the output gem file of the over-represented Gene Ontology Biological Process and Cellular Component terms was loaded to Cytoscape v3.8.2 [88]. The enrichment map was created with the EnrichmentMap v3.3.2. application based on the instructions of Reimand and colleagues with <0.1 adjusted p-value similarity score [89].

6.2.6 Functional protein-protein interaction and network clustering analysis

Protein-protein interactions analysis among the identified proteins was performed with STRING v11.5 database (https://string-db.org) [90] using the default 0.4 medium confidence and 5% false discovery rate stringency values. Without any modification, the resulting protein-protein interactions chart was incorporated into Cytoscape and modified using the STRINGApp v1.7.0 and STRING Enrichment applications [91]. Cluster analysis was performed with clusterMaker2 v1.3.1 using Markov Clustering Algorithm. The clustering was based on the combined score calculated from experimental and computational interaction values assigned by the STRING database.

6.2.7 Gene set enrichment analysis of the proteomic dataset

Enriched gene sets from the whole, unfiltered proteomics data were explored with Gene Set Enrichment Analysis (GSEA) software v4.1.0 [92]. The preprocessed raw dataset was ranked according to calculated fold change values and GSEA was performed with all the annotated ontology sets from the Molecular Signatures Database collections [93]. Only gene sets with a false discovery rate (FDR) value of <0.1 was considered as significant enrichment. Interaction analysis was performed on gene sets falling into FDR 0.1 > criteria and was visualized with Cytoscape as described in the previous sections. Subsequent leading edge analysis was performed from the core enrichment proteins of the significantly enriched gene sets with the in-built plugin of the GSEA software.

All the proteins which contributed to the core enrichment of the previously described GSEA analysis were further analyzed and classified according to the Kyoto Encyclopedia of Genes and Genome (KEGG) resource using Pathview Web (https://pathview.uncc.edu/home) [94, 95].

6.3 Influence of hypercholesterolemia on preconditioning-induced miR-125b-1-3p expression

6.3.1 Experimental setup

In a separate set of experiments, hypercholesterolemia was induced as described above. At the end of the eight-week feeding period, serum samples were collected for cholesterol and triglyceride measurements, and hearts from both feeding groups were isolated and perfused according to Langendorff. Isolated hearts were divided into global I/R or IPre subgroups. The time-matched I/R control group hearts were equilibrated for 45 min before 35 min global ischemia and 120 min reperfusion. In the IPre group after 15 min equilibration time, three intermittent cycles of 5 min no-flow ischemia, separated by 5 min aerobic perfusion was applied before the onset of global ischemia to induce IPre. At the end of the reperfusion, either infarct size was determined or left ventricles were snap-frozen in liquid nitrogen and stored at −80 °C for subsequent miR analysis.

6.3.2 Infarct size determination

After the end of reperfusion, atria were removed, and the ventricles were used to determine the infarcted area. Briefly, frozen ventricles were cut into 7–8 equal slices and incubated in triphenyl tetrazolium chloride (TTC) solution (Sigma, Saint Louis, MO, USA). As a result, the surviving area turned to red-stained while the necrotic area remained pale [96]. Digitalized images from the stained heart slices were evaluated with planimetry method and the amount of myocardial necrosis was expressed as infarct size/area at risk %.

6.3.3 Creatine-kinase release measurement

Coronary effluents were collected after 2, 5, 30, and 120 minutes of the beginning of the reperfusion to measure the release of cardiac-specific creatine kinase (CK-MB) enzyme. Enzyme release was measured via kinetic enzyme activity assay using colorimetric assay detecting kits (Diagnosticum, Hungary) and a microplate reader (Clariostar Plus, BMG Labtech). Enzyme activity was normalized to the volume of coronary effluent and the total weight of the respective heart. Enzyme releases were expressed as U/min/g.

6.3.4 Measurement of cardiac miR-125b-1-3p level with miR-sequencing

In a separate set of experiments, hearts were isolated and perfused as described above to identify differentially expressed miRs. Six heart samples from each group were used for

miR-sequencing. Total RNA was isolated from left ventricles with Qiagen miRNeasy Mini kit. Total RNA samples were quality checked and quantified by capillary gel electrophoresis in an Agilent Bioanalyzer 2100 instrument using Agilent 6000 RNA Nano Kit. Then 1000 ng total RNA samples were used to prepare sequencing libraries using NEBNext Multiplex Small RNA Library Prep Set for Illumina (New England Biolabs) following the recommendations of the manufacturer. Sequencing libraries were size selected with AMPure XP beads (Beckman Coulter). Validated library pools were loaded in MiSeq Reagent Kit V3-150 and sequenced with an Illumina MiSeq instrument generating 36 nucleotides long single-end reads. Sequencing reads were quality checked with FastQC and were trimmed using Cutadapt ver. 1.8.1. Trimmed oligos were analyzed with the mirdeep2 package. Reads were aligned to the rat reference genome assembly ver. 6.0. Differential expression analyses were performed with Deseq2. Fold change greater than 1.5 (log_2=0.585) and $p<0.05$ were used as criteria for differentially expressed miRs.

6.4 The effect of skeletal muscle electrical stimulation on cardioprotection and muscle-derived myokine levels

6.4.1 Experimental setup

Aiming to test whether EMS could be a feasible alternative to cardiac preconditioning a similar ex vivo heart perfusion setup was applied as described above, involving only normocholesterolemic rats. EMS treatment was performed in sedated control animals with stimulating electrodes placed on the *gastrocnemius* muscles of the rats. Three EMS sessions were applied; each included 10 Hz frequency continuous stimulation for 35 minutes daily. Twenty-four hours after the last EMS treatment, rats were anesthetized with an intraperitoneal injection of 50 mg/kg sodium pentobarbital, then blood and *gastrocnemius* muscle samples were collected for myokine level measurements. Hearts from EMS-treated and untreated animals were isolated and perfused according to Langendorff; equilibrated for 15 min followed by 30 min global ischemia and 120 min reperfusion. During reperfusion, coronary effluents were collected and used to measure cardiac lactate-dehydrogenase (LDH) and CK-MB release. At the end of the reperfusion, infarct size was determined by TTC staining as described above.

6.4.2 Electrical muscle stimulation

EMS treatment was performed with a portable electrostimulation device (Sanitas SEM 44 digital EMS/TENS, Hans Dinslage GmbH, Germany). Rats were sedated with a 40 mg/kg^{-1} sodium pentobarbital solution (Produlab Pharma b.v., Raamsdonksveer, The Netherlands), placed in a heating pad in a supine position, and hind limbs were fixed. Bilateral EMS was applied to target the gastrocnemius muscles with stimulating electrodes once a day for three consecutive days. The EMS treatment consisted of 35 minutes of continuous stimulation with applied bipolar rectangular pulses at 10 Hz frequency and 250 μs pulse width with minimal intensity to produce a visible muscle contraction. The control group underwent the same procedure, without turning on the EMS equipment.

6.4.3 Determination of skeletal muscle myokine expression and secretion

Total RNA was isolated from the *gastrocnemius* muscles with the phenol-chloroform extraction method and total RNA concentration was determined. Reverse transcription of 500 ng RNA was performed with iScript cDNA Synthesis Kit (BioRad, CA, USA), and the resulting cDNA was used as the template for qPCR measurement of myokine expression levels using SYBR Green PCR Super Mix (BioRad) and CFX96 Touch Real-Time PCR machine (BioRad). Relative expression levels were determined with the $2^{\wedge-\Delta\Delta Ct}$ method with GAPDH used as the housekeeping gene.

Double-antibody sandwich ELISA kits (Fine Test, Wuhan, China) specific for rat Irisin, Decorin, Myonectin, Myoglobin, IL-6, IL15, and FSTL1 proteins, respectively, were used to measure protein content in gastrocnemius and serum samples according to the manufacturer's instructions. Myokine content was determined with a colorimetric detection method using a microplate reader (Clariostar Plus, BMG Labtech).

6.4.4 Western Blot analysis

Frozen left ventricular samples were homogenized with an ultrasonicator in Radio Immunoprecipitation Assay (RIPA) buffer (Cell Signaling) supplemented with a protease inhibitor cocktail and phosphatase inhibitors phenylmethane sulfonyl fluoride and sodium fluoride. Homogenates were centrifuged, and protein concentrations of the supernatants were determined using BCA Protein Assay Kit (Pierce, Rockford, IL, USA). Twenty μg of reduced and denatured protein was loaded in 10% polyacrylamide gel, and SDS gel electrophoresis was performed. Separated proteins were transferred to 0.22 μM pore size nitrocellulose membranes. After checking the transfer efficiency with Ponceau-staining, membranes were

blocked for 1 h in 5% (w/v) bovine serum albumin (BSA) at room temperature. Blocked membranes were incubated with the following primary antibodies in the concentrations of 1:1000 phosphorylated-AKT (Ser473), AKT, phosphorylated-ERK1/2 (Thr202/Tyr204), ERK1/2, phosphorylated-STAT3 (Tyr705) and STAT3, respectively, and in 1:5000 concentration against GAPDH at 4 °C overnight. After incubation with horseradish peroxidase (HRP)-conjugated goat anti-rabbit secondary antibody membranes were developed with an enhanced chemiluminescence kit. After the development of phosphorylated signals of AKT, ERK1/2, and STAT3 membranes were stripped and reassessed for the total amount of proteins. Signals were analyzed and evaluated by Quantity One Software (BioRad).

6.5 Statistics

All values are expressed as the mean + SEM. Student's t-test was used to evaluate the effect of the cholesterol-enriched diet on body weight, serum or plasma lipid levels, and echocardiographic parameters. The Shapiro-Wilk normality test was used to test the normal distribution of the data. Two-way analysis of variance (ANOVA) with *post hoc* Fisher's Least Significant Difference test was used to evaluate the infarct size limiting effect of IPre in normo- and hypercholesterolemic animals. For proteomic data, the two-one-sided test was used for the equivalence test and the statistical significance was tested using an unpaired Welch test. Multiple testing correction was applied in the pathway-enriched analysis. Wald test was performed in differential miR expression analysis and expression ratio with p-value <0.05 and >1.5 fold change were considered as significant expression differences.

Student's t-test was used to evaluate the effect of EMS on infarct size. For the evaluation of LDH and CK-MB releases repeated measures ANOVA with Holm-Sidak all pairwise multiple comparison method was applied. Relative expression levels of myokines were determined with the 2^-ΔΔCt method. For all statistical evaluations through the experiments, a p-value < 0.05 was considered as an indicator of significant difference among the groups.

7 Results

7.1 Characterization and network analysis of the left ventricular proteome in the settings of hypercholesterolemia

7.1.1 Effect of cholesterol-enriched diet on plasma lipid levels

At the end of the eight-week feeding period, there was no significant difference in the body weight and the left ventricular tissue weight of the animals receiving a cholesterol-enriched diet or a standard diet (Table 1). Nevertheless, the total plasma cholesterol showed a marked elevation in the cholesterol-fed group, supporting the manifestation of diet-induced hypercholesterolemia. The plasma total triglyceride level also increased significantly in the hypercholesterolemic animals.

	Normochol	**Hyperchol**
Body weight (g)	485 ± 22	521 ± 17
Tibia length (cm)	4.20 ± 0.08	4.21 ± 0.05
Left ventricle weight (mg)	1242 ± 42	1230 ± 48
Total cholesterol (mmol/L)	1.52 ± 0.11	4.35 ± 0.21*
Total triglyceride (mmol/L)	0.44 ± 0.03	1.18 ± 0.08*

Table 1. General characterization of normocholesterolemic (Normochol) and hypercholesterolemic (Hyperchol) rats after eight weeks. Data are expressed as mean ± SEM; n=6; *p<0.05

7.1.2 Cardiac function assessed by transthoracic echocardiography

Transthoracic echocardiography was performed at the end of the feeding period to investigate the effects of diet-induced hypercholesterolemia on cardiac morphology and function. After eight weeks, gross cardiac morphology remained unaffected, as shown by systolic and diastolic wall thickness parameters (Table 2). Furthermore, there were no differences in left ventricular end-diastolic and end-systolic volume, fractional shortening, and ejection fraction, respectively. Interestingly, heart rate was significantly decreased in the settings of hypercholesterolemia. Early (E) and late (A) ventricular filling velocities showed a trend toward a decrease, thus significantly elevating the E/A ratio in the hypercholesterolemic hearts, suggesting impaired diastolic function. The presence of diastolic dysfunction was further supported by significantly decreased mitral annulus velocity (e') and mitral valve deceleration time. The E/e' ratio was unaffected.

	Normochol	Hyperchol	p-value
AWTs (mm)	3.86 ± 0.01	3.74 ± 0.13	0.471
AWTd (mm)	2.03 ± 0.10	2.17 ± 0.13	0.420
IWTs (mm)	3.88 ± 0.12	3.62 ± 0.13	0.154
IWTd (mm)	2.39 ± 0.13	2.30 ± 0.14	0.660
PWTs (mm)	3.71 ± 0.09	3.70 ± 0.22	0.938
PWTd (mm)	2.46 ± 0.20	2.43 ± 0.13	0.902
SWTs (mm)	3.81 ± 0.05	3.69 ± 0.13	0.442
SWTd (mm)	2.18 ± 0.06	2.27 ± 0.13	0.548
LVESD (mm)	2.39 ± 0.10	2.85 ± 0.28	0.155
LVEDD (mm)	6.32 ± 0.30	6.72 ± 0.25	0.343
FS (%)	62.06 ± 1.43	63.89 ± 4.06	0.679
EF (%)	93.61 ± 0.63	90.56 ± 2.18	0.209
MV E velocity (m/s)	1.28 ± 0.19	0.80 ± 0.14	0.067
MV A velocity (m/s)	0.95 ± 0.16	0.50 ± 0.16	0.076
E/A	1.39 ± 0.06	1.81 ± 0.17*	**0.043**
e' (m/s)	0.06 ± 0.00	0.04 ± 0.00 *	**0.005**
E/e'	20.78 ± 3.38	20.08 ± 3.80	0.894
E deceleration time	79.00 ± 9.08	51.56 ± 6.12*	**0.031**
Heart rate (1/min)	350.33 ± 10.89	323.50 ± 5.00*	**0.049**

Table 2. Left ventricular morphological and functional parameters examined by echocardiography after the feeding period in both normocholesterolemic (Normochol) and hypercholesterolemic (Hyperchol) rats. Values are mean ± SEM (n=6), *p<0.05. A: mitral late flow velocity, AWT: anterior wall thickness, d: diastolic, E: mitral early flow velocity, e': septal mitral annular velocity, EF: ejection fraction, FS: fractional shortening, IWT: inferior wall thickness, LVEDD: left ventricular end-diastolic diameter, LVESD: left ventricular end-systolic diameter, MV: mitral valve, PWT: posterior wall thickness, s: systolic, SWT: septal wall thickness.

7.1.3 Proteomic characterization of the hypercholesterolemic left ventricle

Altogether, 901 proteins were reliably identified from left ventricular samples through mass spectrometry. Statistical analysis (Welch's t-test) performed on the identified proteins revealed altered levels ($p<0.05$) of 75 proteins due to hypercholesterolemia. Among the significant hits, proteins with at least a 1.2-fold change value were considered for further network analyses. Based on these criteria, we observed the upregulation of 23 proteins and downregulation of 22 in the left ventricle of hypercholesterolemic animals compared with the normocholesterolemic controls (Table 3, Figure 3).

UniProt ID	Gene Symbol	Protein Name	Fold Change
P09895	*Rpl5*	60S ribosomal protein L5	2.60
Q03626	*Mug1*	Murinoglobulin-1	1.96
O35814	*Stip1*	Stress-induced-phosphoprotein 1	1.91
P09006	*Serpina3n*	Serine protease inhibitor A3N	1.90
P52873	*Pc*	Pyruvate carboxylase	1.54
P02680	*Fgg*	Fibrinogen gamma chain	1.45
P02564	*Myh7*	Myosin-7	1.42
P06399	*Fga*	Fibrinogen alpha chain	1.42
P01026	*C3*	Complement C3	1.35
D3ZWC6	*Sntb1*	Syntrophin, basic 1	1.31
P25113	*Pgam1*	Phosphoglycerate mutase 1	1.30
P29147	*Bdh1*	D-beta-hydroxybutyrate dehydrogenase	1.30
Q68FP1	*Gsn*	Gelsolin	1.29
P05545	*Serpina3k*	Serine protease inhibitor A3K	1.27
Q5RKI0	*Wdr1*	WD repeat-containing protein 1	1.27
P07335	*Ckb*	Creatine kinase B-type	1.25
A0A0G2K542	*Ugp2*	UTP--glucose-1-phosphate uridylyltransferase	1.22
Q99PD4	*Arpc1a*	Actin-related protein 2/3 complex subunit 1A	1.22
P50137	*Tkt*	Transketolase	1.22
D4A5W5	*Recql4*	RecQ-like helicase 4	1.22
P63102	*Ywhaz*	14-3-3 protein zeta/delta	1.21
P61589	*Rhoa*	Transforming protein RhoA	1.21
Q08163	*Cap1*	Adenylyl cyclase-associated protein 1	1.21
G3V885	*Myh6*	Myosin-6	0.83
Q925Q9	*Sh3kbp1*	SH3 domain-containing kinase-binding protein 1	0.83
F1LNF0	*Myh14*	Myosin heavy chain 14	0.83
F1M7L9		Uncharacterized protein	0.82
P38650	*Dync1h1*	Cytoplasmic dynein 1 heavy chain 1	0.81
Q925F0	*Smpx*	Small muscular protein	0.78
O35115	*Fhl2*	Four and a half LIM domains protein 2	0.77
P02401	*Rplp2*	60S acidic ribosomal protein P2	0.77
Q6PCU8	*Ndufv3*	NADH dehydrogenase [ubiquinone] flavoprotein 3	0.76
P41123	*Rpl13*	60S ribosomal protein L13	0.76
Q5XIG9	*Mtfp1*	Mitochondrial fission process 1	0.74
P02650	*Apoe*	Apolipoprotein E	0.68
P62902	*Rpl31*	60S ribosomal protein L31	0.66
C0KUC6	*Lims1*	LIM and senescent cell antigen-like-containing domain protein	0.61
Q924S5	*Lonp1*	Lon protease homolog	0.58
P02466	*Col1a2*	Collagen alpha-2(I) chain	0.52
P60711	*Actb*	Beta-actin	0.47
A0A0G2K1W9	*Ldhd*	Lactate dehydrogenase D	0.37
M0RB63	*LOC684509*	NADH-ubiquinone oxidoreductase B9 subunit	0.34
A0A0G2KAA3	*Ndufa3*	NADH:ubiquinone oxidoreductase subunit A3	0.34
P13697	*Me1*	NADP-dependent malic enzyme	0.34
Q9QZA6	*Cd151*	CD151 antigen	0.28

Table 3. List of hypercholesterolemia-induced significant alterations in the left ventricular proteins. Fold-change cut-off values of significantly expressed proteins were set as > 1.2 for upregulated and < 0.83 for downregulated levels, respectively. The fold change values are shown as ratio pairs.

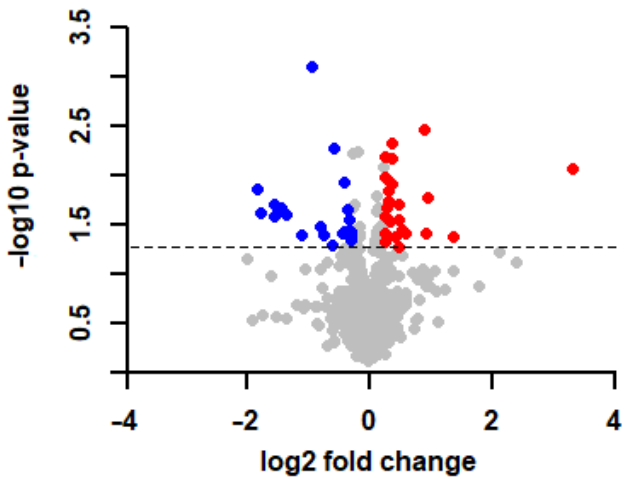

Figure 3. Diet-induced hypercholesterolemia leads to alterations in the myocardial proteome. Volcano plot showing the significantly ($p<0.05$ of Welch's t-test and 1.2-fold changes) altered proteins induced by hypercholesterolemia in the left ventricles of rats. Each dot represents one distinct protein. The downregulated (blue) and upregulated (red) proteins are highlighted in the plot. The dashed line indicates the threshold value of statistical significance.

7.1.4 Pathway enrichment analysis of the significantly altered proteins

To assign biological functions and reveal potential networks for the significantly changed proteins, Gene Ontology (GO) and subsequent pathway enrichment analyses were carried out. The GO analysis covered all three independent ontology categories, including molecular function (MF), biological process (BP), and cellular component (CC). We observed the enrichment of 31 GO terms at FDR < 0.1, altogether (Figure 4). Interestingly, according to the GO terminology, a substantial number of the enriched nodes were in the CC category, possibly indicating hypercholesterolemia-induced rearrangements of subcellular structures and macromolecular complexes in the left ventricle. Based on the GO analysis, the enriched ontology terms involved proteins associated with contractile function and cytoskeletal organization (Figure 4). Additionally in the same analysis, a minor enrichment of mitochondrial proteins was also observed. Overall, the involvement of the observed processes might contribute to the initiation of the subcellular structural remodeling and subsequent contractile impairment of the myocardium in hypercholesterolemic animals.

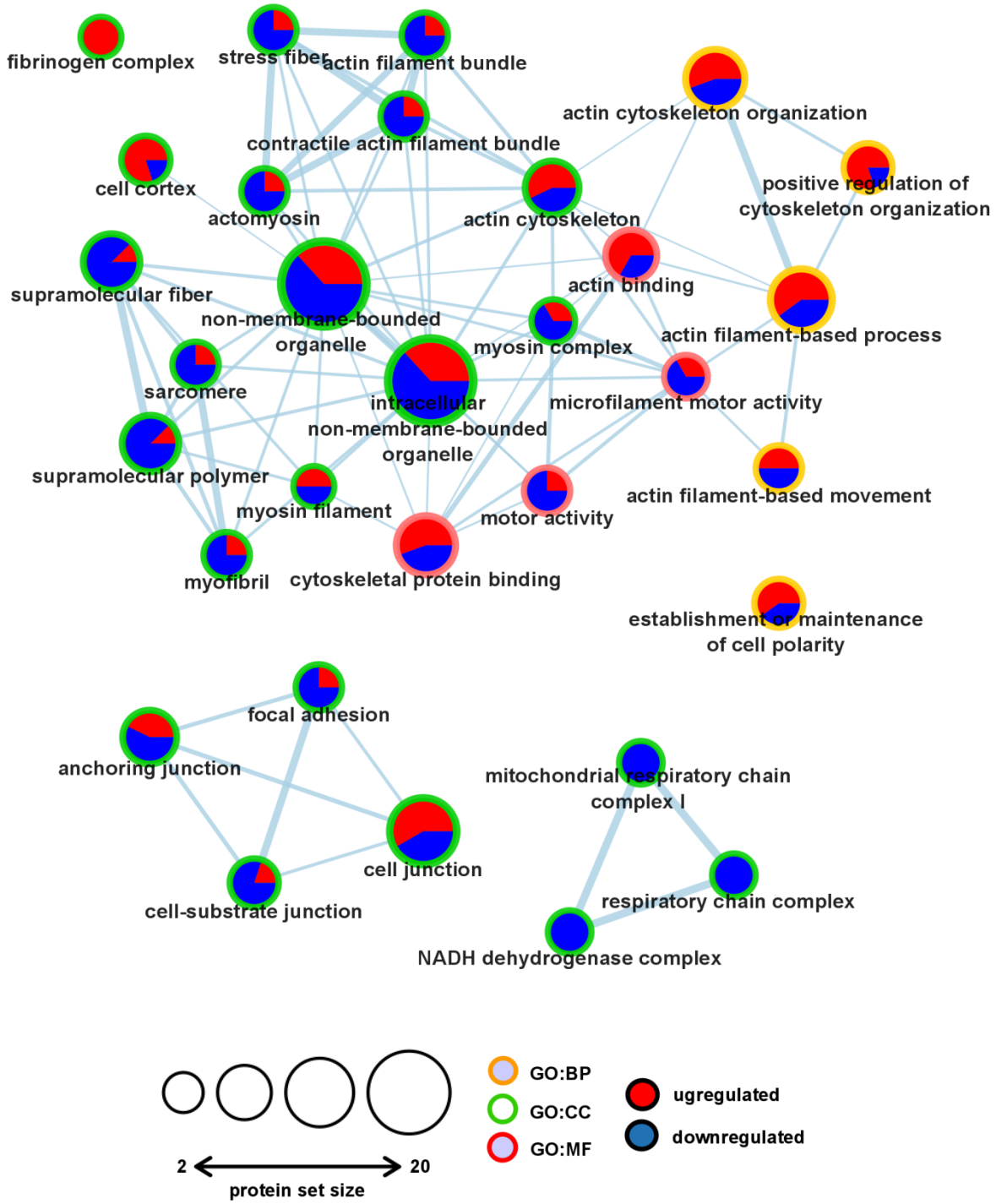

Figure 4. Pathway enrichment analysis of the proteomic results revealed enrichment of proteins related to the contractile and cytoskeletal systems. Significantly changed proteins were subjected to gene ontology (GO) and pathway enrichment analysis, and visualized with Cytoscape v. 3.8.2. The size of the nodes corresponds to the number of proteins falling into the respective category, while the GO terminologies are marked as differently colored borders (MF: molecular function, BP: biological process, CC: cellular component). Edges (lines) represent overlaps and functional interactions among the nodes. The width of each edge corresponds to the similarity score between the nodes. The numbers of up (red) and downregulated (blue) proteins were incorporated into the nodes as pie charts.

7.1.5 Functional interaction analysis of the differentially expressed proteins

As the next step, we assessed the functional interactions and conducted subsequent cluster analysis within the significantly altered proteins. Our analyses revealed a modest number of connections among the identified proteins (Figure 5). Interestingly, beta-actin (ACTB) was downregulated in the hypercholesterolemic myocardium and ACTB established a prominent hub of the revealed network. ACTB turned out to be connected to both structural and accessory proteins. Among these interactions, many proteins were upregulated, such as Actin-related protein 2/3 complex subunit 1A (ARPC1A), Adenylyl cyclase-associated protein 1 (CAP1), WD repeat-containing protein 1 (WDR1), Myosin-7 (MYH7), Gelsolin (GSN), and Ras homolog family member A (RHOA). At the same time, the levels of Myosin-6 (MYH6), Myosin heavy chain 14 (MYH14), Collagen type 1 alpha 2 chains (COL1A2), and Cytoplasmic dynein heavy chain 1 (DYNC1H1) were downregulated (Figure 5).

Additionally, the cluster analysis revealed other minor subnetworks among the resulting interactions, which might implicate disturbed metabolic functions and subsequent energy production. For instance, the resulting functional interaction network contains a couple of metabolic enzymes with altered expression such as Pyruvate carboxylase (PC), Phosphoglycerate mutase 1 (PGAM1), Transketolase (TKT), Creatine kinase (CKB), Malic enzyme 1 (ME1) and Lactate dehydrogenase, respectively (Figure 5). Moreover, three subunits of the NADH dehydrogenase complex showed significantly downregulated expression and formed one of the loops in the network (Figure 5). These subnetworks suggest an impaired mitochondrial function and imbalance in the energy production of the hypercholesterolemic myocardium.

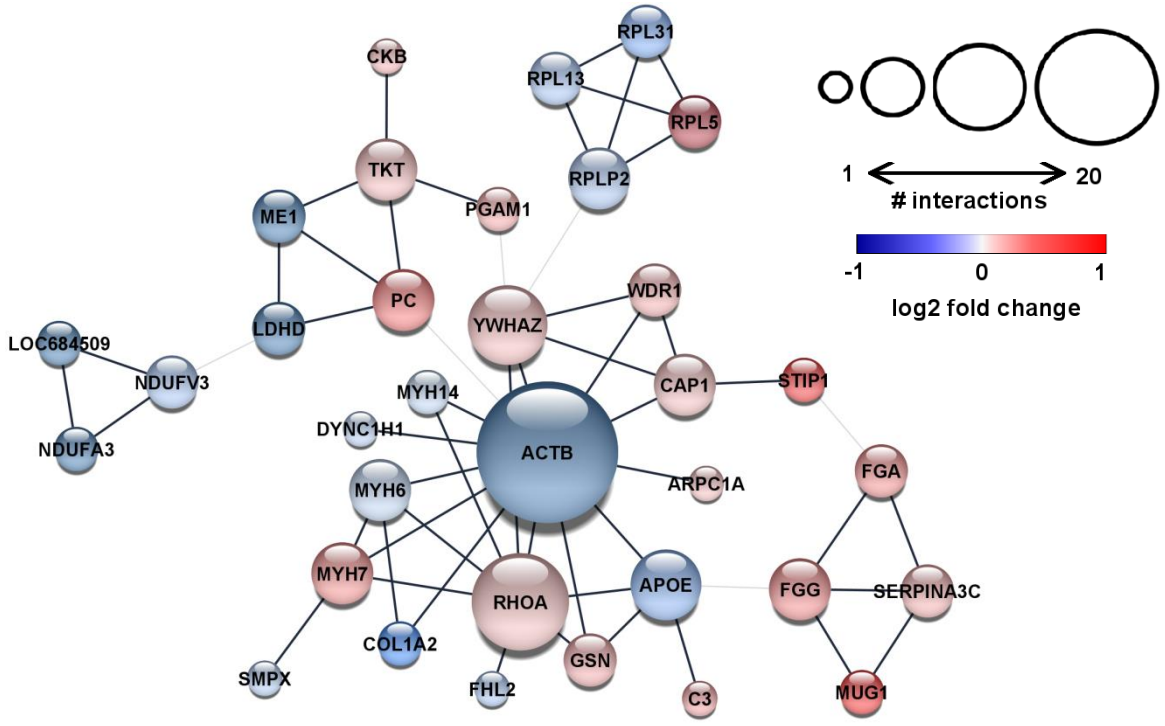

Figure 5. Downregulated beta-actin was established as a prominent hub of the protein interaction network in the hypercholesterolemic myocardium. Each node (circle) represents one protein and is labeled according to gene IDs. The node size corresponds with the number of interactions of the respective protein. The color of each node indicates the fold change values (red for upregulated and blue for downregulated expression). Edges (grey lines) represent the interactions between nodes, with their thickness indicating interactions within the clusters (wide edges) or among the proteins in different clusters (narrow edges).

7.1.6 Protein-specific gene set enrichment analysis

For deeper analyses of the global changes in the left ventricular proteome, a gene set enrichment analysis (GSEA) was performed on the unfiltered, whole proteomic dataset. The GSEA identified similar downregulated expression patterns among the proteins associated with mitochondrial complexes, with particular emphasis on the elements of the respiratory chain complexes (Figure 6). Additionally, our analysis revealed downregulated expression patterns of proteins previously assigned to heart development processes according to the GO terminology. Then, subsequent leading-edge analysis was carried out to determine which subsets of proteins contributed the most to the enriched GO terms. As expected, proteins of the respiratory chain complexes, i.e., subunits of the NADH:Ubiquinone oxidoreductase complex (NDFU), were among the leading enrichment set (Figure 7). Furthermore, another set of leading-edge proteins could be identified with important roles in

normal cardiac contractile function (Figure 7). For instance, downregulated expression patterns were observed in the case of cardiac-specific isoforms of the troponin complex, such as Troponin T2 (TNNT2), Troponin C1 (TNNC1), Troponin I3 (TNNI3), and Tropomyosin 1 (TPM1). Furthermore, hypercholesterolemia seemed to negatively affect the protein expression pattern of the ventricular isoform of myosin light chain (MYL3), as well as myosin heavy chain 6 (MYH6), which is preferably expressed in the ventricles of smaller mammals with rapid heart rates.

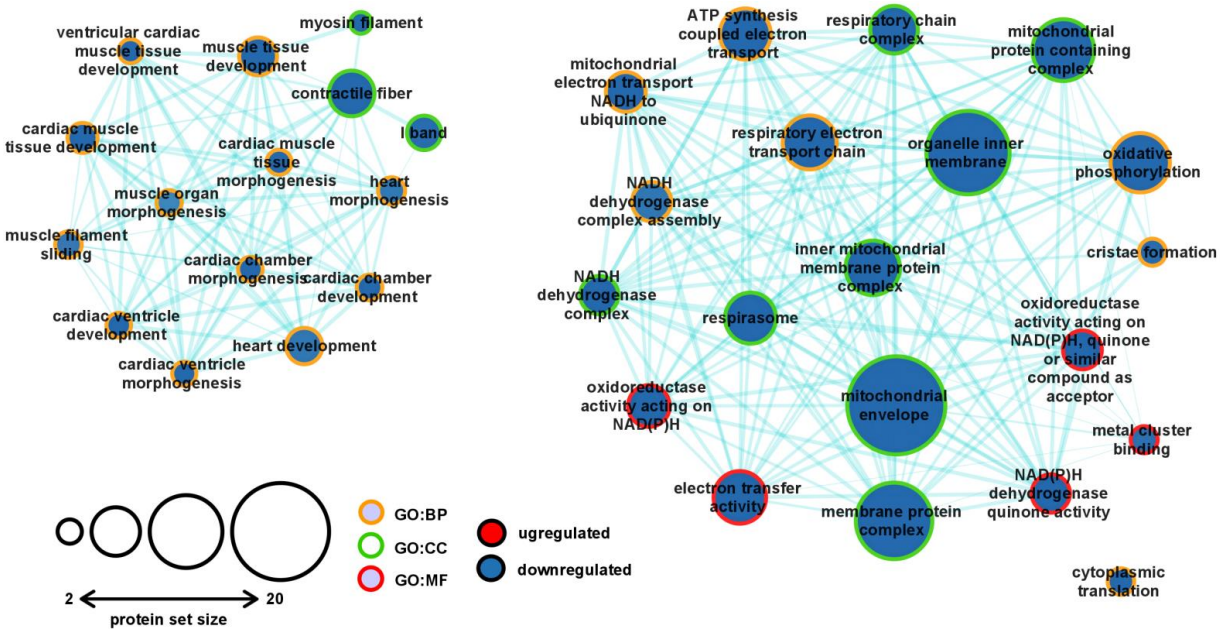

Figure 6. Enrichment map of the major GO sets influenced by hypercholesterolemia at the whole proteome level. Pathway enrichment analysis was performed with protein-specific GSEA. The nodes represent enriched gene sets. The node size corresponds with the number of proteins falling into a respective gene set category. The color of each node represents the trend of quantitative change in the hypercholesterolemic left ventricle, while the color of the nodes' border indicates the respective GO category. Edges represent similarity among the gene sets, as the thickness of each edge corresponds with the overlap between the nodes. The enriched gene sets were visualized with Cytoscape v3.8.2.

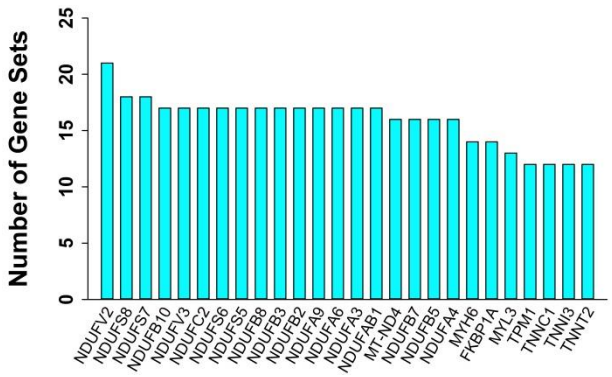

Figure 7. The output of leading edge analysis of the enriched ontology terms. The numbers of the horizontal axis indicate the appearance of the respective protein in the significantly enriched subsets.

Furthermore, the core enrichment proteins from the previous GSEA analysis were further analyzed according to the Kyoto Encyclopedia of Genes and Genomes (KEGG). Expression levels of proteins related to cardiac muscle contraction were affected by hypercholesterolemia, as shown by the concordant downregulated expression patterns of cardiac-specific troponins and myosin complex in the left ventricle of hypercholesterolemic animals (Figure 8). Additionally, the results of the KEGG-based analysis of our protein sets further support the possible deterioration of the mitochondrial function in the hypercholesterolemic left ventricle, affecting the expression of components of all the five major complexes of the respiratory chain system responsible for oxidative phosphorylation (Figure 9).

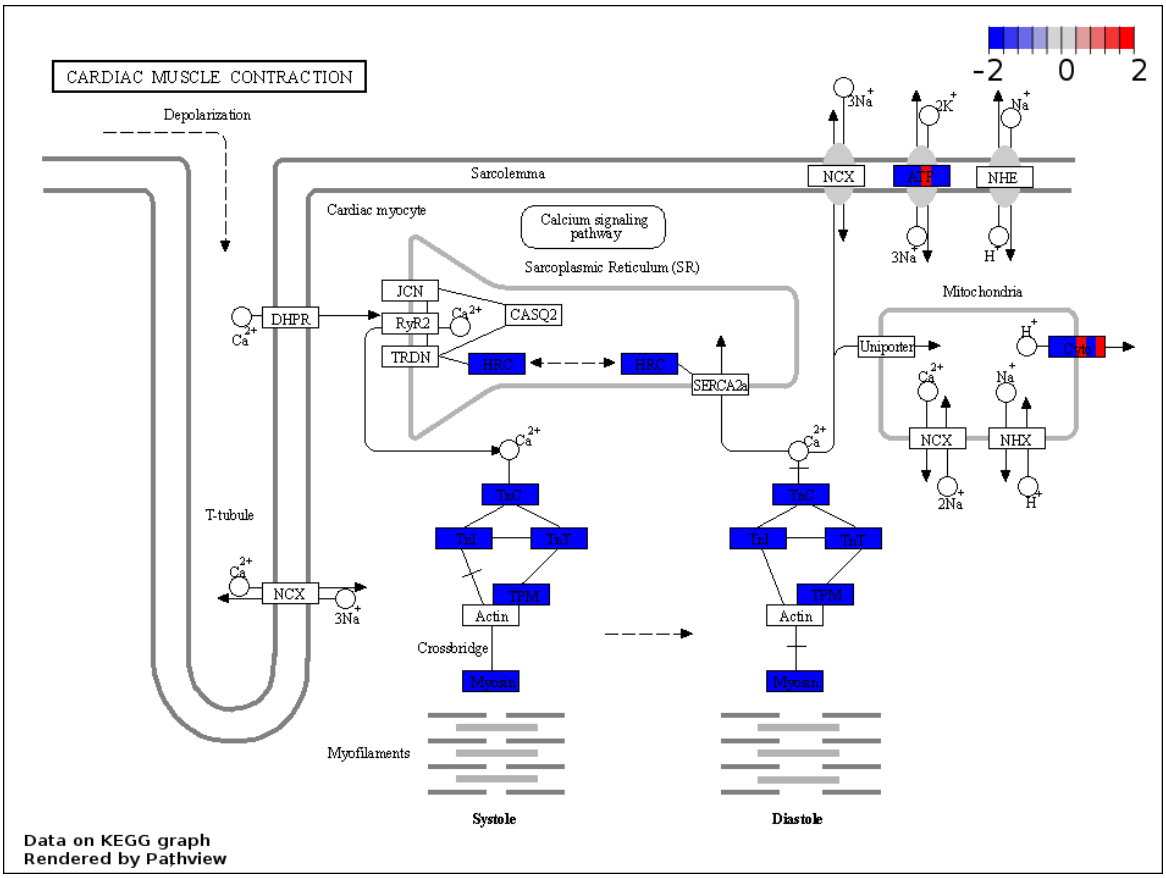

Figure 8. KEGG analysis showed concordant downregulated expression patterns of cardiac-specific troponins and the myosin complex. Visual representation of leading-edge protein subsets based on the Kyoto Encyclopedia of Genes and Genomes database. Each protein was divided into six sections and was colored based on the relative expression count compared with the normocholesterolemic group. Pathway graphs were created with Pathview Web **(https://pathview.uncc.edu/home).**

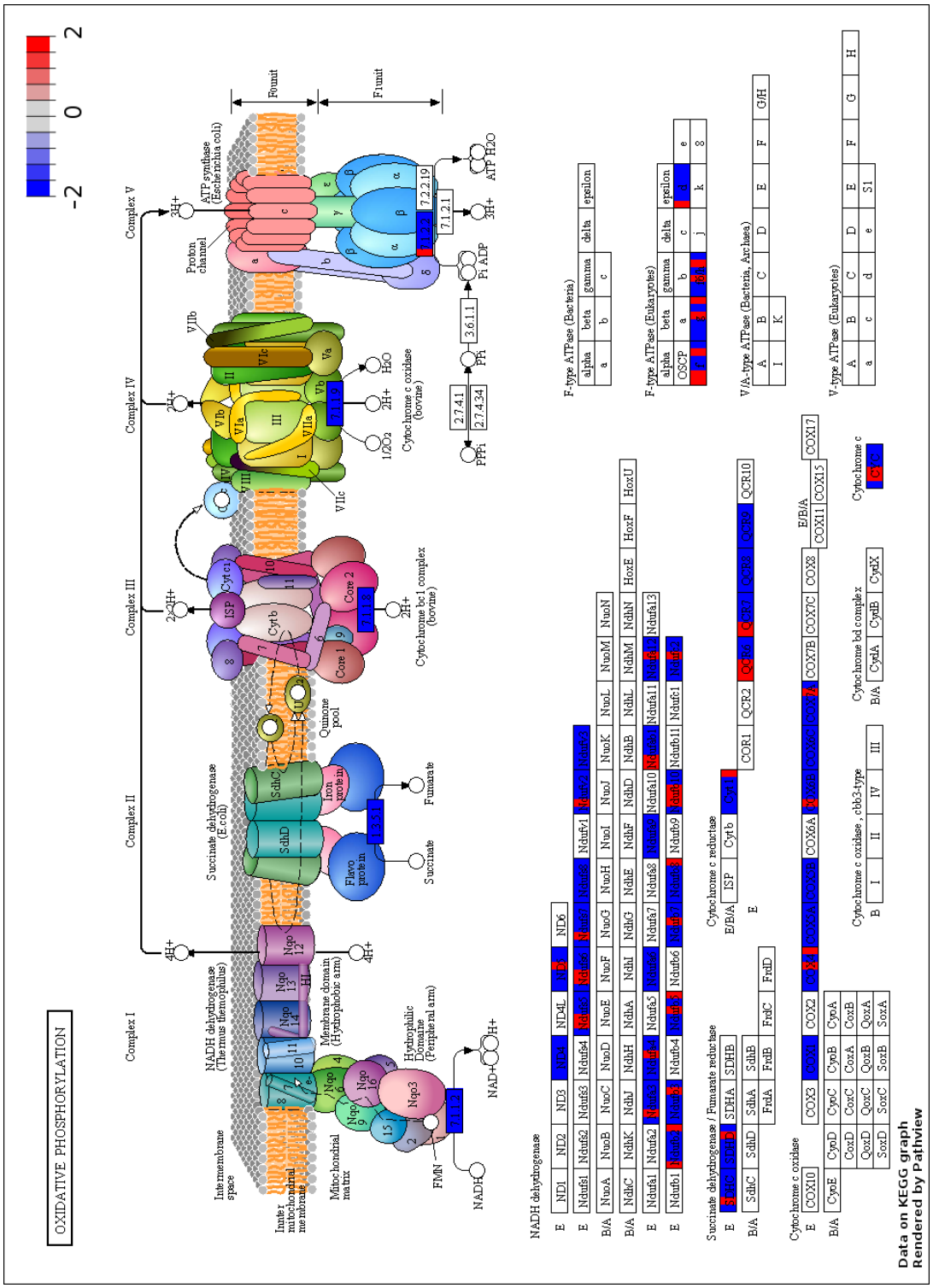

Figure 9. KEGG analysis showed concordant downregulated expression changes in protein components of the respiratory chain in the hypercholesterolemic left ventricle. Visual representation of leading-edge protein subsets based on the Kyoto Encyclopedia of Genes and Genomes database. Each protein was divided into six sections and was colored based on the relative expression count compared with the normocholesterolemic group. Pathway graphs were created with Pathview Web.

7.2 Testing the effect of hypercholesterolemia on ischemic preconditioning-induced miR-125b-1-3p upregulation and cardioprotection

7.2.1 Verification of hypercholesterolemia

In a separate set of experiments, hypercholesterolemia was induced in male rats similarly as described above. At the end of the eight-week diet period, the body weight of animals receiving a cholesterol-enriched diet was not different from the weight of control animals fed with a standard diet (Table 4). Serum total cholesterol as well as triglyceride levels were significantly higher in cholesterol-fed rats when compared to control animals fed with a standard chow.

	Normochol	**Hyperchol**
Body weight (g)	504 ± 8.6	502 ± 9.5
Total cholesterol (mmol/L)	1.73 ± 0.12	6.04 ± 1.11*****
Total triglyceride (mmol/L)	0.52 ± 0.06	1.07 ± 0.10*****

Table 4. Body weight and serum lipid parameters of normo- (Normochol) and hypercholesterolemic (Hyperchol) animals. Data are expressed as mean ± SEM; n=16/group. *p<0.05

7.2.2 Effect of hypercholesterolemia on ischemic preconditioning

To assess the cardioprotective effect of IPre, infarct size was measured in hearts undergoing I/R. In the hearts of normocholesterolemic rats, IPre significantly decreased infarct size compared to the I/R control group (Figure 10). However, IPre failed to significantly attenuate infarct size in the hearts of hypercholesterolemic animals.

Additionally, CK-MB enzyme release was measured from the coronary effluents collected at different time points of the reperfusion. We found that at the end of the reperfusion, IPre significantly decreased CK-MB enzyme release activity only in normocholesterolemic but not in hypercholesterolemic hearts (Figure 11).

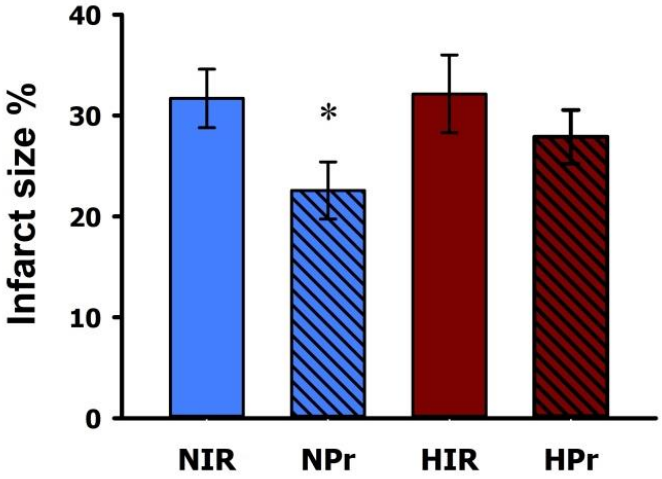

Figure 10. Infarct size values at the end of ex vivo heart perfusion. Hearts isolated from normo- and hypercholesterolemic rats were subjected to 35 min global ischemia and 120 min reperfusion (I/R) with or without ischemic preconditioning (3 × 5 min cycles of I/R applied before index ischemia; IPre). Data are expressed as mean ± SEM; n=8/group. *p<0.05 vs. corresponding I/R group. N: normocholesterolemia, H: hypercholesterolemia, IR: ischemia/reperfusion, Pr: ischemic preconditioning, respectively.

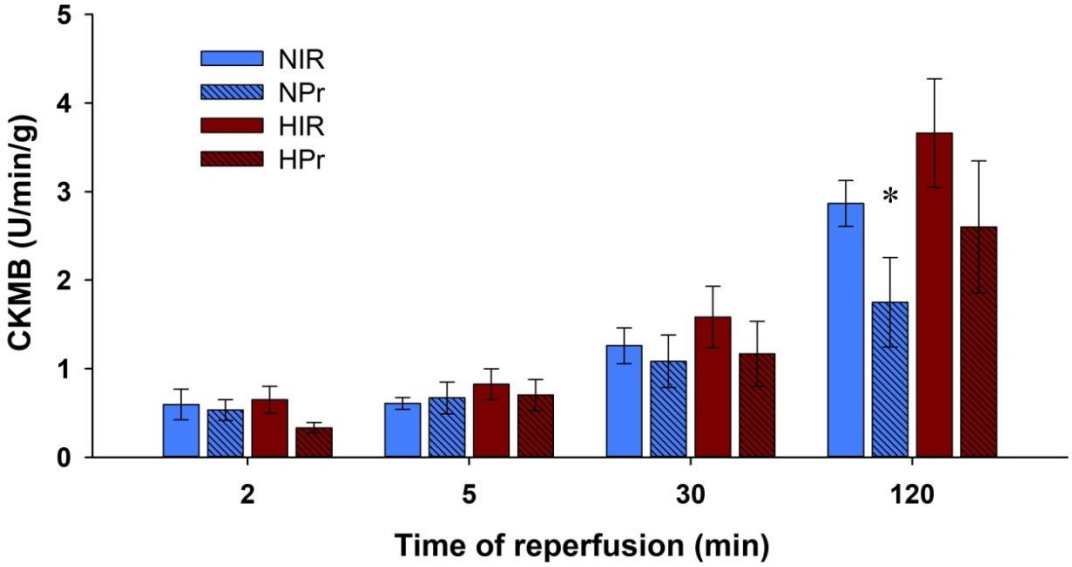

Figure 11. IPre decreased CK-MB enzyme release in normo- but not in hypercholesterolemic hearts. Coronary effluents were collected at different time points of the reperfusion and used for colorimetric CK-MB enzyme activity measurement. Data are expressed as mean ± SEM; n=8. *p<0.05 vs. corresponding I/R group. The abbreviations are N: normocholesterolemia, H: hypercholesterolemia, IR: ischemia/reperfusion, and Pr: ischemic preconditioning, respectively.

7.2.3 The effect of preconditioning on miR-125b-1-3p levels

To assess if miR-125b-1-3p correlates with cardioprotection, miR expression was determined in hearts subjected to I/R with or without IPre in both normo- and hypercholesterolemic groups (Figure 12). At the end of reperfusion, IPre significantly upregulated miR-125b-1-3p in normocholesterolemic hearts compared to I/R controls. In contrast, IPre failed to increase significantly miR-125b-1-3p levels in the hearts of hypercholesterolemic animals, thereby showing a clear correlation with the blunted cardioprotective effects of IPre in the settings of hypercholesterolemia.

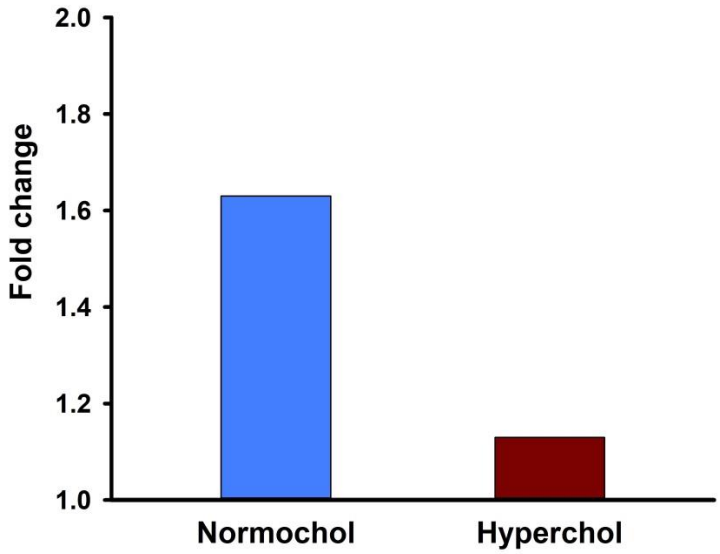

Figure 12. miR-125b-1-3p expression changes induced by ischemic preconditioning (IPre) in the hearts of normocholesterolemic and hypercholesterolemic rats. Values are log2 expression changes ± SEM calculated with Deseq2. Normochol and Hyperchol refer to normo- and hypercholesterolemia, respectively.

7.3 The effect of electrical stimulation of skeletal muscle against cardiac ischemia/reperfusion and on muscle-derived myokine levels

7.3.1 Effect of skeletal muscle EMS on ex vivo perfused hearts

To assess the cardioprotective effect of EMS, ex vivo heart perfusion was performed on isolated hearts from EMS-treated and untreated control rats. Cardiac CK-MB and LDH release were significantly lower upon EMS at the end of reperfusion (Figure 13). Furthermore, myocardial infarct size was also determined at the end of reperfusion, and although the mean value of infarct size tended to be lower in the EMS group compared to the nonstimulated control group (approximately by 20%), the applied EMS treatment failed to attenuate infarct size significantly (Figure 14).

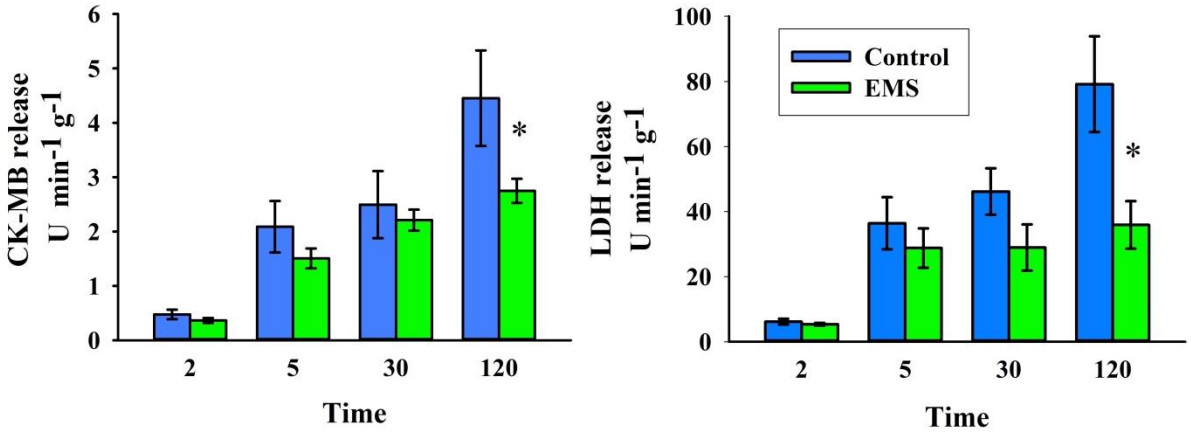

Figure 13. Testing the potential preconditioning effect of EMS treatment against I/R in ex vivo perfused hearts. CK-MB and LDH enzyme release measurement. Coronary effluents were collected at different time points of the reperfusion and used for colorimetric CK-MB and LDH enzyme activity measurement. Data are expressed as mean ± SEM; n=6/group. *p<0.05.

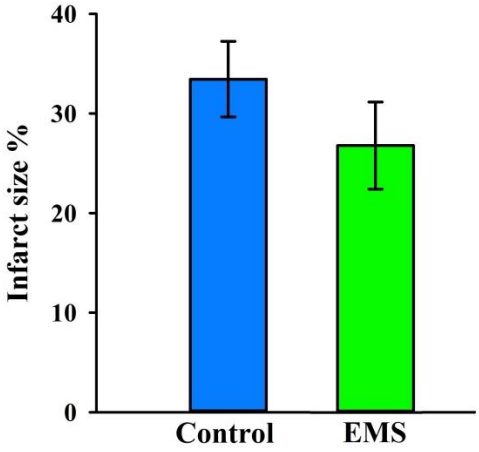

Figure 14. Infarct size values at the end of ex vivo heart perfusion. Hearts isolated from EMS-treated and untreated rats were subjected to 30 min global ischemia and 120 min reperfusion (I/R). The infarcted area/area at risk (IS/AAR%) Data are expressed as mean ± SEM; n=6/group.

7.3.2 Assessment of myokine expression levels in the stimulated muscle

To determine the possible mediators of EMS-associated cardioprotection, myokine expression was measured in the stimulated gastrocnemius muscles. Among the investigated myokines the applied EMS treatment upregulated *Fstl1, Il6,* and *Igf1* mRNA expression in the gastrocnemius muscle (Table 3). Additionally, *Il15* mRNA content was downregulated in response to EMS. Next, we assessed the protein content of some selected myokines in the stimulated gastrocnemius muscle. Irisin, Decorin, Myonectin, FSTL1, and Myoglobin proteins were upregulated as a consequence of EMS (Table 4). Nevertheless, IL-6 and IL-15 protein levels remained unaffected upon EMS treatment, despite their altered mRNA levels.

Myokine	Relative mRNA expression levels	
	Control	EMS
Fstl1	1.02 ± 0.08	2.80 ± 0.59*
Fgf21	1.55 ± 0.47	1.44 ± 0.38
Il6	1.11 ± 0.17	3.90 ± 1.10*
Bdnf	1.10 ± 0.15	0.93 ± 0.19
Erfe	1.07 ± 0.16	0.98 ± 0.11
Igf1	0.93 ± 0.07	1.42 ± 0.19*
Lif	1.91 ± 0.70	1.50 ± 0.61
Dcn	1.08 ± 0.11	1.31 ± 0.21
Fndc5	1.06 ± 0.12	0.92 ± 0.15
Il15	1.04 ± 0.09	0.56 ± 0.07*

Table 5. Myokine RNA expression in the gastrocnemius muscle after EMS treatment. *Fstl1*: Follistatin-like 1, *Fgf21*: Fibroblast growth factor 21, *Il6*: Interleukin-6, *Bdnf*: Brain-derived neurotrophic factor, *Erfe*: Erythroferrone / myonectin, *Igf1*: Insulin-like growth factor 1, *Lif*: Leukemia inhibitory factor, *Dcn*: Decorin, *Fndc5*: Fibronectin type III domain-containing protein 5 / Irisin precursor, *Il15*: Interleukin-15, respectively. Data are expressed as mean ± SEM; n=10, *p<0.05.

Myokine	Tissue protein content (ng mg^{-1})	
	Control	EMS
Irisin	22.14 ± 3.52	39.59 ± 5.26*
Decorin	0.24 ± 0.05	0.55 ± 0.09*
Myonectin	2.13 ± 0.32	4.84 ± 0.94*
FSTL1	25.46 ± 2.52	33.00 ± 1.87*
IL-6	9.28 ± 0.89	10.61 ± 1.12
IL-15	0.97 ± 0.08	0.94 ± 0.08
Myoglobin	0.57 ± 0.10	1.31 ± 0.34*

Table 6. Myokine protein levels in the stimulated gastrocnemius muscle. Protein concentration values are expressed as ng mg^{-1} tissue protein. FSTL1: Follistatin-like 1, IL-6: Interleukin 6, IL-15: Interleukin-15. All data are mean ± SEM; n = 8/group, * $p < 0.05$.

7.3.3 Measurement of serum myokine levels upon EMS

To elucidate whether skeletal muscle-derived myokines may contribute to the cardioprotective effects of EMS, serum myokine levels were measured by ELISA. However, at the time of serum sampling none of the measured myokines showed significant differences in the blood compared to the untreated control animals (Table 5).

Myokine	Serum protein content (ng mg^{-1})	
	Control	EMS
Irisin	6.13 ± 0.62	6.22 ± 0.96
Decorin	1.11 ± 0.01	1.20 ± 0.01
Myonectin	0.22 ± 0.01	0.22 ± 0.01
FSTL1	2.51 ± 0.18	2.63 ± 0.30
Myoglobin	6.64 ± 0.80	6.95 ± 0.84

Table 7. Serum myokine levels. Protein concentration values expressed as ng mg^{-1} serum protein FSTL1: Follistatin-like 1, Data are mean±SEM; n=8/group, *$p<0.05$

7.3.4 Effect of EMS on cardiac conditioning-associated pathways

To further clarify the possible cardioprotective effect of the skeletal muscle EMS, the key protein elements of the RISK and the SAFE pathways were investigated in ventricular samples at the end of the reperfusion. Regarding the RISK pathway, phosphorylation of AKT was not affected significantly upon EMS, while phosphorylation of ERK1 and ERK2 showed a trend toward an increase ($p=0.18$ and 0.21, respectively) in the hearts of EMS-treated animals compared to the untreated controls (Figure 15). Additionally, phosphorylation of STAT3, the key transcription factor of the SAFE pathway, was not affected in the left ventricles either.

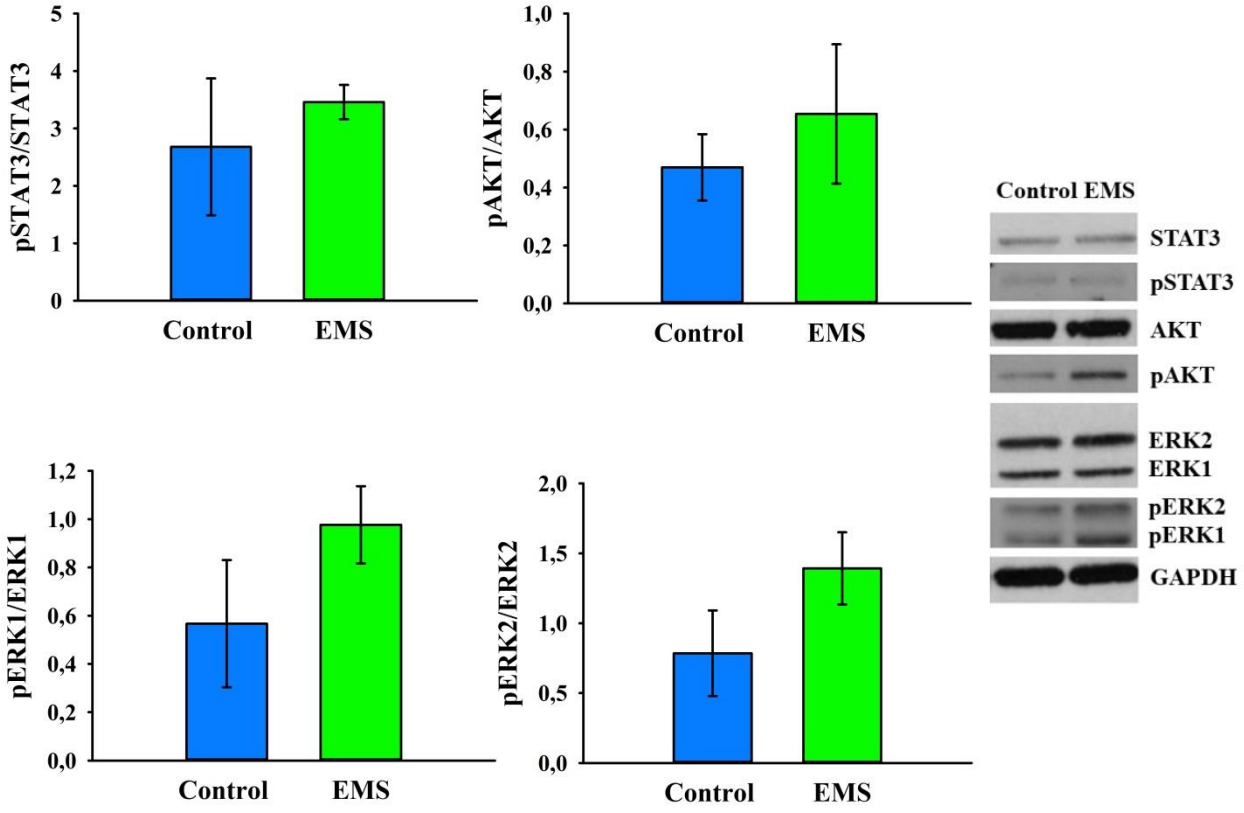

Figure 15. Effect of skeletal muscle EMS training on the phosphorylation of STAT3, AKT, and ERK1/2 proteins assessed by Western blots. Data are expressed as mean ± SEM; n=4, * $p<0.05$.

8 Discussion

In the present thesis, we investigated different aspects of myocardial infarction and its major risk factor, hypercholesterolemia. Based on our results, hypercholesterolemia alters the expression of proteins related to the maintenance of the contractile and cytoskeletal structure and energy generation processes. We have also shown an inverse correlation between the attenuated cardioprotective effect of IPre in hypercholesterolemia with diminished miR-125b-1-3p induction, suggesting that miR-125b-1-3p may be an important activator of IPre-induced cardioprotection and its decreased expression level seems to interfere with the infarct size limiting effect of IPre in hypercholesterolemia. Furthermore, despite the lack of significant infarct size reduction in normocholesterolemia, EMS application seems to influence the course of cellular damage due to I/R and alters the expression levels of several myokines in the skeletal muscle, which might be potential mediators of the beneficial effects of EMS in the cardiovascular system.

8.1 New findings

The novel findings of the present thesis can be summarized as follows:

- Hypercholesterolemia is associated with an altered left ventricular proteome.
- Pathway enrichment and interaction analyses revealed hypercholesterolemia-associated protein changes in contractile and cytoskeletal systems as well as in the protein components of the mitochondrial respiratory chain.
- Upregulation of miR-125b-1-3p induced by preconditioning is lost in settings of hypercholesterolemia.
- EMS treatment seems to alleviate the I/R damage of ex vivo perfused normocholesterolemic hearts
- EMS is associated with modified myokine mRNA and protein levels in the targeted gastrocnemius muscle tissue

8.2 Alterations in the contractile and cytoskeletal system and mitochondrial respiratory chain possibly contribute to hypercholesterolemia-associated cardiac dysfunction

Independently from its proatherogenic effect, high blood cholesterol level exerts direct adverse effects on the myocardium leading to cardiac dysfunction and disturbed stress adaptation against I/R injury. These processes might involve proteome-level changes and

altered molecular interactions and networks. Therefore, we utilized the advantages of downstream bioinformatics analyses of the proteomics dataset to clarify the underlying protein expression changes associated with the direct cardiac effects of hypercholesterolemia. Mild diastolic dysfunction developed in hypercholesterolemic rats as reported previously [31, 35, 97]. In line with the impaired cardiac function, the proteome scale analyses of the hypercholesterolemic myocardium revealed modest quantitative changes on the left ventricular proteome which is in line with other proteomics-based studies of the left ventricle with impaired contractile function [98, 99]. One of the most notable changes in the level of an individual protein was observed in the case of the downregulated expression of ACTB, an essential component of the non-contractile cytoskeleton system and distributions in actin filament assembly and dynamics are implicated to contribute to heart diseases [100, 101]. The central role of ACTB in hypercholesterolemia-induced cardiac dysfunction was further supported by the protein-protein interactions network analysis, which showed that ACTB formed the hub of the revealed network, thus forming many interactions with other accessory proteins (e.g., CAP1, WDR1, GSN, RHOA, and ARPC1A, respectively), which might indicate cytoskeletal rearrangements. Similarly, metabolic perturbations such as hyperglycemia and hyperlipidemia reduced ACTB in both ventricles, which was associated with further impairment of cellular elasticity and disorganized myocardial actin cytoskeleton [102-104]. Possible rearrangements of subcellular structures and macromolecular complexes in the left ventricle upon hypercholesterolemia is further supported by our GO analysis of the differentially expressed proteins as the resulting network implicates alterations in the contractile apparatus and cytoskeletal system of the hypercholesterolemic left ventricle. Previous studies suggested that hyperlipidemia, especially hypercholesterolemia, leads to the augmentation of oxidative and nitrosative stress and enhanced proinflammatory cytokine production, consequently contributing to cardiac and endothelial dysfunction [3,4,16]. The related oxidative damage possibly involves contractile and cytoskeletal proteins and, hence, likely contributes to contractile impairment. Nevertheless, in this study, quantitative changes in myofibrillar proteins were also demonstrated which might also be responsible for the direct cardiac effects of hypercholesterolemia.

A deeper analysis of the whole, unfiltered left ventricular proteome turned out that hypercholesterolemia negatively influenced many protein components of the mitochondrial respiratory chain system in the heart. Although the individual expression of the majority of the proteins in the enriched protein sets failed to meet the criteria of significant change, as a group their coordinated downregulation was significant. Impaired mitochondrial function is

implicated in the adverse cardiac effects of hypercholesterolemia [105]. Mitochondrial cholesterol accumulation interferes with the normal function of mitochondrial membrane proteins and transporters [106], as well as disturbs myocardial ATP synthesis and bioenergetics [62], which might be associated with the downregulation of the elements of the respiratory chain complex. However, further proof-of-concept studies are recommended to confirm the causal role of the proteins or network of proteins identified in our study in diastolic dysfunction in the heart using targeted proteomics or immunochemical methods.

8.3 The attenuated cardioprotective effect of ischemic preconditioning upon hypercholesterolemia is correlated with diminished miR-125b-1-3p induction

IPre is one of the most powerful endogenous cardioprotective approaches as it markedly enhances the ability of the heart to withstand ischemic injury [107]. Although several signaling pathways have been implicated in IPre, the exact mechanism is still not entirely clear. Previous findings suggested that miR-125b-1-3p upregulation might be an important mediator of IPre-induced cardioprotection [17, 21]. In our study, the application of IPre in the presence of hypercholesterolemia failed to upregulate miR-125b-1-3p expression as compared to I/R. This is in line with previous reports demonstrating that hypercholesterolemia abolished the infarct size-limiting effect conferred by IPre [49, 57, 108, 109]. Additionally, hypercholesterolemia seems to alter cardiac miRNA expression profile, which is possibly associated with the alleviated protective effect of ischemic conditioning. For instance, the downregulation of miR-25 mediates oxidative/nitrosative stress in the myocardium upon diet-induced hypercholesterolemia in rats [32]. Moreover, cardiac miRNA interactome analysis of hypercholesterolemic rats revealed that mRNA targets of the differentially expressed miRNAs are likely associated with hypercholesterolemia-induced cardiac dysfunction [110]. Although several studies revealed relationships between IPre and cardiac miRNA levels in normocholesterolemic subjects, this is the first demonstration that hypercholesterolemia influences miRNA expression changes induced by IPre.

Upregulation of miR-125b-1-3p is considered an adaptive response of IPre, however, the mRNA targets in the myocardium are still not clear. The cytoprotective role of the miR-125b family members possibly comprises the alleviation of oxidative damage ensuing apoptosis of cardiomyocytes [22, 111, 112]. Nevertheless, miR-125b-1-3p expression is enhanced by nuclear factor erythroid 2-related factor 2 (NRF2) protein. Acting as a transcription factor, NRF2 binds to a cis-regulatory sequence, called antioxidant response element, in the promoter region of the miR-125b-1 gene, thereby enhancing miR-125b-1

expression level [113, 114]. Additionally, there are existing data in the literature about the cardioprotective role of NRF2 through the modulation of oxidative stress [115] which further supports a positive effect of miR-125b-1-3p upregulation to alleviate cardiac I/R injury. Our study suggests that the upregulation of miR-125b-1-3p in response to IPre may be an important element in the cardioprotective mechanism, however, further studies need to confirm a direct causative relationship.

8.4 Electromyostimulation treatment seems to mitigate I/R injury on ex vivo perfused heart – the possible role of myokines

EMS has been long utilized to either supplement or substitute muscle strengthening in several rehabilitation settings [116]. Although inferior to conventional training, nevertheless, the encouragement of muscle strength and improvements in exercise capacity make EMS a feasible alternative for exercise, therefore patients can start to perform more daily activities [117, 118]. To test whether EMS could be a feasible alternative for cardiac conditioning, an ex vivo heart perfusion method was applied. In our perfusion model, LDH and CK-MB release during the reperfusion was significantly decreased in the ex vivo perfused hearts of animals that received EMS. However, EMS before global I/R failed to significantly decrease the infarcted area. Our results suggest that despite the lack of significant infarct size reduction EMS treatment might initiate different cardioprotective mechanisms which were partially retained during the ex vivo heart perfusion. The effect of electrical stimulation as a cardiac remote preconditioning maneuver was tested previously with different experimental setups. In an early study, the combination of remote ischemic preconditioning and electrical stimulation of the gastrocnemius muscle conferred cardioprotection in a rabbit model of in vivo I/R [119]. Interestingly, the same approach failed to enhance the efficiency of preconditioning of human patients who underwent coronary angioplasty [120]. Nevertheless, previous research mainly focused on the direct electrical stimulation of peripheral nerves rather than the muscle contraction-mediated preconditioning effects. Targeted electrical stimulation of peripheral nerves of the limbs straight before I/R mitigated myocardial infarct size and improved the post-ischemic cardiac performance in rodents. [71, 121-123].

Several hundred cytokines and oligopeptides, termed myokines, are produced and released by muscle in response to muscle contractions [124]. These molecules may act as mediators which link muscle exercise to the whole body physiology, nevertheless, the majority of myokines were also shown to exert protection against ischemia. Based on our findings, the applied EMS protocol increased *Il6* mRNA, but not IL-6 protein content in the

gastrocnemius muscle. In the skeletal muscle, the exercise-induced release of IL-6 seems to exert anti-inflammatory actions [125] and could act as one of the major mediators of exercise-induced cardioprotection against myocardial I/R injury [126]. Another myokine, FSTL1 was the only myokine upregulated both in mRNA and protein levels in the muscle, without any change in the bloodstream upon EMS. Exercise-induced FSTL1 expression has been implicated with improved endothelial cell function, mitigation of myocardial ischemic injury, and revascularization in ischemic heart [127-129]. Additionally, without changes in mRNA content, EMS induced an increment in the protein levels of Decorin, Irisin, Myonectin, and Myoglobin, respectively, after three days of the stimulation period. However, none of the selected myokines showed altered levels in the serum of EMS-treated animals. To the best of our knowledge, Decorin, Irisin, and Myonectin levels were not yet investigated upon EMS treatment and the disclosure of their paracrine and endocrine functions might provide great value to the better understanding of the systemic effects of involuntary contractions of the skeletal muscles elicited by electrical stimulations. Notably, previous studies suggested the importance of intact peripheral nerves for triggering electrical stimulation-driven cardioprotection. However, the produced myokines might overcome the necessity of damaged peripheral sensory nerves which further strengthens their prominent role in the possible protection of the myocardium during the application of EMS [130].

8.5 Limitations and future perspectives

Similar to all experimental investigations, our study is not without limitations. First of all, since we have applied a rodent model of hypercholesterolemia in our present study, further confirmation of our results is urged in the future in humans due to potential species-dependent differences in the cardiac effects of hypercholesterolemia. Moreover, we applied a shotgun proteomic analysis in the present study, which may have higher limits of detection than targeted approaches; however, it provides the possibility to obtain quantitative information about as many proteins as possible. Our study and the applied protocols were focused on the detection of differences in the expression of proteins, and the identification of possible changes in posttranslational modifications of proteins was outside of the scope of the present study.

We have analyzed microRNA at a single time-point, i.e. at 2 h of reperfusion. This may limit proper interpretation of early molecular changes in the course of cardioprotection, therefore assaying miR-125b-1-3p and triggers for miR-125-b-1-3p induction at earlier time-points in future studies may have some added value. Although we have demonstrated a

correlation between miR-125b-1-3p expression and cardioprotection of IPre, there is limited information about the putative mRNA targets and biological role of miR-125b-1-3p against I/R injury. Despite these limitations, the present data might provide valuable information regarding the effect of experimental hypercholesterolemia on some aspects of the potential molecular mechanism of ischemic preconditioning.

To test the potential preconditioning effect of EMS, we applied an ex vivo heart perfusion system, where global ischemia was induced. This approach is different from the stress during in vivo occurring I/R. As known, ischemic preconditioning triggered cardioprotection of the second window of preconditioning may be less robust than that of the first window, which requires further consideration of the exact time of testing EMS. Despite there being clear evidence of the beneficial effect of EMS measuring secondary endpoints, like the incidence of myocardial arrhythmias might also be helpful to determine the preconditioning effect of EMS.

Additionally, myokine levels were only measured after one day of the last EMS session, which could also hide changes upon EMS due to the fast turnover of circulating proteins. Nevertheless, more robust changes in circulating myokine levels might happen with the involvement of greater muscle mass. Therefore, different sampling times for serum myokine measurements as well as assessment of previously described myokine-evoked molecular changes in the heart might elucidate the conditional role of several myokines in EMS-induced cardioprotection.

9 Conclusions

In this thesis, we focused (i) on the underlying molecular mechanism leading to the direct adverse cardiac effects on hypercholesterolemia and (ii) the application of electrical stimuli provoked involuntary contraction of the skeletal muscle to trigger remote cardioprotection.

Based on the findings of the present thesis we can conclude that hypercholesterolemia induced quantitative changes in the left ventricular proteome, affecting both the contractile and cytoskeletal apparatus as well as the mitochondrial respiratory chain system. These alterations might provide a feasible explanation for the mild cardiac dysfunction observed in hypercholesterolemia. Nevertheless, these results of our network and enrichment analyses might contribute to a better understanding and development of further therapeutic approaches mitigating cardiac dysfunction in the presence of metabolic risk factors.

As suggested previously, IPre-associated miR-125b-1-3p upregulation is an adaptive response to prevent I/R-induced cellular damage. However, hypercholesterolemia attenuates IPre-induced miR-125b-1-3p upregulation, which is likely associated with the loss of cardioprotection. Therefore modulation of cardiac miR-125b-1-3p could be a feasible target for cardioprotection even in cases when risk factors and comorbidities are present; however, this hypothesis remained to be confirmed in future experimental studies.

Despite the lack of significant infarct size reduction, EMS seems to influence the course of cellular damage due to I/R in normocholesterolemic animals. We conclude that electrical stimulation of the skeletal muscle might provide an alternative remote preconditioning approach; nevertheless, further optimization of the protocol is warranted before deeper investigations of the method. Still, our data might serve as the basis of future research. Similarly to voluntary exercise, myokines might be also involved in the cardioprotective effects of EMS, however, verification of their mechanistic role remains for the scope of future studies.

10 Acknowledgment

Our studies were supported by the grants OTKA-NKFIH (K115990), EFOP 3.6.2-16-2017-00006, GINOP 2.3.2-15-2016-00006, GINOP-2.3.2-15-2016-00040 and TKP2021-EGA-32 project. Furthermore, the present work was supported by the ÚNKP-19-3-SZTE-269 grant provided by the New National Excellence Program of the Ministry for Innovation and Technology.

I would like to express my sincere gratitude to Prof. Dr. László Dux for providing me with the possibility to join the Department of Biochemistry.

I owe my greatest gratitude to my supervisors, Dr. Tamás Csont and Dr. Csaba Csonka for their scientific guidance, encouragement, and loads of helpful suggestions through the past years in both professional and personal aspects.

I am also thankful to the senior members of our research group, Dr. Márton Pipicz, Dr. Márta Sárközy, and Dr. Gergő Szűcs for their practical suggestions and advice.

This endeavor would not have been possible without the invaluable contribution of Dr. Renáta Molnár-Gáspár as well as my fellow Ph.D. students, Dr. Andrea Apjok-Sója, Dr. Virág Demján, and Petra Diószegi.

I owe a special thanks to all the members of the Department of Biochemistry especially Atina Čolić, Dóra Csóré, Éva Plechl, Réka Somogyi, Ildikó Engi, Tünde Bodnár, Imre Ocsovszki, and József Papp for their technical support and willingness to help me anytime. I am also grateful to my former undergraduate students, Dr. Réka Marik and Dr. Kamilla Nagy for their enthusiasm during our common scientific work.

I would like to thank our cooperation partners Dr. László Bodai and Dr. Nóra Zsindely to make us possible to perform miRNA sequencing, also for Dr. Zoltán Szabó and Bella Bruszel for the quantitative proteomics.

I am deeply indebted to my mentor during my undergraduate years, Dr. Attila Borics whom I learned the scientific perspective.

I could not have undertaken this journey without the emotional support of my mother, my father, my mother's husband Árpi, my sister Tina, my brothers Patrik, Oli, and Levi, as well my best friend Tomi. Above all, words cannot express my gratitude to my wife, Anikó; her never-ending love and enormous effort to provide stable background to our little daughter have always kept my spirits and motivation high during this process.

11 References

1. Timmis, A.; Vardas, P.; Townsend, N.; Torbica, A.; Katus, H.; De Smedt, D.; Gale, C. P.; Maggioni, A. P.; Petersen, S. E.; Huculeci, R.; Kazakiewicz, D.; de Benito Rubio, V.; Ignatiuk, B.; Raisi-Estabragh, Z.; Pawlak, A.; Karagiannidis, E.; Treskes, R.; Gaita, D.; Beltrame, J. F.; McConnachie, A.; Bardinet, I.; Graham, I.; Flather, M.; Elliott, P.; Mossialos, E. A.; Weidinger, F.; Achenbach, S.; European Society of, C.; on behalf of the Atlas Writing, G., European Society of Cardiology: cardiovascular disease statistics 2021. *Eur. Heart J.* **2022**, ehab892.
2. Timmis, A.; Townsend, N.; Gale, C. P.; Torbica, A.; Lettino, M.; Petersen, S. E.; Mossialos, E. A.; Maggioni, A. P.; Kazakiewicz, D.; May, H. T.; De Smedt, D.; Flather, M.; Zuhlke, L.; Beltrame, J. F.; Huculeci, R.; Tavazzi, L.; Hindricks, G.; Bax, J.; Casadei, B.; Achenbach, S.; Wright, L.; Vardas, P.; European Society of, C., European Society of Cardiology: Cardiovascular Disease Statistics 2019. *Eur. Heart J.* **2020,** 41, (1), 12-85.
3. Reed, G. W.; Rossi, J. E.; Cannon, C. P., Acute myocardial infarction. *The Lancet* **2017,** 389, (10065), 197-210.
4. Frank, A.; Bonney, M.; Bonney, S.; Weitzel, L.; Koeppen, M.; Eckle, T., Myocardial ischemia reperfusion injury: from basic science to clinical bedside. *Seminars in cardiothoracic and vascular anesthesia* **2012,** 16, (3), 123-32.
5. Hausenloy, D. J.; Yellon, D. M., Myocardial ischemia-reperfusion injury: a neglected therapeutic target. *The Journal of Clinical Investigation* **2013,** 123, (1), 92-100.
6. Heusch, G., Myocardial ischaemia–reperfusion injury and cardioprotection in perspective. *Nature Reviews Cardiology* **2020,** 17, (12), 773-789.
7. Murry, C. E.; Jennings, R. B.; Reimer, K. A., Preconditioning with ischemia: a delay of lethal cell injury in ischemic myocardium. *Circulation* **1986,** 74, (5), 1124-1136.
8. Hausenloy, D. J.; Yellon, D. M., Ischaemic conditioning and reperfusion injury. *Nature reviews. Cardiology* **2016,** 13, (4), 193-209.
9. Perrelli, M. G.; Pagliaro, P.; Penna, C., Ischemia/reperfusion injury and cardioprotective mechanisms: Role of mitochondria and reactive oxygen species. *World journal of cardiology* **2011,** 3, (6), 186-200.
10. García-Niño, W. R.; Zazueta, C.; Buelna-Chontal, M.; Silva-Palacios, A., Mitochondrial Quality Control in Cardiac-Conditioning Strategies against Ischemia-Reperfusion Injury. *Life* **2021,** 11, (11), 1123.
11. Bartel, D. P., MicroRNAs: target recognition and regulatory functions. *Cell* **2009,** 136, (2), 215-33.
12. Dong, S.; Cheng, Y.; Yang, J.; Li, J.; Liu, X.; Wang, X.; Wang, D.; Krall, T. J.; Delphin, E. S.; Zhang, C., MicroRNA expression signature and the role of microRNA-21 in the early phase of acute myocardial infarction. *J Biol Chem* **2009,** 284, (43), 29514-29525.
13. Duan, X.; Ji, B.; Wang, X.; Liu, J.; Zheng, Z.; Long, C.; Tang, Y.; Hu, S., Expression of microRNA-1 and microRNA-21 in different protocols of ischemic conditioning in an isolated rat heart model. *Cardiology* **2012,** 122, (1), 36-43.
14. Cheng, Y.; Zhu, P.; Yang, J.; Liu, X.; Dong, S.; Wang, X.; Chun, B.; Zhuang, J.; Zhang, C., Ischaemic preconditioning-regulated miR-21 protects heart against ischaemia/reperfusion injury via anti-apoptosis through its target PDCD4. *Cardiovascular Research* **2010,** 87, (3), 431-439.

15. Pan, Y. L.; Han, Z. Y.; He, S. F.; Yang, W.; Cheng, J.; Zhang, Y.; Chen, Z. W., miR-133b-5p contributes to hypoxic preconditioning-mediated cardioprotection by inhibiting the activation of caspase-8 and caspase-3 in cardiomyocytes. *Molecular medicine reports* **2018,** 17, (5), 7097-7104.
16. Wang, X.; Zhu, H.; Zhang, X.; Liu, Y.; Chen, J.; Medvedovic, M.; Li, H.; Weiss, M. J.; Ren, X.; Fan, G.-C., Loss of the miR-144/451 cluster impairs ischaemic preconditioning-mediated cardioprotection by targeting Rac-1. *Cardiovascular Research* **2012,** 94, (2), 379-390.
17. Wang, Y.; Tan, J.; Wang, L.; Pei, G.; Cheng, H.; Zhang, Q.; Wang, S.; He, C.; Fu, C.; Wei, Q., MiR-125 Family in Cardiovascular and Cerebrovascular Diseases. *Front Cell Dev Biol* **2021,** 9, 799049.
18. Chao, C. T.; Yeh, H. Y.; Yuan, T. H.; Chiang, C. K.; Chen, H. W., MicroRNA-125b in vascular diseases: An updated systematic review of pathogenetic implications and clinical applications. *J Cell Mol Med* **2019,** 23, (9), 5884-5894.
19. Yang, J.-S.; Phillips, M. D.; Betel, D.; Mu, P.; Ventura, A.; Siepel, A. C.; Chen, K. C.; Lai, E. C., Widespread regulatory activity of vertebrate microRNA* species. *RNA* **2011,** 17, (2), 312-326.
20. Ohanian, M.; Humphreys, D. T.; Anderson, E.; Preiss, T.; Fatkin, D., A heterozygous variant in the human cardiac miR-133 gene, MIR133A2, alters miRNA duplex processing and strand abundance. *BMC Genet.* **2013,** 14, 18.
21. Varga, Z. V.; Zvara, A.; Faragó, N.; Kocsis, G. F.; Pipicz, M.; Gáspár, R.; Bencsik, P.; Görbe, A.; Csonka, C.; Puskás, L. G.; Thum, T.; Csont, T.; Ferdinandy, P., MicroRNAs associated with ischemia-reperfusion injury and cardioprotection by ischemic pre- and postconditioning: protectomiRs. *American Journal of Physiology. Heart and Circulatory Physiology* **2014,** 307, (2), H216-227.
22. Wang, X.; Ha, T.; Zou, J.; Ren, D.; Liu, L.; Zhang, X.; Kalbfleisch, J.; Gao, X.; Williams, D.; Li, C., MicroRNA-125b protects against myocardial ischaemia/reperfusion injury via targeting p53-mediated apoptotic signalling and TRAF6. *Cardiovascular Research* **2014,** 102, (3), 385-395.
23. Xiao, C.; Wang, K.; Xu, Y.; Hu, H.; Zhang, N.; Wang, Y.; Zhong, Z.; Zhao, J.; Li, Q.; Zhu, D.; Ke, C.; Zhong, S.; Wu, X.; Yu, H.; Zhu, W.; Chen, J.; Zhang, J.; Wang, J. a.; Hu, X., Transplanted Mesenchymal Stem Cells Reduce Autophagic Flux in Infarcted Hearts via the Exosomal Transfer of miR-125b. *Circ Res* **2018,** 123, (5), 564-578.
24. Zhu, L.-P.; Tian, T.; Wang, J.-Y.; He, J.-N.; Chen, T.; Pan, M.; Xu, L.; Zhang, H.-X.; Qiu, X.-T.; Li, C.-C.; Wang, K.-K.; Shen, H.; Zhang, G.-G.; Bai, Y.-P., Hypoxia-elicited mesenchymal stem cell-derived exosomes facilitates cardiac repair through miR-125b-mediated prevention of cell death in myocardial infarction. *Theranostics* **2018,** 8, (22), 6163-6177.
25. Virani, S. S.; Alonso, A.; Aparicio, H. J.; Benjamin, E. J.; Bittencourt, M. S.; Callaway, C. W.; Carson, A. P.; Chamberlain, A. M.; Cheng, S.; Delling, F. N.; Elkind, M. S. V.; Evenson, K. R.; Ferguson, J. F.; Gupta, D. K.; Khan, S. S.; Kissela, B. M.; Knutson, K. L.; Lee, C. D.; Lewis, T. T.; Liu, J.; Loop, M. S.; Lutsey, P. L.; Ma, J.; Mackey, J.; Martin, S. S.; Matchar, D. B.; Mussolino, M. E.; Navaneethan, S. D.; Perak, A. M.; Roth, G. A.; Samad, Z.; Satou, G. M.; Schroeder, E. B.; Shah, S. H.; Shay, C. M.; Stokes, A.; VanWagner, L. B.; Wang, N. Y.; Tsao, C. W., Heart Disease and Stroke Statistics-2021 Update: A Report From the American Heart Association. *Circulation* **2021,** 143, (8), e254-e743.
26. Cordain, L.; Eaton, S. B.; Sebastian, A.; Mann, N.; Lindeberg, S.; Watkins, B. A.; O'Keefe, J. H.; Brand-Miller, J., Origins and evolution of the Western diet: health

implications for the 21st century. *The American Journal of Clinical Nutrition* **2005,** 81, (2), 341-354.

27. Hu, P.; Dharmayat, K. I.; Stevens, C. A. T.; Sharabiani, M. T. A.; Jones, R. S.; Watts, G. F.; Genest, J.; Ray, K. K.; Vallejo-Vaz, A. J., Prevalence of Familial Hypercholesterolemia Among the General Population and Patients With Atherosclerotic Cardiovascular Disease: A Systematic Review and Meta-Analysis. *Circulation* **2020,** 141, (22), 1742-1759.
28. Danese, M. D.; Sidelnikov, E.; Kutikova, L., The prevalence, low-density lipoprotein cholesterol levels, and treatment of patients at very high risk of cardiovascular events in the United Kingdom: a cross-sectional study. *Current medical research and opinion* **2018,** 34, (8), 1441-1447.
29. Csonka, C.; Baranyai, T.; Tiszlavicz, L.; Fébel, H.; Szűcs, G.; Varga, Z. V.; Sárközy, M.; Puskás, L. G.; Antal, O.; Siska, A.; Földesi, I.; Ferdinandy, P.; Czakó, L.; Csont, T., Isolated hypercholesterolemia leads to steatosis in the liver without affecting the pancreas. *Lipids Health Dis* **2017,** 16, (1), 144.
30. Elustondo, P.; Martin, L. A.; Karten, B., Mitochondrial cholesterol import. *Biochimica et biophysica acta. Molecular and cell biology of lipids* **2017,** 1862, (1), 90-101.
31. Csont, T.; Bereczki, E.; Bencsik, P.; Fodor, G.; Görbe, A.; Zvara, A.; Csonka, C.; Puskás, L. G.; Sántha, M.; Ferdinandy, P., Hypercholesterolemia increases myocardial oxidative and nitrosative stress thereby leading to cardiac dysfunction in apoB-100 transgenic mice. *Cardiovascular Research* **2007,** 76, (1), 100-109.
32. Varga, Z. V.; Kupai, K.; Szűcs, G.; Gáspár, R.; Pálóczi, J.; Faragó, N.; Zvara, A.; Puskás, L. G.; Rázga, Z.; Tiszlavicz, L.; Bencsik, P.; Görbe, A.; Csonka, C.; Ferdinandy, P.; Csont, T., MicroRNA-25-dependent up-regulation of NADPH oxidase 4 (NOX4) mediates hypercholesterolemia-induced oxidative/nitrative stress and subsequent dysfunction in the heart. *J Mol Cell Cardiol* **2013,** 62, 111-121.
33. McCommis, K. S.; McGee, A. M.; Laughlin, M. H.; Bowles, D. K.; Baines, C. P., Hypercholesterolemia increases mitochondrial oxidative stress and enhances the MPT response in the porcine myocardium: beneficial effects of chronic exercise. *American journal of physiology. Regulatory, integrative and comparative physiology* **2011,** 301, (5), R1250-8.
34. Talini, E.; Di Bello, V.; Bianchi, C.; Palagi, C.; Delle Donne, M. G.; Penno, G.; Nardi, C.; Canale, M. L.; Del Prato, S.; Mariani, M.; Miccoli, R., Early impairment of left ventricular function in hypercholesterolemia and its reversibility after short term treatment with rosuvastatin A preliminary echocardiographic study. *Atherosclerosis* **2008,** 197, (1), 346-54.
35. Huang, Y.; Walker, K. E.; Hanley, F.; Narula, J.; Houser, S. R.; Tulenko, T. N., Cardiac systolic and diastolic dysfunction after a cholesterol-rich diet. *Circulation* **2004,** 109, (1), 97-102.
36. Li, D.; Zhang, Y.; Ma, J.; Ling, W.; Xia, M., Adenosine monophosphate activated protein kinase regulates ABCG1-mediated oxysterol efflux from endothelial cells and protects against hypercholesterolemia-induced endothelial dysfunction. *Arterioscler Thromb Vasc Biol* **2010,** 30, (7), 1354-62.
37. Sozen, E.; Yazgan, B.; Sahin, A.; Ince, U.; Ozer, N. K., High Cholesterol Diet-Induced Changes in Oxysterol and Scavenger Receptor Levels in Heart Tissue. *Oxid Med Cell Longev* **2018,** 2018, 8520746.
38. Han, Q.; Yeung, S. C.; Ip, M. S. M.; Mak, J. C. W., Dysregulation of cardiac lipid parameters in high-fat high-cholesterol diet-induced rat model. *Lipids Health Dis* **2018,** 17, (1), 255.

39. Canton, M.; Menazza, S.; Sheeran, F. L.; Polverino de Laureto, P.; Di Lisa, F.; Pepe, S., Oxidation of myofibrillar proteins in human heart failure. *J Am Coll Cardiol* **2011,** 57, (3), 300-9.
40. Csonka, C.; Murlasits, Z.; Ferdinandy, P.; Csont, T., Ischemic stress adaptation of the myocardium in the disease states: Role of hyperlipidemia. In *Advances in Cardiomyocyte Research*, Nánási, P., Ed. Transworld Research Network: Kerala, India, 2009; pp 245-265.
41. Varga, Z. V.; Kupai, K.; Szűcs, G.; Gáspár, R.; Pálóczi, J.; Faragó, N.; Zvara, A.; Puskás, L. G.; Rázga, Z.; Tiszlavicz, L.; Bencsik, P.; Görbe, A.; Csonka, C.; Ferdinandy, P.; Csont, T., MicroRNA-25-dependent up-regulation of NADPH oxidase 4 (NOX4) mediates hypercholesterolemia-induced oxidative/nitrative stress and subsequent dysfunction in the heart. *J Mol Cell Cardiol* **2013,** 62, 111-21.
42. Saracoglu, E.; Kılıç, S.; Vuruşkan, E.; Düzen, I.; Çekici, Y.; Kuzu, Z.; Yıldırım, A.; Küçükosmanoğlu, M.; Çetin, M., Prediction of subtle left ventricular systolic dysfunction in homozygous and heterozygous familial hypercholesterolemia: Genetic analyses and speckle tracking echocardiography study. *Echocardiography (Mount Kisco, N.Y.)* **2018,** 35, (9), 1289-1299.
43. Muthuramu, I.; Mishra, M.; Aboumsallem, J. P.; Postnov, A.; Gheysens, O.; De Geest, B., Cholesterol lowering attenuates pressure overload-induced heart failure in mice with mild hypercholesterolemia. *Aging (Albany NY)* **2019,** 11, (17), 6872-6891.
44. Rubinstein, J.; Pelosi, A.; Vedre, A.; Kotaru, P.; Abela, G. S., Hypercholesterolemia and myocardial function evaluated via tissue doppler imaging. *Cardiovascular ultrasound* **2009,** 7, 56.
45. Yao, Y. S.; Li, T. D.; Zeng, Z. H., Mechanisms underlying direct actions of hyperlipidemia on myocardium: an updated review. *Lipids Health Dis* **2020,** 19, (1), 23-23.
46. Luo, T. Y.; Su, M. J.; Yang, Y. F.; Liu, Y. B.; Liang, H. C.; Wu, C. C.; Lee, Y. T., Effect of hypercholesterolemia on myocardial function in New Zealand white rabbits. *J Biomed Sci* **2004,** 11, (6), 829-37.
47. Pluijmert, N. J.; den Haan, M. C.; van Zuylen, V. L.; Steendijk, P.; de Boer, H. C.; van Zonneveld, A. J.; Fibbe, W. E.; Schalij, M. J.; Quax, P. H. A.; Atsma, D. E., Hypercholesterolemia affects cardiac function, infarct size and inflammation in APOE*3-Leiden mice following myocardial ischemia-reperfusion injury. *PLoS One* **2019,** 14, (6), e0217582-e0217582.
48. Ungi, I.; Ungi, T.; Ruzsa, Z.; Nagy, E.; Zimmermann, Z.; Csont, T.; Ferdinandy, P., Hypercholesterolemia attenuates the anti-ischemic effect of preconditioning during coronary angioplasty. *Chest* **2005,** 128, (3), 1623-1628.
49. Ueda, Y.; Kitakaze, M.; Komamura, K.; Minamino, T.; Asanuma, H.; Sato, H.; Kuzuya, T.; Takeda, H.; Hori, M., Pravastatin restored the infarct size-limiting effect of ischemic preconditioning blunted by hypercholesterolemia in the rabbit model of myocardial infarction. *J. Am. Coll. Cardiol.* **1999,** 34, (7), 2120-2125.
50. Szilvassy, Z.; Ferdinandy, P.; Szilvassy, J.; Nagy, I.; Karcsu, S.; Lonovics, J.; Dux, L.; Koltai, M., The loss of pacing-induced preconditioning in atherosclerotic rabbits: role of hypercholesterolaemia. *J Mol Cell Cardiol* **1995,** 27, (12), 2559-2569.
51. Wu, N.; Zhang, X.; Jia, P.; Jia, D., Hypercholesterolemia abrogates the protective effect of ischemic postconditioning by induction of apoptosis and impairment of activation of reperfusion injury salvage kinase pathway. *Biochemical and Biophysical Research Communications* **2015,** 458, (1), 148-153.
52. Kupai, K.; Csonka, C.; Fekete, V.; Odendaal, L.; Rooyen, J. v.; Marais, D. W.; Csont, T.; Ferdinandy, P., Cholesterol diet-induced hyperlipidemia impairs the

cardioprotective effect of postconditioning: role of peroxynitrite. *American Journal of Physiology-Heart and Circulatory Physiology* **2009,** 297, (5), H1729-H1735.
53. Ma, L. L.; Kong, F. J.; Guo, J. J.; Zhu, J. B.; Shi, H. T.; Li, Y.; Sun, R. H.; Ge, J. B., Hypercholesterolemia Abrogates Remote Ischemic Preconditioning-Induced Cardioprotection: Role of Reperfusion Injury Salvage Kinase Signals. *Shock (Augusta, Ga.)* **2017,** 47, (3), 363-369.
54. Csonka, C.; Sárközy, M.; Pipicz, M.; Dux, L.; Csont, T., Modulation of Hypercholesterolemia-Induced Oxidative/Nitrative Stress in the Heart. *Oxid Med Cell Longev* **2016,** 2016, 3863726.
55. Landim, M. B.; Dourado, P. M.; Casella-Filho, A.; Chagas, A. C.; da-Luz, P. L., High plasma concentrations of asymmetric dimethylarginine inhibit ischemic cardioprotection in hypercholesterolemic rats. *Brazilian journal of medical and biological research = Revista brasileira de pesquisas medicas e biologicas* **2013,** 46, (5), 454-9.
56. Tang, X.-L.; Takano, H.; Xuan, Y.-T.; Sato, H.; Kodani, E.; Dawn, B.; Zhu, Y.; Shirk, G.; Wu, W.-J.; Bolli, R., Hypercholesterolemia Abrogates Late Preconditioning via a Tetrahydrobiopterin-Dependent Mechanism in Conscious Rabbits. *Circulation* **2005,** 112, (14), 2149-2156.
57. Giricz, Z.; Lalu, M. M.; Csonka, C.; Bencsik, P.; Schulz, R.; Ferdinandy, P., Hyperlipidemia attenuates the infarct size-limiting effect of ischemic preconditioning: role of matrix metalloproteinase-2 inhibition. *J. Pharmacol. Exp. Ther.* **2006,** 316, (1), 154-161.
58. Kocsis, G. F.; Csont, T.; Varga-Orvos, Z.; Puskas, L. G.; Murlasits, Z.; Ferdinandy, P., Expression of genes related to oxidative/nitrosative stress in mouse hearts: effect of preconditioning and cholesterol diet. *Med. Sci. Monit.* **2010,** 16, (1), BR32-39.
59. Giricz, Z.; Koncsos, G.; Rajtík, T.; Varga, Z. V.; Baranyai, T.; Csonka, C.; Szobi, A.; Adameová, A.; Gottlieb, R. A.; Ferdinandy, P., Hypercholesterolemia downregulates autophagy in the rat heart. *Lipids Health Dis* **2017,** 16, (1), 60.
60. Wang, T. D.; Chen, W. J.; Mau, T. J.; Lin, J. W.; Lin, W. W.; Lee, Y. T., Attenuation of increased myocardial ischaemia-reperfusion injury conferred by hypercholesterolaemia through pharmacological inhibition of the caspase-1 cascade. *Br J Pharmacol* **2003,** 138, (2), 291-300.
61. Dost, T.; Cohen, M. V.; Downey, J. M., Redox signaling triggers protection during the reperfusion rather than the ischemic phase of preconditioning. *Basic Res Cardiol* **2008,** 103, (4), 378-84.
62. Csonka, C.; Kupai, K.; Bencsik, P.; Görbe, A.; Pálóczi, J.; Zvara, A.; Puskás, L. G.; Csont, T.; Ferdinandy, P., Cholesterol-enriched diet inhibits cardioprotection by ATP-sensitive K+ channel activators cromakalim and diazoxide. *American Journal of Physiology. Heart and Circulatory Physiology* **2014,** 306, (3), H405-413.
63. Ferko, M.; Farkasova, V.; Jasova, M.; Kancirova, I.; Ravingerova, T.; Duris Adameova, A.; Andelova, N.; Waczulikova, I., Hypercholesterolemia antagonized heart adaptation and functional remodeling of the mitochondria observed in acute diabetes mellitus subjected to ischemia/reperfusion injury. *Journal of physiology and pharmacology : an official journal of the Polish Physiological Society* **2018,** 69, (5).
64. Pedersen, B. K., The Physiology of Optimizing Health with a Focus on Exercise as Medicine. *Annual review of physiology* **2019,** 81, 607-627.
65. Kern, H.; Carraro, U., Home-Based Functional Electrical Stimulation for Long-Term Denervated Human Muscle: History, Basics, Results and Perspectives of the Vienna Rehabilitation Strategy. *European journal of translational myology* **2014,** 24, (1), 3296.

66. de Oliveira, T. M. D.; Felício, D. C.; Filho, J. E.; Durigan, J. L. Q.; Fonseca, D. S.; José, A.; Oliveira, C. C.; Malaguti, C., Effects of whole-body electromyostimulation on function, muscle mass, strength, social participation, and falls-efficacy in older people: A randomized trial protocol. *PLoS One* **2021,** 16, (1), e0245809.
67. McGregor, G.; Ennis, S.; Powell, R.; Hamborg, T.; Raymond, N. T.; Owen, W.; Aldridge, N.; Evans, G.; Goodby, J.; Hewins, S.; Banerjee, P.; Krishnan, N. S.; Ting, S. M. S.; Zehnder, D., Feasibility and effects of intra-dialytic low-frequency electrical muscle stimulation and cycle training: A pilot randomized controlled trial. *PLoS One* **2018,** 13, (7), e0200354.
68. Palau, P.; Domínguez, E.; López, L.; Ramón, J. M.; Heredia, R.; González, J.; Santas, E.; Bodí, V.; Miñana, G.; Valero, E.; Mollar, A.; Bertomeu González, V.; Chorro, F. J.; Sanchis, J.; Lupón, J.; Bayés-Genís, A.; Núñez, J., Inspiratory Muscle Training and Functional Electrical Stimulation for Treatment of Heart Failure With Preserved Ejection Fraction: The TRAINING-HF Trial. *Revista espanola de cardiologia (English ed.)* **2019,** 72, (4), 288-297.
69. van Buuren, F.; Mellwig, K. P.; Fründ, A.; Bogunovic, N.; Oldenburg, O.; Kottmann, T.; Wagner, O.; Dahm, J. B.; Horstkotte, D.; Fritzsche, D., [Electrical myostimulation: improvement of quality of life, oxygen uptake and left ventricular function in chronic heart failure]. *Die Rehabilitation* **2014,** 53, (5), 321-6.
70. Redington, K. L.; Disenhouse, T.; Strantzas, S. C.; Gladstone, R.; Wei, C.; Tropak, M. B.; Dai, X.; Manlhiot, C.; Li, J.; Redington, A. N., Remote cardioprotection by direct peripheral nerve stimulation and topical capsaicin is mediated by circulating humoral factors. *Basic Res Cardiol* **2012,** 107, (2), 241.
71. Dong, J. H.; Liu, Y. X.; Zhao, J.; Ma, H. J.; Guo, S. M.; He, R. R., High-frequency electrical stimulation of femoral nerve reduces infarct size following myocardial ischemia-reperfusion in rats. *Sheng li xue bao : [Acta physiologica Sinica]* **2004,** 56, (5), 620-4.
72. Matsuo, K.; Yoneki, K.; Tatsuki, H.; Mibu, K.; Furuzono, K.; Kobayashi, K.; Yasuda, S.; Tamiya, S., Effect of Electrical Muscle Stimulation on the Reduction of Muscle Volume Loss in Acute Heart Failure Patients. *International heart journal* **2022,** 63, (6), 1141-1149.
73. Poltavskaya, M.; Sviridenko, V.; Giverts, I.; Patchenskaya, I.; Kozlovskaya, I.; Tomilovskaya, E.; Veliyev, G. O.; Andreev, D.; Syrkin, A.; Saner, H., In-hospital electrical muscle stimulation for patients early after heart failure decompensation: results from a prospective randomised controlled pilot trial. *Open heart* **2022,** 9, (2), e001965.
74. Powers, S. K., Exercise: Teaching myocytes new tricks. *J Appl Physiol (1985)* **2017,** 123, (2), 460-472.
75. Lee, J. H.; Jun, H.-S., Role of Myokines in Regulating Skeletal Muscle Mass and Function. *Frontiers in physiology* **2019,** 10.
76. Pedersen, B. K.; Steensberg, A.; Fischer, C.; Keller, C.; Keller, P.; Plomgaard, P.; Febbraio, M.; Saltin, B., Searching for the exercise factor: is IL-6 a candidate? *Journal of muscle research and cell motility* **2003,** 24, (2-3), 113-9.
77. Pedersen, B. K.; Febbraio, M. A., Muscles, exercise and obesity: skeletal muscle as a secretory organ. *Nature reviews. Endocrinology* **2012,** 8, (8), 457-65.
78. Penna, C.; Alloatti, G.; Crisafulli, A., Mechanisms Involved in Cardioprotection Induced by Physical Exercise. *Antioxidants & redox signaling* **2020,** 32, (15), 1115-1134.
79. Cabrera-Fuentes, H. A.; Aragones, J.; Bernhagen, J.; Boening, A.; Boisvert, W. A.; Bøtker, H. E.; Bulluck, H.; Cook, S.; Di Lisa, F.; Engel, F. B.; Engelmann, B.;

Ferrazzi, F.; Ferdinandy, P.; Fong, A.; Fleming, I.; Gnaiger, E.; Hernández-Reséndiz, S.; Kalkhoran, S. B.; Kim, M. H.; Lecour, S.; Liehn, E. A.; Marber, M. S.; Mayr, M.; Miura, T.; Ong, S. B.; Peter, K.; Sedding, D.; Singh, M. K.; Suleiman, M. S.; Schnittler, H. J.; Schulz, R.; Shim, W.; Tello, D.; Vogel, C. W.; Walker, M.; Li, Q. O.; Yellon, D. M.; Hausenloy, D. J.; Preissner, K. T., From basic mechanisms to clinical applications in heart protection, new players in cardiovascular diseases and cardiac theranostics: meeting report from the third international symposium on "New frontiers in cardiovascular research". *Basic Res Cardiol* **2016,** 111, (6), 69.

80. Ouchi, N.; Ohashi, K.; Shibata, R.; Murohara, T., Protective Roles of Adipocytokines and Myokines in Cardiovascular Disease. *Circulation journal : official journal of the Japanese Circulation Society* **2016,** 80, (10), 2073-80.
81. Otaka, N.; Shibata, R.; Ohashi, K.; Uemura, Y.; Kambara, T.; Enomoto, T.; Ogawa, H.; Ito, M.; Kawanishi, H.; Maruyama, S.; Joki, Y.; Fujikawa, Y.; Narita, S.; Unno, K.; Kawamoto, Y.; Murate, T.; Murohara, T.; Ouchi, N., Myonectin Is an Exercise-Induced Myokine That Protects the Heart From Ischemia-Reperfusion Injury. *Circ Res* **2018,** 123, (12), 1326-1338.
82. Ho, M. Y.; Wang, C. Y., Role of Irisin in Myocardial Infarction, Heart Failure, and Cardiac Hypertrophy. *Cells* **2021,** 10, (8).
83. Chow, L. S.; Gerszten, R. E.; Taylor, J. M.; Pedersen, B. K.; van Praag, H.; Trappe, S.; Febbraio, M. A.; Galis, Z. S.; Gao, Y.; Haus, J. M.; Lanza, I. R.; Lavie, C. J.; Lee, C.-H.; Lucia, A.; Moro, C.; Pandey, A.; Robbins, J. M.; Stanford, K. I.; Thackray, A. E.; Villeda, S.; Watt, M. J.; Xia, A.; Zierath, J. R.; Goodpaster, B. H.; Snyder, M. P., Exerkines in health, resilience and disease. *Nature Reviews Endocrinology* **2022,** 18, (5), 273-289.
84. Searle, B. C.; Pino, L. K.; Egertson, J. D.; Ting, Y. S.; Lawrence, R. T.; MacLean, B. X.; Villén, J.; MacCoss, M. J., Chromatogram libraries improve peptide detection and quantification by data independent acquisition mass spectrometry. *Nature Communications* **2018,** 9, (1), 5128.
85. Gessulat, S.; Schmidt, T.; Zolg, D. P.; Samaras, P.; Schnatbaum, K.; Zerweck, J.; Knaute, T.; Rechenberger, J.; Delanghe, B.; Huhmer, A.; Reimer, U.; Ehrlich, H.-C.; Aiche, S.; Kuster, B.; Wilhelm, M., Prosit: proteome-wide prediction of peptide tandem mass spectra by deep learning. *Nature Methods* **2019,** 16, (6), 509-518.
86. Tyanova, S.; Temu, T.; Sinitcyn, P.; Carlson, A.; Hein, M. Y.; Geiger, T.; Mann, M.; Cox, J., The Perseus computational platform for comprehensive analysis of (prote)omics data. *Nature Methods* **2016,** 13, (9), 731-740.
87. Raudvere, U.; Kolberg, L.; Kuzmin, I.; Arak, T.; Adler, P.; Peterson, H.; Vilo, J., g:Profiler: a web server for functional enrichment analysis and conversions of gene lists (2019 update). *Nucleic Acids Res* **2019,** 47, (W1), W191-W198.
88. Shannon, P.; Markiel, A.; Ozier, O.; Baliga, N. S.; Wang, J. T.; Ramage, D.; Amin, N.; Schwikowski, B.; Ideker, T., Cytoscape: a software environment for integrated models of biomolecular interaction networks. *Genome research* **2003,** 13, (11), 2498-504.
89. Reimand, J.; Isserlin, R.; Voisin, V.; Kucera, M.; Tannus-Lopes, C.; Rostamianfar, A.; Wadi, L.; Meyer, M.; Wong, J.; Xu, C.; Merico, D.; Bader, G. D., Pathway enrichment analysis and visualization of omics data using g:Profiler, GSEA, Cytoscape and EnrichmentMap. *Nature Protocols* **2019,** 14, (2), 482-517.
90. Szklarczyk, D.; Gable, A. L.; Nastou, K. C.; Lyon, D.; Kirsch, R.; Pyysalo, S.; Doncheva, N. T.; Legeay, M.; Fang, T.; Bork, P.; Jensen, L. J.; von Mering, C., The STRING database in 2021: customizable protein-protein networks, and functional

characterization of user-uploaded gene/measurement sets. *Nucleic Acids Res* **2021,** 49, (D1), D605-d612.

91. Doncheva, N. T.; Morris, J. H.; Gorodkin, J.; Jensen, L. J., Cytoscape StringApp: Network Analysis and Visualization of Proteomics Data. *Journal of proteome research* **2019,** 18, (2), 623-632.
92. Subramanian, A.; Tamayo, P.; Mootha, V. K.; Mukherjee, S.; Ebert, B. L.; Gillette, M. A.; Paulovich, A.; Pomeroy, S. L.; Golub, T. R.; Lander, E. S.; Mesirov, J. P., Gene set enrichment analysis: a knowledge-based approach for interpreting genome-wide expression profiles. *Proc Natl Acad Sci U S A* **2005,** 102, (43), 15545-50.
93. Liberzon, A.; Subramanian, A.; Pinchback, R.; Thorvaldsdóttir, H.; Tamayo, P.; Mesirov, J. P., Molecular signatures database (MSigDB) 3.0. *Bioinformatics (Oxford, England)* **2011,** 27, (12), 1739-1740.
94. Luo, W.; Brouwer, C., Pathview: an R/Bioconductor package for pathway-based data integration and visualization. *Bioinformatics (Oxford, England)* **2013,** 29, (14), 1830-1.
95. Luo, W.; Pant, G.; Bhavnasi, Y. K.; Blanchard, S. G., Jr.; Brouwer, C., Pathview Web: user friendly pathway visualization and data integration. *Nucleic Acids Res* **2017,** 45, (W1), W501-W508.
96. Csonka, C.; Kupai, K.; Kocsis, G. F.; Novák, G.; Fekete, V.; Bencsik, P.; Csont, T.; Ferdinandy, P., Measurement of myocardial infarct size in preclinical studies. *J Pharmacol Toxicol Methods* **2010,** 61, (2), 163-170.
97. Liu, L.; Mu, Y.; Han, W.; Wang, C., Association of hypercholesterolemia and cardiac function evaluated by speckle tracking echocardiography in a rabbit model. *Lipids Health Dis* **2014,** 13, 128-128.
98. Hołda, M. K.; Stachowicz, A.; Suski, M.; Wojtysiak, D.; Sowińska, N.; Arent, Z.; Palka, N.; Podolec, P.; Kopeć, G., Myocardial proteomic profile in pulmonary arterial hypertension. *Scientific Reports* **2020,** 10, (1), 14351.
99. Szűcs, G.; Sója, A.; Péter, M.; Sárközy, M.; Bruszel, B.; Siska, A.; Földesi, I.; Szabó, Z.; Janáky, T.; Vígh, L.; Balogh, G.; Csont, T., Prediabetes Induced by Fructose-Enriched Diet Influences Cardiac Lipidome and Proteome and Leads to Deterioration of Cardiac Function prior to the Development of Excessive Oxidative Stress and Cell Damage. *Oxid Med Cell Longev* **2019,** 2019, 3218275.
100. Sequeira, V.; Nijenkamp, L. L. A. M.; Regan, J. A.; van der Velden, J., The physiological role of cardiac cytoskeleton and its alterations in heart failure. *Biochimica et Biophysica Acta (BBA) - Biomembranes* **2014,** 1838, (2), 700-722.
101. Ehler, E., Actin-associated proteins and cardiomyopathy-the 'unknown' beyond troponin and tropomyosin. *Biophys Rev* **2018,** 10, (4), 1121-1128.
102. Yang, M.; Yan, J.; Wu, A.; Zhao, W.; Qin, J.; Pogwizd, S. M.; Wu, X.; Yuan, S.; Ai, X., Alterations of housekeeping proteins in human aged and diseased hearts. *Pflügers Archiv - European Journal of Physiology* **2021,** 473, (3), 351-362.
103. Michaelson, J.; Hariharan, V.; Huang, H., Hyperglycemic and Hyperlipidemic Conditions Alter Cardiac Cell Biomechanical Properties. *Biophysical Journal* **2014,** 106, (11), 2322-2329.
104. Varela, R.; Rauschert, I.; Romanelli, G.; Alberro, A.; Benech, J. C., Hyperglycemia and hyperlipidemia can induce morphophysiological changes in rat cardiac cell line. *Biochem Biophys Rep* **2021,** 26, 100983.
105. Castillo, R. L.; Herrera, E. A.; Gonzalez-Candia, A.; Reyes-Farias, M.; de la Jara, N.; Peña, J. P.; Carrasco-Pozo, C., Quercetin Prevents Diastolic Dysfunction Induced by a High-Cholesterol Diet: Role of Oxidative Stress and Bioenergetics in Hyperglycemic Rats. *Oxid Med Cell Longev* **2018,** 2018, 7239123-7239123.

106. Elustondo, P.; Martin, L. A.; Karten, B., Mitochondrial cholesterol import. *Biochimica et Biophysica Acta (BBA) - Molecular and Cell Biology of Lipids* **2017,** 1862, (1), 90-101.
107. Heusch, G., Molecular basis of cardioprotection: signal transduction in ischemic pre-, post-, and remote conditioning. *Circ Res* **2015,** 116, (4), 674-699.
108. Ferdinandy, P.; Szilvássy, Z.; Horváth, L. I.; Csont, T.; Csonka, C.; Nagy, E.; Szentgyörgyi, R.; Nagy, I.; Koltai, M.; Dux, L., Loss of pacing-induced preconditioning in rat hearts: role of nitric oxide and cholesterol-enriched diet. *J Mol Cell Cardiol* **1997,** 29, (12), 3321-3333.
109. Iliodromitis, E. K.; Zoga, A.; Vrettou, A.; Andreadou, I.; Paraskevaidis, I. A.; Kaklamanis, L.; Kremastinos, D. T., The effectiveness of postconditioning and preconditioning on infarct size in hypercholesterolemic and normal anesthetized rabbits. *Atherosclerosis* **2006,** 188, (2), 356-362.
110. Ágg, B.; Baranyai, T.; Makkos, A.; Vető, B.; Faragó, N.; Zvara, Á.; Giricz, Z.; Veres, D. V.; Csermely, P.; Arányi, T.; Puskás, L. G.; Varga, Z. V.; Ferdinandy, P., MicroRNA interactome analysis predicts post-transcriptional regulation of ADRB2 and PPP3R1 in the hypercholesterolemic myocardium. *Scientific Reports* **2018,** 8, (1), 10134.
111. Luo, C.; Ling, G.-x.; Lei, B.-f.; Feng, X.; Xie, X.-y.; Fang, C.; Li, Y.-g.; Cai, X.-w.; Zheng, B.-s., Circular RNA PVT1 silencing prevents ischemia-reperfusion injury in rat by targeting microRNA-125b and microRNA-200a. *J Mol Cell Cardiol* **2021,** 159, 80-90.
112. Zhang, B.; Mao, S.; Liu, X.; Li, S.; Zhou, H.; Gu, Y.; Liu, W.; Fu, L.; Liao, C.; Wang, P., MiR-125b inhibits cardiomyocyte apoptosis by targeting BAK1 in heart failure. *Molecular Medicine* **2021,** 27, (1), 72.
113. Shah, N. M.; Zaitseva, L.; Bowles, K. M.; MacEwan, D. J.; Rushworth, S. A., NRF2-driven miR-125B1 and miR-29B1 transcriptional regulation controls a novel anti-apoptotic miRNA regulatory network for AML survival. *Cell death and differentiation* **2015,** 22, (4), 654-64.
114. Joo, M. S.; Lee, C. G.; Koo, J. H.; Kim, S. G., miR-125b transcriptionally increased by Nrf2 inhibits AhR repressor, which protects kidney from cisplatin-induced injury. *Cell Death Dis* **2013,** 4, (10), e899.
115. Mata, A.; Cadenas, S., The Antioxidant Transcription Factor Nrf2 in Cardiac Ischemia-Reperfusion Injury. *Int J Mol Sci* **2021,** 22, (21).
116. Sañudo, B.; Bartolomé, D.; Tejero, S.; Ponce-González, J. G.; Loza, J. P.; Figueroa, A., Impact of Active Recovery and Whole-Body Electromyostimulation on Blood-Flow and Blood Lactate Removal in Healthy People. *Frontiers in physiology* **2020,** 11, 310.
117. Banerjee, P.; Caulfield, B.; Crowe, L.; Clark, A. L., Prolonged electrical muscle stimulation exercise improves strength, peak VO2, and exercise capacity in patients with stable chronic heart failure. *Journal of cardiac failure* **2009,** 15, (4), 319-26.
118. Ploesteanu, R. L.; Nechita, A. C.; Turcu, D.; Manolescu, B. N.; Stamate, S. C.; Berteanu, M., Effects of neuromuscular electrical stimulation in patients with heart failure - review. *J Med Life* **2018,** 11, (2), 107-118.
119. Birnbaum, Y.; Hale, S. L.; Kloner, R. A., Ischemic preconditioning at a distance: reduction of myocardial infarct size by partial reduction of blood supply combined with rapid stimulation of the gastrocnemius muscle in the rabbit. *Circulation* **1997,** 96, (5), 1641-6.

120. Reinthaler, M.; Jung, F.; Empen, K., Remote ischemic preconditioning of the heart: Combining lower limb ischemia and electronic stimulation of the gastrocnemius muscle. *Clinical hemorheology and microcirculation* **2018,** 70, (4), 381-389.
121. Tsou, M. T.; Huang, C. H.; Chiu, J. H., Electroacupuncture on PC6 (Neiguan) attenuates ischemia/reperfusion injury in rat hearts. *The American journal of Chinese medicine* **2004,** 32, (6), 951-65.
122. Redington, K. L.; Disenhouse, T.; Li, J.; Wei, C.; Dai, X.; Gladstone, R.; Manlhiot, C.; Redington, A. N., Electroacupuncture reduces myocardial infarct size and improves post-ischemic recovery by invoking release of humoral, dialyzable, cardioprotective factors. *The journal of physiological sciences : JPS* **2013,** 63, (3), 219-23.
123. Merlocco, A. C.; Redington, K. L.; Disenhouse, T.; Strantzas, S. C.; Gladstone, R.; Wei, C.; Tropak, M. B.; Manlhiot, C.; Li, J.; Redington, A. N., Transcutaneous electrical nerve stimulation as a novel method of remote preconditioning: in vitro validation in an animal model and first human observations. *Basic Res Cardiol* **2014,** 109, (3), 406.
124. Feng, L.; Li, B.; Tian, Z., Exerkines: opening the way to protecting ischemic heart. *Current Opinion in Physiology* **2023,** 31, 100615.
125. Truong, A. D.; Kho, M. E.; Brower, R. G.; Feldman, D. R.; Colantuoni, E.; Needham, D. M., Effects of neuromuscular electrical stimulation on cytokines in peripheral blood for healthy participants: a prospective, single-blinded Study. *Clinical physiology and functional imaging* **2017,** 37, (3), 255-262.
126. McGinnis, G. R.; Ballmann, C.; Peters, B.; Nanayakkara, G.; Roberts, M.; Amin, R.; Quindry, J. C., Interleukin-6 mediates exercise preconditioning against myocardial ischemia reperfusion injury. *American Journal of Physiology-Heart and Circulatory Physiology* **2015,** 308, (11), H1423-H1433.
127. Ouchi, N.; Oshima, Y.; Ohashi, K.; Higuchi, A.; Ikegami, C.; Izumiya, Y.; Walsh, K., Follistatin-like 1, a Secreted Muscle Protein, Promotes Endothelial Cell Function and Revascularization in Ischemic Tissue through a Nitric-oxide Synthase-dependent Mechanism. *J Biol Chem* **2008,** 283, (47), 32802-32811.
128. Yang, W.; Duan, Q.; Zhu, X.; Tao, K.; Dong, A., Follistatin-Like 1 Attenuates Ischemia/Reperfusion Injury in Cardiomyocytes via Regulation of Autophagy. *BioMed Research International* **2019,** 2019, 9537382.
129. Xi, Y.; Hao, M.; Liang, Q.; Li, Y.; Gong, D. W.; Tian, Z., Dynamic resistance exercise increases skeletal muscle-derived FSTL1 inducing cardiac angiogenesis via DIP2A-Smad2/3 in rats following myocardial infarction. *Journal of sport and health science* **2020**.
130. Sajer, S.; Guardiero, G. S.; Scicchitano, B. M., Myokines in Home-Based Functional Electrical Stimulation-Induced Recovery of Skeletal Muscle in Elderly and Permanent Denervation. *European journal of translational myology* **2018,** 28, (4), 7905.

12 Annex

I.

International Journal of
Molecular Sciences

MDPI

Article

Hypercholesterolemia Interferes with Induction of miR-125b-1-3p in Preconditioned Hearts

Márton R. Szabó [1,2], Renáta Gáspár [1,2], Márton Pipicz [1,2], Nóra Zsindely [3], Petra Diószegi [1,2], Márta Sárközy [1,2], László Bodai [4] and Tamás Csont [1,2,*]

1 Metabolic Diseases and Cell Signaling (MEDICS) Research Group, Department of Biochemistry, Faculty of Medicine, University of Szeged, Dóm tér 9., H-6720 Szeged, Hungary; szabo.marton@med.u-szeged.hu (M.R.S.); gaspar.renata@med.u-szeged.hu (R.G.); pipicz.marton@med.u-szeged.hu (M.P.); dioszegi.petra@med.u-szeged.hu (P.D.); sarkozy.marta@med.u-szeged.hu (M.S.)

2 Interdisciplinary Centre of Excellence, University of Szeged, Dugonics tér 13., H-6720 Szeged, Hungary

3 Department of Microbiology, Faculty of Science and Informatics, University of Szeged, Közép fasor 52., H-6726 Szeged, Hungary; zsindizsn@yahoo.com

4 Department of Biochemistry and Molecular Biology, Faculty of Science and Informatics, University of Szeged, Közép fasor 52., H-6726 Szeged, Hungary; bodai@bio.u-szeged.hu

* Correspondence: csont.tamas@med.u-szeged.hu; Tel.: +36-62-545-096

Received: 31 March 2020; Accepted: 20 May 2020; Published: 26 May 2020

Abstract: Ischemic preconditioning (IPre) reduces ischemia/reperfusion (I/R) injury in the heart. The non-coding microRNA miR-125b-1-3p has been demonstrated to play a role in the mechanism of IPre. Hypercholesterolemia is known to attenuate the cardioprotective effect of preconditioning; nevertheless, the exact underlying mechanisms are not clear. Here we investigated, whether hypercholesterolemia influences the induction of miR-125b-1-3p by IPre. Male Wistar rats were fed with a rodent chow supplemented with 2% cholesterol and 0.25% sodium-cholate hydrate for 8 weeks to induce high blood cholesterol levels. The hearts of normo- and hypercholesterolemic animals were then isolated and perfused according to Langendorff, and were subjected to 35 min global ischemia and 120 min reperfusion with or without IPre (3 × 5 min I/R cycles applied before index ischemia). IPre significantly reduced infarct size in the hearts of normocholesterolemic rats; however, IPre was ineffective in the hearts of hypercholesterolemic animals. Similarly, miR-125b-1-3p was upregulated by IPre in hearts of normocholesterolemic rats, while in the hearts of hypercholesterolemic animals IPre failed to increase miR-125b-1-3p significantly. Phosphorylation of cardiac Akt, ERK, and STAT3 was not significantly different in any of the groups at the end of reperfusion. Based on these results we propose here that hypercholesterolemia attenuates the upregulation of miR-125b-1-3p by IPre, which seems to be associated with the loss of cardioprotection.

Keywords: hypercholesterolaemia; cardioprotection; miR-125b; miR-125b*; miRNA; protectomiR; risk factor; comorbidity; RISK; SAFE

1. Introduction

Myocardial infarction, characterized by restriction of blood flow to the myocardium, is a major cause of death worldwide [1,2]. Nevertheless, the heart is able to adapt remarkably to withstand the detrimental effects of ischemic injury. One of the most powerful strategies to trigger endogenous cardioprotective mechanisms in the myocardium is ischemic preconditioning (IPre), i.e., when short, repetitive cycles of ischemia/reperfusion (I/R) are applied before the sustained lethal ischemia [3]. The molecular mechanism of IPre is complex and still not entirely clear. Trigger molecules (e.g., adenosine, opioids, bradykinin, and nitric oxide) induced by preconditioning has been shown

to activate G-protein-coupled receptors and cardioprotective protein kinases (e.g., Akt, Erk, STAT3, and PKG), thereby leading to cell survival [4,5]. Besides activation of several signaling pathways, changes in protein-coding gene expression of the heart in response to preconditioning have been demonstrated, too. Moreover, non-coding microRNAs (miRNA) have emerged as regulators of preconditioning [6]. Indeed, we have previously shown that preconditioning alters the expression of several miRNAs in the heart in settings of ischemia/reperfusion [7]. We have identified miR-125b*, more specifically miR-125b-1-3p, as a cardioprotective miRNA, since preconditioning enhanced its expression and cardiac cells transfected with miR-125b* mimics showed significant survival rate during simulated ischemia/reperfusion injury [7].

Interestingly, metabolic diseases like diabetes or hyperlipidemia may interfere with the efficacy of IPre [8]. Hypercholesterolemia is a well-known risk factor for myocardial infarction due to its promoting effect on coronary atherosclerosis [2]. Nevertheless, independently from its proatherogenic effect, a high blood cholesterol level exerts a direct adverse effect on the myocardium leading to cardiac dysfunction, altered tolerance to I/R injury, and disturbed stress adaptation [8,9]. High cholesterol level is thought to induce oxidative/nitrosative stress in the myocardium [9,10], thereby leading to dysregulation of cardioprotective signaling pathways (e.g., decreases in nitric oxide bioavailability, and in activation of cardioprotective protein kinases). In addition, hypercholesterolemia was shown to alter cardiac gene expression of mRNAs as well as miRNAs. We have demonstrated for instance, that downregulation of cardiac miR-25 in hypercholesterolemic rats mediates oxidative/nitrative stress in the heart [11]. Nevertheless, the exact underlying mechanisms responsible for the attenuated cardioprotective effect of preconditioning in hypercholesterolemia are unclear; therefore we investigated whether hypercholesterolemia influences miR-125b-1-3p upregulation induced by preconditioning.

2. Results

2.1. Verification of Hypercholesterolemia

At the end of the 8-week diet period, the body weight of animals receiving cholesterol-enriched diet was not different from the weight of control animals fed a standard diet (Figure 1A). In order to verify the development of hypercholesterolemia in our model, total blood cholesterol level was measured. Total cholesterol was significantly higher in cholesterol-fed rats when compared to control animals fed with standard chow (Figure 1B).

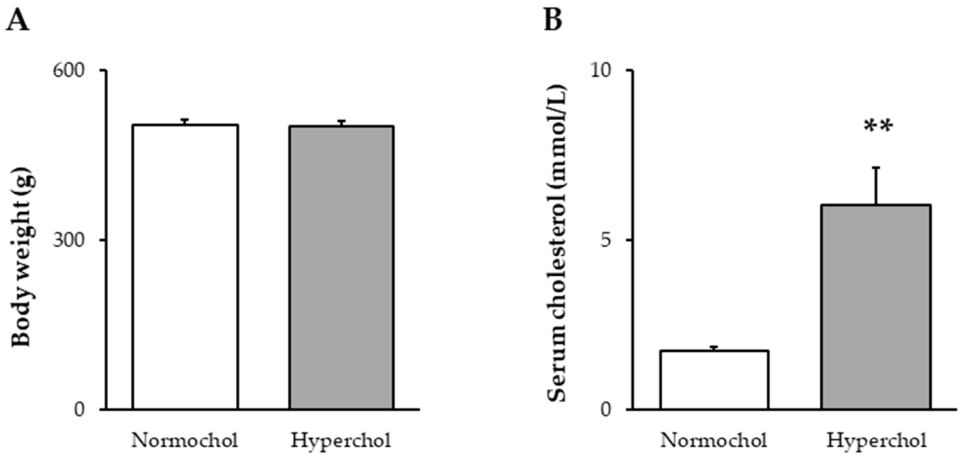

Figure 1. Body weight (**A**) and serum total cholesterol levels (**B**) at the end of 8 weeks of cholesterol diet. Data are expressed as mean ± SEM; n = 14–16. ** $p < 0.01$ vs. Normochol. Normochol and Hyperchol refer to normo- and hypercholesterolemia, respectively.

2.2. Hypercholesterolemia Attenuates the Infarct Size-Limiting Effect of Ischemic Preconditioning

To assess the cardioprotective effect of IPre, infarct size was measured in hearts undergoing I/R. In the hearts of normocholesterolemic rats, IPre significantly decreased infarct size compared to the I/R control group (Figure 2). However, IPre failed to significantly attenuate infarct size in the hearts of hypercholesterolemic animals (Figure 2).

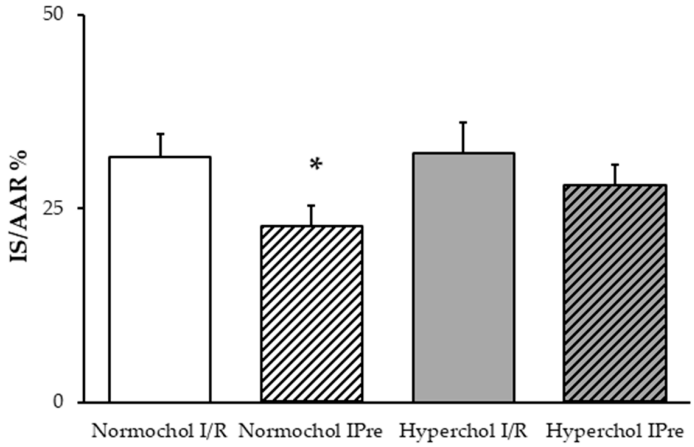

Figure 2. Infarct size values at the end of ex vivo heart perfusion. Hearts isolated from normo- and hypercholesterolemic rats were subjected to 35 min global ischemia and 120 min reperfusion (ischemia/reperfusion (I/R)) with or without ischemic preconditioning (3 × 5 min cycles of I/R applied before index ischemia; IPre). IS/AAR = infarct size/area at risk %. Data are expressed as mean ± SEM; $n = 8$. * $p < 0.05$ vs. corresponding I/R group. Normochol and Hyperchol refer to normo- and hypercholesterolemia, respectively.

2.3. Upregulation of miR-125b-1-3p Induced by Preconditioning is Lost in Settings of Hypercholesterolemia

In order to assess if miR-125b-1-3p correlates with cardioprotection, miRNA expression was determined in hearts subjected to I/R with or without IPre in both normo- and hypercholesterolemic groups. At the end of reperfusion, IPre significantly upregulated miR-125b-1-3p in normocholesterolemic hearts compared to I/R controls (Figure 3). In contrast, IPre failed to increase significantly miR-125b-1-3p level in hearts of hypercholesterolemic animals (Figure 3).

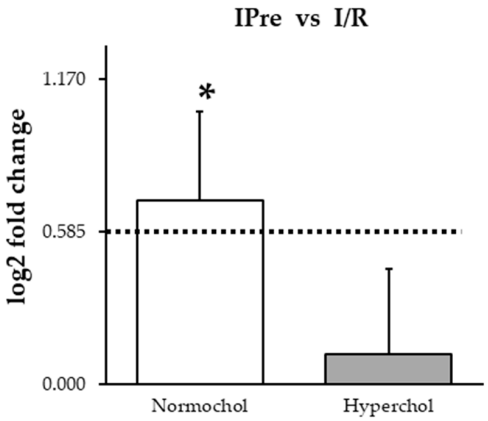

Figure 3. miR-125b-1-3p expression changes induced by ischemic preconditioning (IPre) in hearts of normocholesterolemic and hypercholesterolemic rats. Values are log2 expression changes ± SEM calculated with Deseq2. * $p < 0.05$ and log2 fold change is greater than 0.585 vs. corresponding ischemia/reperfusion (I/R) control group. Normochol and Hyperchol refer to normo- and hypercholesterolemia, respectively.

2.4. Ischemic Preconditioning Failed to Affect the RISK and SAFE Pathways at the End of Reperfusion

To elucidate the possible downstream mechanism of IPre in normo- and hypercholesterolemic conditons, Reperfusion Injury Salvage Kinases (RISK) and Survivor Activating Factor Enhancement (SAFE) pathways were investigated in ventricular samples obtained at the end of reperfusion. Although, a slight decrease of Akt phosphorylation and a slight increase in ERK2 and STAT3 phosphorylation may be seen in preconditioned normocholesterolemic hearts compared to I/R controls, the phosphorylation of Akt, ERK1/2, and STAT3 were not affected significantly by any of the interventions (Figure 4). In hypercholesterolemic groups phosphorylation of Akt, ERK1/2, and STAT3 were not affected by IPre.

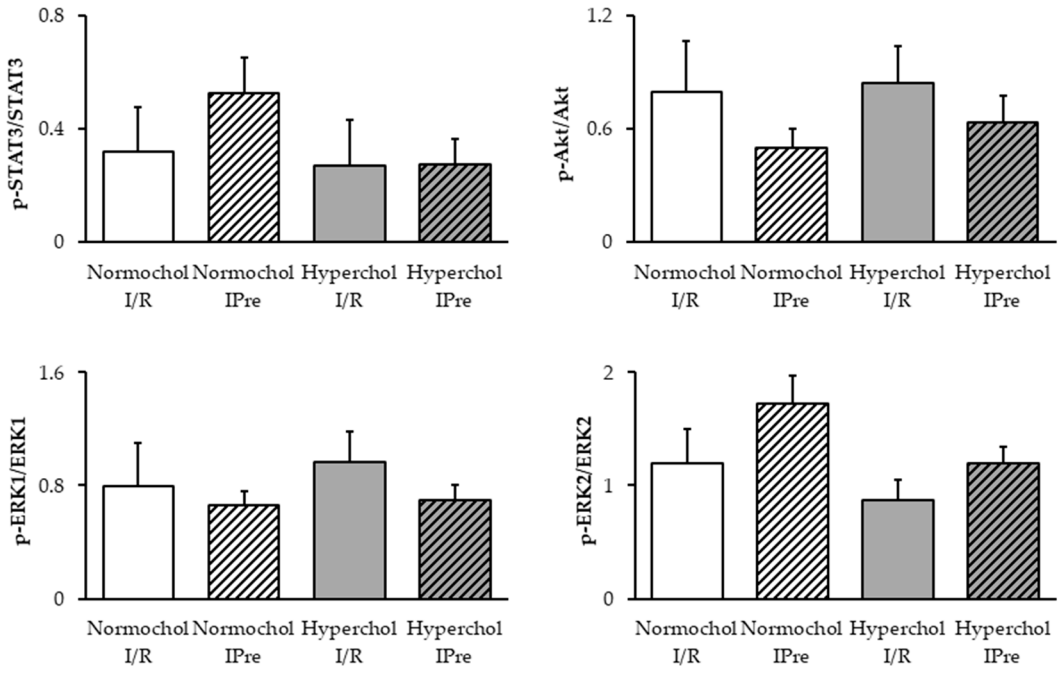

Figure 4. Delayed phosphorylation of STAT3, Akt, and ERK1/2 proteins assessed by Western blots. Ventricular samples were harvested at the end of reperfusion from normo- and hypercholesterolemic hearts subjected to ischemia/reperfusion (I/R) with or without ischemic preconditioning (IPre). Data are expressed as mean ± SEM; $n = 5$, Two-way ANOVA. Normochol and Hyperchol refer to normo- and hypercholesterolemia, respectively.

3. Discussion

In the present study, we have shown an association of the attenuated cardioprotective effect of IPre in hypercholesterolemia with diminished miR-125b-1-3p induction. This is the first demonstration that diet-induced hypercholesterolemia blunts the cardiac overexpression of miR-125b-1-3p triggered by IPre. Together with previous findings, our present results suggest that miR-125b-1-3p may be an important activator of IPre-induced cardioprotection and its decreased expression level seems to interfere with the infarct size limiting effect of IPre in hypercholesterolemia.

Similarly to literature data [5], in our isolated perfused heart model, the application of IPre in normocholesterolemic hearts decreased infarct size compared to the I/R group. IPre is one of the most powerful endogenous cardioprotective approaches as it markedly enhances the ability of the heart to withstand a subsequent ischemic injury. The early phase of IPre (i.e., classic preconditioning or first window of protection) manifested within minutes after preconditioning stimulus, was first described by Murry and colleagues [3]. The protective effect of IPre against myocardial infarction was confirmed using numerous species in several experimental models [4]. Although a number of signaling pathways have been implicated in IPre, the exact mechanism is still not entirely clear.

Non-protein-coding miRNAs have been proposed to play a role in IPre [4,5,7]. MiR-125b-1-3p (previously named miR-125b*) is the passenger antisense strand of miR-125b-1 stem-loop precursor. Antisense miRNAs are considered to be degraded during miRNA maturation. However, recent data suggest that passenger strands also have biological functions [12,13]. So far, only a few studies have revealed that miR-125b-1 protects the heart against I/R injury. In the present study, we investigated the expression levels of miR-125b-1-3p in ex vivo perfused hearts, and we showed upregulation of miR-125b-1-3p by IPre in normocholesterolemic hearts, suggesting that miR-125b-1-3p may play a role in IPre-induced cardioprotection. This finding is in accordance with our previous studies, when we identified miR-125b-1-3p as a protectomiR since both IPre and postconditioning induced miR-125b-1-3p expression in the setting of I/R [7]. Moreover, in the same study, cardiomyocytes transfected with miR-125b-1-3p showed enhanced cell viability following simulated I/R injury. In contrast, Li and colleagues found that decreased level of miR-125b-1-3p is associated with rutin-induced cardioprotection in HL-1 cells [14]. These discrepancies may arise due to substantial differences in the applied models since the molecular mechanism of I/R may differ from the mechanisms of drug–induced cardiotoxicity. Interestingly, literature data support the cardioprotective effect of the predominantly expressed sense strand of mature miR-125b-1 as well. Myocardial infarction was lower in precursor miR-125b-1 (encoding both 125b-1-3p and -5p) overexpressing transgenic mice, possibly due to inhibition of apoptotic signaling [15]. In a separate study, pharmacological induction of miR-125b-5p conferred cardioprotection against ischemia/reperfusion by suppressing Bak1 and Kfl13 protein expressions [16]. Furthermore, pretreatment with miR-125b-5p containing exosomes derived from mesenchymal stem cells protected the murine heart from myocardial infarction and cultured cardiomyocytes against simulated I/R injury [17,18]. Nevertheless, the expression of miR-125b-5p seems to have adverse effects in the failing heart through inducing cardiac fibrosis [19–21].

In the present study, we have found that hypercholesterolemia abolished the infarct size limiting effect of IPre. This is in line with previous reports from our group and others, demonstrating that hypercholesterolemia interferes with cardioprotection [22–26]. However, here we found that in contrast to findings obtained in normocholesterolemia, the application of IPre in hypercholesterolemia failed to upregulate miR-125b-1-3p expression as compared to I/R. We have previously demonstrated that diet-induced hypercholesterolemia alters cardiac miRNA expression profile, and as a consequence, downregulation of miR-25 mediates oxidative/nitrosative stress in the myocardium [11]. Although several studies revealed relationships between IPre and cardiac miRNA levels in normocholesterolemic subjects, this is the first demonstration that hypercholesterolemia influences miRNA expression changes induced by IPre. Our study suggests that the upregulation of miR-125b-1-3p in response to IPre may be an important element in the cardioprotective mechanism; however, further studies need to confirm a direct causative relationship.

In our current study, we also looked at possible downstream signaling mechanism of IPre as an attempt to relate the observed alterations in miR-125b-1-3p expression with known cardioprotective mechanisms. Therefore, we have assessed phosphorylation rates of Akt, ERK1/2, and STAT3 at the end of reperfusion, as both infarct size and miR analysis was performed at that timepoint in the current study. IPre in normocholesterolemic hearts failed to increase significantly the delayed phosphorylation of Akt, ERK1/2, and STAT3 proteins, respectively. This seems to be against the general view that these kinases contribute to the protective effect of IPre. The discrepancies may be explained by the experimental protocol that we used. We have determined kinase phosphorylations 2 h after the onset of reperfusion, while the phosphorylation status of IPre-related kinases is mostly investigated at the beginning of reperfusion. Nevertheless, some studies have already assessed the late activation of cardiac RISK and SAFE pathways after 30, 120, or 180 min of reperfusion in response to ischemic conditionings [27–29]. Our present findings do not exclude the possible activation of the RISK and/or SAFE pathways by IPre in earlier phases of the protocol we used. However, at the late phase, when miR-125b-1-3p induction was evident, the activation of RISK and SAFE pathways does not seem to play a crucial role in the cardioprotective mechanism of IPre. This may be a valuable conclusion as some other microRNAs has

been linked to STAT3 modulation, e.g., miR-874 inhibition targeting STAT3 has been shown to protect the heart against I/R injury by attenuating cardiomyocyte apoptosis in a mouse model [30]. Based on our results, one may speculate that upregulation of miR-125b-1-3p is rather a consequence of the activation of RISK and SAFE pathways; however, further research is needed to prove this hypothesis. We have found in the current study that IPre failed to affect significantly the delayed phosphorylation of Akt and ERK1/2 proteins in hypercholesterolemic hearts. Interestingly, Akt may stimulate nitric oxide production via activation of endothelial nitric oxide synthase (eNOS) in response to preconditioning stimuli [31,32] and a decreased cardiac nitric oxide content was suggested to correlate with impaired cardioprotection due to IPre in cholesterol-fed rats [9,22,33]. Based on our present results, it is unlikely that miR-125b-1-3p would regulate Akt-eNOS-nitric oxide-PKG signaling in our model, however, whether nitric oxide is able to affect cardiac miR-125b-1-3p expression in normocholesterolemia needs to be assessed in the future. Our current results also show that hypercholesterolemia does not affect STAT3 phosphorylation after I/R with or without IPre, thereby providing a deeper insights into the rather unclear effects of metabolic disorders on cardiac STAT3 signaling [34].

Similarly to all experimental investigations, our study is not without limitations. We have analyzed microRNA expression and the RISK and SAFE pathways at a single time-point, i.e., at 2 h of reperfusion. This may limit proper interpretation of early molecular changes in the course of cardioprotection, therefore assaying miR-125b-1-3p, triggers for miR-125-b-1-3p induction and survival kinases at earlier time-points in future studies may have some added value. Although it is clinically less relevant, a common feature of studies performed on I/R—including ours—is that the ischemic tissue may contain both viable and non-viable cells, and the lack of separation of these cells for biochemical analysis may potentially affect overall molecular markers of the tissue. This is especially problematic when regional ischemia is used, because it is almost impossible to separate the non-ischemic, ischemic-viable, and ischemic-non-viable cells. Therefore, in the present study we applied global ischemia, where all cells were exposed to the same stress (i.e., ischemia). Despite these limitations our study provides valuable data regarding the effect of experimental hypercholesterolemia on some aspects of the potential molecular mechanism of ischemic preconditioning.

We conclude that miR-125b-1-3p upregulation is an adaptive response to prevent cellular damage induced by I/R, however, the exact role and molecular targets of miR-125b-1-3p should be further analyzed in future studies. This is the first demonstration that hypercholesterolemia attenuates IPre-induced miR-125b-1-3p upregulation, which is likely associated with the loss of cardioprotection. These results may suggest that modulation of cardiac miR-125b-1-3p could be a feasible target for cardioprotection even in cases when risk factors and comorbidities are present; however, this hypothesis remained to be confirmed in future experimental studies.

4. Materials and Methods

4.1. Animals

A total of 56 adult male Wistar rats were used in this study. All experiments conformed to the Guide for the Care and Use of Laboratory Animals published by the US National Institutes of Health (NIH publication No. 85-23, revised 1996) and was approved by the Animal Research Ethics Committee of Csongrád County (approval code: XV.1181/2013) and the local animal ethics committee of the University of Szeged.

4.2. Experimental Setup

Male Wistar rats (250–300 g) were fed for 8 weeks with a laboratory chow enriched with 2% (*w/w*) cholesterol and 0.25% sodium-cholate hydrate (*w/w*). The control animals were fed with standard rodent chow. At the end of the diet period rats were anesthetized with intraperitoneal injection of sodium pentobarbital (50 mg/kg; Produlab Pharma b.v., Raamsdonksveer, The Netherlands), blood samples were collected from the thoracic aorta and hearts were isolated and placed into ice-cold Krebs–Henseleit

buffer. After cannulation of the aorta, isolated hearts were perfused with an oxygenated Krebs–Henseleit buffer at 37 °C in a retrograde manner according to Langendorff as described previously [35–37]. Then hearts from both feeding groups were divided into global ischemia/reperfusion (I/R) or ischemic preconditioning (IPre) groups (Figure 5). The time-matched I/R control group hearts were equilibrated for 45 min before 35 min global ischemia and 120 min reperfusion. In the IPre group after 15 min equilibration time IPre was induced by 3 intermittent cycles of 5 min no-flow ischemia, separated by 5 min aerobic perfusion before the onset of global ischemia. At 120 min after the onset of reperfusion, either infarct size was determined (n = 8 in each group) or left ventricles were snap-frozen in liquid nitrogen and stored at −80 °C for miRNA analysis and Western blot experiments (n = 6 in each group). Global ischemia was used in this study in order to apply the same degree of stress (i.e., ischemia) for the entire myocardium.

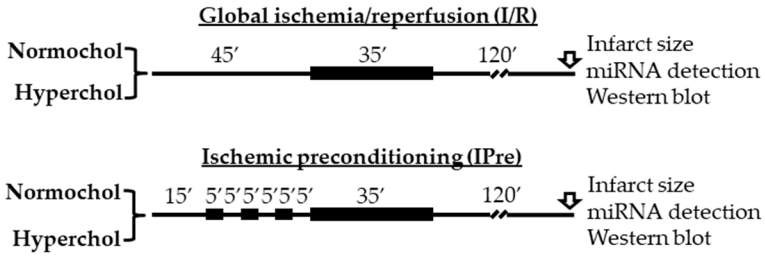

Figure 5. Experimental protocols for ex vivo ischemia/reperfusion (IR) and IR with ischemic preconditioning (IPre). At the end of reperfusion infarct size, miRNA expression analyses and Western blotting measurements were performed from the left ventricles. Normochol and Hyperchol refer to normo- and hypercholesterolemia, respectively.

4.3. Serum Total Cholesterol Measurement

Serum was separated from the freshly collected blood samples and used to determine total cholesterol concentrations using a colorimetric cholesterol detecting kit (Diagnosticum, Budapest, Hungary) and a microplate reader (BMG Labtech, Ortenberg, Germany) as described previously [10,11].

4.4. Infarct Size Determination

In a separate set of experiments, hearts were isolated and perfused as described above. After the end of reperfusion, atria were removed, and the total ventricles were used to determine the infarcted area as described previously [38,39]. Briefly, frozen ventricles were cut to 7–8 equal slices and placed into triphenyl-tetrazoliumchloride solution (Sigma-Aldrich, Saint Louis, MO, USA) for 10 min at 37 °C followed by a 10 min formaldehyde fixation and phosphate buffer washing steps. As a result, survived area were red-stained while the necrotic area become pale. Digitalized images from the stained heart slices were evaluated with planimetry method and the amount of myocardial necrosis was expressed as infarct size/area at risk %.

4.5. Measurement of Cardiac miR-125b-1-3p Level

Six heart sample from each group were used for miRNA-sequencing. Total RNA was isolated from left ventricles with miRNeasy Mini kit (Qiagen, Hilden, Germany). Total RNA samples were quality checked and quantified by capillary gel electrophoresis in an Agilent Bioanalyzer 2100 instrument using Agilent 6000 RNA Nano Kit (Agilent Technologies, Santa Clara, CA, USA). Then 1000 ng total RNA samples were used to prepare sequencing libraries using NEBNext Multiplex Small RNA Library Prep Set for Illumina (New England Biolabs, Iswich, MA, USA) following the recommendations of the manufacturer. Sequencing libraries were size selected with AMPure XP beads (Beckman Coulter, Pasadena, CA, USA) then validated and quantitated in an Agilent 2100 Bioalyzer using Agilent DNA 1000 kit. Validated library pools were denatured and loaded in MiSeq Reagent Kit V3-150

(New England Biolabs, Iswich, MA, USA) and sequenced with an Illumina MiSeq (Illumina Inc, San Diego, CA, USA) instrument generating 36 nucleotides long single-end reads.

4.6. Bioinformatic Analysis

Sequencing reads were quality checked with FastQC (Babraham Bioinformatics, UK) and adapter trimmed using Cutadapt ver. 1.8.1 [40]. Trimmed oligos were analyzed with mirdeep2 [41]. Reads were aligned to the rat reference genome using the mapper module than sequenced reads were mapped to predefined miRNA precursors, and the expression of the corresponding miRNAs were determined using the quantifier module. Differential expression analysis were performed with Deseq2 [42].

4.7. Western Blotting

Frozen left ventricular samples were homogenized in Radio Immunoprecipitation Assay buffer (Cell Signaling Technology, Danvers, MA, USA) supplemented with protease inhibitor cocktail, phenylmethane sulfonyl fluoride and sodium fluoride (Sigma-Aldrich, Saint Louis, MO, USA) as described previously [37,43–45]. Homogenates were centrifuged, and protein concentrations of the supernatants were determined using BCA Protein Assay Kit (Pierce, Rockford, IL, USA). Twenty-five micrograms of reduced and denatured protein was loaded in 10% polyacrylamide gel, and SDS gel electrophoresis was performed. Separated proteins were transferred to 0.22 μM pore size nitrocellulose membranes. After checking, the transfer efficiency with Ponceau-stained membranes were blocked for 1 h in 5% (*w/v*) bovine serum albumin (Sigma-Aldrich, Saint Louis, MO, USA) at room temperature. Blocked membranes were incubated with the following primary antibodies in the concentrations of 1:1000 phospho-Akt (Ser473, #4060), Akt (#9272), phospho-ERK1/2 (Thr202/Tyr204, #9101), ERK1/2 (#9102), phospho-STAT3 (Tyr705, #9145), STAT3 (#4904 and in 1:5000 concentration against GAPDH (#2118) at 4 °C overnight (Cell Signaling Technology, Danvers, MA, USA). After incubation with horseradish peroxidase (HRP)-conjugated goat anti-rabbit secondary antibody (Dako, Glostrup, Denmark) membranes were developed with an enhanced chemiluminescence kit. After development of phosphorylated signals of Akt, Erk1/2, and STAT3, respectively, the stripped membranes were reassessed for the total amount of proteins. The developed signals were evaluated by Quantity One Software (Bio-Rad, Hercules, CA, USA).

4.8. Statistical Analysis

Values are expressed as mean ± SEM. Student's t-test was used to evaluate the effect of cholesterol-enriched diet in body weight and serum cholesterol level, while two-way analysis of variance (ANOVA) was used to evaluate infarct size values and Western blotting results. Wald test was performed in differential miRNA expression analysis. MiRNA expression ratio with p-value <0.05 and >1.5 fold change (0.585 log2 fold change) are considered as significant expression difference.

Author Contributions: Conceptualization, T.C.; methodology, M.R.S., R.G., N.Z., P.D., M.S., L.B.; formal analysis, M.R.S., M.P.; writing—original draft preparation, M.R.S., M.P.; writing—review and editing, T.C.; visualization, M.R.S., M.P.; funding acquisition, T.C. All authors have read and agreed to the published version of the manuscript.

Funding: This article was supported by the grants GINOP 2.3.2-15-2016-00006, EFOP 3.6.2-16-2017-00006, OTKA-NKFIH (K115990), and 20391 3/2018/FEKUSTRAT. M.R.S. was supported by the ÚNKP-19-3-SZTE-269 New National Excellence Program of the Ministry for Innovation and Technology. M.S. was supported by the János Bolyai Research Scholarship of the Hungarian Academy of Sciences and the New National Excellence Program of the Ministry of Human Capacities (ÚNKP-18-4-SZTE-63 and ÚNKP-19-4-SZTE-89). L.B. was supported by the ÚNKP-19-4-SZTE-8 New National Excellence Program of the Ministry for Innovation and Technology and by the János Bolyai Research Scholarship (BO/00522/19/8) of the Hungarian Academy of Sciences.

Acknowledgments: We acknowledge the outstanding technical support of Dóra Halmi for Western blot measurements.

Conflicts of Interest: The authors declare no conflict of interest.

Abbreviations

I/R	Ischemia/Reperfusion
IPre	Ischemic Preconditioning
miRNA	microRNA
PKG	Protein kinase G
RISK	Reperfusion Injury Salvage Kinases
SAFE	Survivor Activating Factor Enhancement pathway

References

1. Nowbar, A.N.; Gitto, M.; Howard, J.P.; Francis, D.P.; Al-Lamee, R. Mortality From Ischemic Heart Disease. *Circ. Cardiovasc. Qual. Outcomes* **2019**, *12*, e005375. [CrossRef] [PubMed]
2. Timmis, A.; Townsend, N.; Gale, C.P.; Torbica, A.; Lettino, M.; Petersen, S.E.; Mossialos, E.A.; Maggioni, A.P.; Kazakiewicz, D.; May, H.T.; et al. European Society of Cardiology: Cardiovascular Disease Statistics 2019. *Eur. Heart J.* **2020**, *41*, 12–85. [CrossRef] [PubMed]
3. Murry, C.E.; Jennings, R.B.; Reimer, K.A. Preconditioning with ischemia: A delay of lethal cell injury in ischemic myocardium. *Circulation* **1986**, *74*, 1124–1136. [CrossRef] [PubMed]
4. Yellon, D.M.; Baxter, G.F.; Garcia-Dorado, D.; Heusch, G.; Sumeray, M.S. Ischaemic preconditioning: Present position and future directions. *Cardiovasc. Res.* **1998**, *37*, 21–33. [CrossRef]
5. Heusch, G. Molecular basis of cardioprotection: Signal transduction in ischemic pre-, post-, and remote conditioning. *Circ. Res.* **2015**, *116*, 674–699. [CrossRef] [PubMed]
6. Yin, C.; Salloum, F.N.; Kukreja, R.C. A novel role of microRNA in late preconditioning: Upregulation of endothelial nitric oxide synthase and heat shock protein 70. *Circ. Res.* **2009**, *104*, 572–575. [CrossRef]
7. Varga, Z.V.; Zvara, A.; Faragó, N.; Kocsis, G.F.; Pipicz, M.; Gáspár, R.; Bencsik, P.; Görbe, A.; Csonka, C.; Puskás, L.G.; et al. MicroRNAs associated with ischemia-reperfusion injury and cardioprotection by ischemic pre- and postconditioning: ProtectomiRs. *Am. J. Physiol. Heart Circ. Physiol.* **2014**, *307*, H216–H227. [CrossRef]
8. Csonka, C.; Murlasits, Z.; Ferdinandy, P.; Csont, T. Ischemic stress adaptation of the myocardium in the disease states: Role of hyperlipidemia. In *Advances in Cardiomyocyte Research*; Nánási, P., Ed.; Transworld Research Network: Kerala, India, 2009; pp. 245–265.
9. Csonka, C.; Sárközy, M.; Pipicz, M.; Dux, L.; Csont, T. Modulation of Hypercholesterolemia-Induced Oxidative/Nitrative Stress in the Heart. *Oxid. Med. Cell. Longev.* **2016**, *2016*, 3863726. [CrossRef]
10. Csont, T.; Bereczki, E.; Bencsik, P.; Fodor, G.; Görbe, A.; Zvara, A.; Csonka, C.; Puskás, L.G.; Sántha, M.; Ferdinandy, P. Hypercholesterolemia increases myocardial oxidative and nitrosative stress thereby leading to cardiac dysfunction in apoB-100 transgenic mice. *Cardiovasc. Res.* **2007**, *76*, 100–109. [CrossRef]
11. Varga, Z.V.; Kupai, K.; Szűcs, G.; Gáspár, R.; Pálóczi, J.; Faragó, N.; Zvara, A.; Puskás, L.G.; Rázga, Z.; Tiszlavicz, L.; et al. MicroRNA-25-dependent up-regulation of NADPH oxidase 4 (NOX4) mediates hypercholesterolemia-induced oxidative/nitrative stress and subsequent dysfunction in the heart. J. Mol. *Cell. Cardiol.* **2013**, *62*, 111–121. [CrossRef]
12. Yang, J.-S.; Phillips, M.D.; Betel, D.; Mu, P.; Ventura, A.; Siepel, A.C.; Chen, K.C.; Lai, E.C. Widespread regulatory activity of vertebrate microRNA* species. *RNA N. Y. N* **2011**, *17*, 312–326. [CrossRef] [PubMed]
13. Ohanian, M.; Humphreys, D.T.; Anderson, E.; Preiss, T.; Fatkin, D. A heterozygous variant in the human cardiac miR-133 gene, MIR133A2, alters miRNA duplex processing and strand abundance. *BMC Genet.* **2013**, *14*, 18. [CrossRef] [PubMed]
14. Li, Q.; Qin, M.; Li, T.; Gu, Z.; Tan, Q.; Huang, P.; Ren, L. Rutin protects against pirarubicin-induced cardiotoxicity by adjusting microRNA-125b-1-3p-mediated JunD signaling pathway. *Mol. Cell. Biochem.* **2020**, *466*, 139–148. [CrossRef] [PubMed]
15. Wang, X.; Ha, T.; Zou, J.; Ren, D.; Liu, L.; Zhang, X.; Kalbfleisch, J.; Gao, X.; Williams, D.; Li, C. MicroRNA-125b protects against myocardial ischaemia/reperfusion injury via targeting p53-mediated apoptotic signalling and TRAF6. *Cardiovasc. Res.* **2014**, *102*, 385–395. [CrossRef]
16. Bayoumi, A.S.; Park, K.-M.; Wang, Y.; Teoh, J.-P.; Aonuma, T.; Tang, Y.; Su, H.; Weintraub, N.L.; Kim, I.-M. A carvedilol-responsive microRNA, miR-125b-5p protects the heart from acute myocardial infarction by repressing pro-apoptotic bak1 and klf13 in cardiomyocytes. *J. Mol. Cell. Cardiol.* **2018**, *114*, 72–82. [CrossRef]

17. Xiao, C.; Wang, K.; Xu, Y.; Hu, H.; Zhang, N.; Wang, Y.; Zhong, Z.; Zhao, J.; Li, Q.; Zhu, D.; et al. Transplanted Mesenchymal Stem Cells Reduce Autophagic Flux in Infarcted Hearts via the Exosomal Transfer of miR-125b. *Circ. Res.* **2018**, *123*, 564–578. [CrossRef]
18. Zhu, L.-P.; Tian, T.; Wang, J.-Y.; He, J.-N.; Chen, T.; Pan, M.; Xu, L.; Zhang, H.-X.; Qiu, X.-T.; Li, C.-C.; et al. Hypoxia-elicited mesenchymal stem cell-derived exosomes facilitates cardiac repair through miR-125b-mediated prevention of cell death in myocardial infarction. *Theranostics* **2018**, *8*, 6163–6177. [CrossRef]
19. Nagpal, V.; Rai, R.; Place, A.T.; Murphy, S.B.; Verma, S.K.; Ghosh, A.K.; Vaughan, D.E. MiR-125b Is Critical for Fibroblast-to-Myofibroblast Transition and Cardiac Fibrosis. *Circulation* **2016**, *133*, 291–301. [CrossRef]
20. Bie, Z.-D.; Sun, L.-Y.; Geng, C.-L.; Meng, Q.-G.; Lin, X.-J.; Wang, Y.-F.; Wang, X.-B.; Yang, J. MiR-125b regulates SFRP5 expression to promote growth and activation of cardiac fibroblasts. *Cell Biol. Int.* **2016**, *40*, 1224–1234. [CrossRef]
21. Wang, Y.; Ma, W.; Lu, S.; Yan, L.; Hu, F.; Wang, Z.; Cheng, B. Androgen receptor regulates cardiac fibrosis in mice with experimental autoimmune myocarditis by increasing microRNA-125b expression. *Biochem. Biophys. Res. Commun.* **2018**, *506*, 130–136. [CrossRef]
22. Ferdinandy, P.; Szilvássy, Z.; Horváth, L.I.; Csont, T.; Csonka, C.; Nagy, E.; Szentgyörgyi, R.; Nagy, I.; Koltai, M.; Dux, L. Loss of pacing-induced preconditioning in rat hearts: Role of nitric oxide and cholesterol-enriched diet. *J. Mol. Cell. Cardiol.* **1997**, *29*, 3321–3333. [CrossRef] [PubMed]
23. Ungi, I.; Ungi, T.; Ruzsa, Z.; Nagy, E.; Zimmermann, Z.; Csont, T.; Ferdinandy, P. Hypercholesterolemia attenuates the anti-ischemic effect of preconditioning during coronary angioplasty. *Chest* **2005**, *128*, 1623–1628. [CrossRef] [PubMed]
24. Giricz, Z.; Lalu, M.M.; Csonka, C.; Bencsik, P.; Schulz, R.; Ferdinandy, P. Hyperlipidemia attenuates the infarct size-limiting effect of ischemic preconditioning: Role of matrix metalloproteinase-2 inhibition. *J. Pharmacol. Exp. Ther.* **2006**, *316*, 154–161. [CrossRef] [PubMed]
25. Ueda, Y.; Kitakaze, M.; Komamura, K.; Minamino, T.; Asanuma, H.; Sato, H.; Kuzuya, T.; Takeda, H.; Hori, M. Pravastatin restored the infarct size-limiting effect of ischemic preconditioning blunted by hypercholesterolemia in the rabbit model of myocardial infarction. *J. Am. Coll. Cardiol.* **1999**, *34*, 2120–2125. [CrossRef]
26. Iliodromitis, E.K.; Zoga, A.; Vrettou, A.; Andreadou, I.; Paraskevaidis, I.A.; Kaklamanis, L.; Kremastinos, D.T. The effectiveness of postconditioning and preconditioning on infarct size in hypercholesterolemic and normal anesthetized rabbits. *Atherosclerosis* **2006**, *188*, 356–362. [CrossRef]
27. Heusch, G.; Musiolik, J.; Gedik, N.; Skyschally, A. Mitochondrial STAT3 activation and cardioprotection by ischemic postconditioning in pigs with regional myocardial ischemia/reperfusion. *Circ. Res.* **2011**, *109*, 1302–1308. [CrossRef]
28. Wang, C.; Li, H.; Wang, S.; Mao, X.; Yan, D.; Wong, S.S.; Xia, Z.; Irwin, M.G. Repeated Non-Invasive Limb Ischemic Preconditioning Confers Cardioprotection Through PKC-ϵ/STAT3 Signaling in Diabetic Rats. Cell. Physiol. Biochem. Int. J. Exp. Cell. Physiol. *Biochem. Pharmacol.* **2018**, *45*, 2107–2121. [CrossRef]
29. Zhang, J.; Bian, H.-J.; Li, X.-X.; Liu, X.-B.; Sun, J.-P.; Li, N.; Zhang, Y.; Ji, X.-P. ERK-MAPK signaling opposes rho-kinase to reduce cardiomyocyte apoptosis in heart ischemic preconditioning. *Mol. Med. Camb. Mass* **2010**, *16*, 307–315. [CrossRef]
30. Chen, P.-J.; Shang, A.-Q.; Yang, J.-P.; Wang, W.-W. microRNA-874 inhibition targeting STAT3 protects the heart from ischemia-reperfusion injury by attenuating cardiomyocyte apoptosis in a mouse model. *J. Cell. Physiol.* **2019**, *234*, 6182–6193. [CrossRef]
31. Bellis, A.; Castaldo, D.; Trimarco, V.; Monti, M.G.; Chivasso, P.; Sadoshima, J.; Trimarco, B.; Morisco, C. Cross-talk between PKA and Akt protects endothelial cells from apoptosis in the late ischemic preconditioning. Arterioscler. Thromb. *Vasc. Biol.* **2009**, *29*, 1207–1212. [CrossRef]
32. Yang, C.; Talukder, M.A.H.; Varadharaj, S.; Velayutham, M.; Zweier, J.L. Early ischaemic preconditioning requires Akt- and PKA-mediated activation of eNOS via serine1176 phosphorylation. *Cardiovasc. Res.* **2013**, *97*, 33–43. [CrossRef] [PubMed]
33. Ferdinandy, P.; Csonka, C.; Csont, T.; Szilvássy, Z.; Dux, L. Rapid pacing-induced preconditioning is recaptured by farnesol treatment in hearts of cholesterol-fed rats: Role of polyprenyl derivatives and nitric oxide. *Mol. Cell. Biochem.* **1998**, *186*, 27–34. [CrossRef]

34. Pipicz, M.; Demján, V.; Sárközy, M.; Csont, T. Effects of Cardiovascular Risk Factors on Cardiac STAT3. *Int. J. Mol. Sci.* **2018**, *19*, 3572. [CrossRef] [PubMed]
35. Csonka, C.; Kupai, K.; Bencsik, P.; Görbe, A.; Pálóczi, J.; Zvara, A.; Puskás, L.G.; Csont, T.; Ferdinandy, P. Cholesterol-enriched diet inhibits cardioprotection by ATP-sensitive K+ channel activators cromakalim and diazoxide. *Am. J. Physiol. Heart Circ. Physiol.* **2014**, *306*, H405–H413. [CrossRef] [PubMed]
36. Kocsis, G.F.; Sárközy, M.; Bencsik, P.; Pipicz, M.; Varga, Z.V.; Pálóczi, J.; Csonka, C.; Ferdinandy, P.; Csont, T. Preconditioning protects the heart in a prolonged uremic condition. *Am. J. Physiol. Heart Circ. Physiol.* **2012**, *303*, H1229–H1236. [CrossRef] [PubMed]
37. Pipicz, M.; Varga, Z.V.; Kupai, K.; Gáspár, R.; Kocsis, G.F.; Csonka, C.; Csont, T. Rapid ventricular pacing-induced postconditioning attenuates reperfusion injury: Effects on peroxynitrite, RISK and SAFE pathways. *Br. J. Pharmacol.* **2015**, *172*, 3472–3483. [CrossRef] [PubMed]
38. Csonka, C.; Kupai, K.; Kocsis, G.F.; Novák, G.; Fekete, V.; Bencsik, P.; Csont, T.; Ferdinandy, P. Measurement of myocardial infarct size in preclinical studies. *J. Pharmacol. Toxicol. Methods* **2010**, *61*, 163–170. [CrossRef]
39. Csont, T.; Sárközy, M.; Szűcs, G.; Szűcs, C.; Bárkányi, J.; Bencsik, P.; Gáspár, R.; Földesi, I.; Csonka, C.; Kónya, C.; et al. Effect of a multivitamin preparation supplemented with phytosterol on serum lipids and infarct size in rats fed with normal and high cholesterol diet. *Lipids Health Dis.* **2013**, *12*, 138. [CrossRef]
40. Martin, M. Cutadapt removes adapter sequences from high-throughput sequencing reads. *EMBnet J.* **2011**, *17*, 10–12. [CrossRef]
41. Friedländer, M.R.; Mackowiak, S.D.; Li, N.; Chen, W.; Rajewsky, N. miRDeep2 accurately identifies known and hundreds of novel microRNA genes in seven animal clades. *Nucleic Acids Res.* **2012**, *40*, 37–52. [CrossRef]
42. Anders, S.; Huber, W. Differential expression analysis for sequence count data. *Genome Biol.* **2010**, *11*, R106. [CrossRef] [PubMed]
43. Gáspár, R.; Pipicz, M.; Hawchar, F.; Kovács, D.; Djirackor, L.; Görbe, A.; Varga, Z.V.; Kiricsi, M.; Petrovski, G.; Gácser, A.; et al. The cytoprotective effect of biglycan core protein involves Toll-like receptor 4 signaling in cardiomyocytes. *J. Mol. Cell. Cardiol.* **2016**, *99*, 138–150. [CrossRef] [PubMed]
44. Sárközy, M.; Gáspár, R.; Zvara, Á.; Siska, A.; Kővári, B.; Szűcs, G.; Márványkövi, F.; Kovács, M.G.; Diószegi, P.; Bodai, L.; et al. Chronic kidney disease induces left ventricular overexpression of the pro-hypertrophic microRNA-212. *Sci. Rep.* **2019**, *9*, 1302. [CrossRef] [PubMed]
45. Sárközy, M.; Gáspár, R.; Zvara, Á.; Kiscsatári, L.; Varga, Z.; Kővári, B.; Kovács, M.G.; Szűcs, G.; Fábián, G.; Diószegi, P.; et al. Selective Heart Irradiation Induces Cardiac Overexpression of the Pro-hypertrophic miR-212. *Front. Oncol.* **2019**, *9*. [CrossRef] [PubMed]

II.

International Journal of
Molecular Sciences

MDPI

Article

Diet-Induced Hypercholesterolemia Leads to Cardiac Dysfunction and Alterations in the Myocardial Proteome

Márton Richárd Szabó [1,2], Márton Pipicz [1,2], Márta Sárközy [1,2], Bella Bruszel [2,3], Zoltán Szabó [2,3] and Tamás Csont [1,2,*]

[1] Department of Biochemistry, Albert Szent-Györgyi Medical School, University of Szeged, H-6720 Szeged, Hungary; szabo.marton@med.u-szeged.hu (M.R.S.); pipicz.marton@med.u-szeged.hu (M.P.); sarkozy.marta@med.u-szeged.hu (M.S.)
[2] Interdisciplinary Centre of Excellence, University of Szeged, H-6720 Szeged, Hungary; bruszelbella@gmail.com (B.B.); szabo.zoltan@med.u-szeged.hu (Z.S.)
[3] Institute of Medical Chemistry, Albert Szent-Györgyi Medical School, University of Szeged, H-6720 Szeged, Hungary
* Correspondence: csont.tamas@med.u-szeged.hu

Abstract: Elevated blood cholesterol is a major risk factor for coronary heart disease. Moreover, direct effects on the myocardium also contribute to the adverse effects of hypercholesterolemia. Here, we investigated the effect of hypercholesterolemia on the cardiac proteome. Male Wistar rats were fed with a laboratory rodent chow supplemented with 2% cholesterol for 8 weeks to induce hypercholesterolemia. The protein expression data obtained from the proteomic characterization of left ventricular samples from normo- and hypercholesterolemic animals were subjected to gene ontology (GO) and protein interaction analyses. Elevated circulating cholesterol levels were accompanied by diastolic dysfunction in cholesterol-fed rats. The proteomic characterization of left ventricular samples revealed altered expression of 45 proteins due to hypercholesterolemia. Based on the Gene Ontology analysis, hypercholesterolemia was associated with disturbed expression of cytoskeletal and contractile proteins. Beta-actin was downregulated in the hypercholesterolemic myocardium, and established a prominent hub of the protein interaction network. Analysis of the unfiltered dataset revealed concordant downregulated expression patterns in proteins associated with the arrangement of the contractile system (e.g., cardiac-specific troponins and myosin complex), and in subunits of the mitochondrial respiratory chain. We conclude that the observed changes in the cardiac proteome may contribute to the development of diastolic dysfunction in hypercholesterolemia.

Keywords: hypercholesterolemia; myocardial proteomics; network analysis; cardiac dysfunction; mitochondrial respiratory chain; contractile proteins

Citation: Szabó, M.R.; Pipicz, M.; Sárközy, M.; Bruszel, B.; Szabó, Z.; Csont, T. Diet-Induced Hypercholesterolemia Leads to Cardiac Dysfunction and Alterations in the Myocardial Proteome. *Int. J. Mol. Sci.* **2022**, *23*, 7387. https://doi.org/10.3390/ijms23137387

Academic Editors: Manikandan Panchatcharam, Sumitra Miriyala, Ara Hosne

Received: 10 June 2022
Accepted: 28 June 2022
Published: 2 July 2022

1. Introduction

Metabolic disorders, e.g., dyslipidemia, diabetes mellitus, or metabolic syndrome, are major risk factors for ischemic heart diseases [1]. Imbalance in the lipid metabolism, especially sustained hypercholesterolemia, contributes to the development of cardiovascular diseases through the formation of atherosclerosis and subsequent acute ischemic events [2]. Moreover, independent of the vascular effects, hypercholesterolemia exerts direct adverse effects on the myocardium, which further impair cardiac function and stress tolerance [3–6]. Previous studies reported the presence of mild diastolic dysfunction and blunted adaptation to ischemia in rodent models of diet-induced hypercholesterolemia [7,8].

Despite the well-known adverse cardiac effects of hypercholesterolemia, the underlying molecular mechanisms and involved pathways are still not fully understood. Previous studies suggested that deteriorated mitochondrial function was possibly related to

the adverse cardiac effects of hypercholesterolemia [9,10]. Moreover, endothelial dysfunction and enhanced oxidative damage-related mechanisms, such as increased NADPH oxidase activity [3,4], were also implied in the direct cardiac consequences of hypercholesterolemia.

The recent advances in the field of 'omics' methods provide a great and effective tool for the high-throughput screening and molecular profiling of different diseases. Microarray screening revealed transcriptomic alterations in the myocardium induced by hyperlipidemia and metabolic syndrome, showing altered expression of genes related to energy production, structural development, and stress [11–13]. However, to date, there are no comprehensive data regarding the global left ventricular proteome changes in the setting of hypercholesterolemia. Therefore, in the present study, we aimed to investigate the global changes in the left ventricular proteome in a rat model of diet-induced hypercholesterolemia using shotgun proteomic analyses. Subsequently, bioinformatic analyses (pathway enrichment and protein interaction analyses) were performed on the proteomic data in order to elucidate the potential underlying molecular mechanisms and pathways regarding the direct adverse cardiac effects of hypercholesterolemia.

2. Results

2.1. Eight Weeks of Cholesterol-Enriched Diet in Rats Resulted in Elevated Plasma Lipid Levels

At the end of an 8-week feeding period, there was no difference in the body weight and the left ventricular tissue weight of the animals receiving a cholesterol-enriched diet or a standard diet (Table 1). However, the total plasma cholesterol was markedly elevated in the cholesterol-fed group, supporting the manifestation of diet-induced hypercholesterolemia. Interestingly, the plasma total triacylglycerol level also increased significantly in the hypercholesterolemic group compared with the control rats.

Table 1. Cholesterol-enriched-diet-induced high blood cholesterol. General characterization of normocholesterolemic (Normochol) and hypercholesterolemic (Hyperchol) rats after the 8-week diet period. * $p < 0.05$; $n = 6$.

	Normochol	Hyperchol
Body weight (g)	485 ± 22	521 ± 17
Tibia length (cm)	4.20 ± 0.08	4.21 ± 0.05
Left ventricular weight (mg)	1242 ± 42	1230 ± 48
Total cholesterol (mmol/L)	1.52 ± 0.11	4.35 ± 0.21 *
Total triglyceride (mmol/L)	0.44 ± 0.03	1.18 ± 0.08 *

2.2. Cholesterol-Enriched-Diet-Induced Diastolic Dysfunction in the Heart

Transthoracic echocardiography was performed at the end of the feeding period to investigate the morphological and functional effects of diet-induced hypercholesterolemia on the myocardium. After 8 weeks of the diet, the cardiac morphology remained unaffected, as shown by the systolic and diastolic wall thickness parameters (Table 2). Furthermore, there were no differences in the left ventricular end-diastolic and end-systolic diameters, fractional shortening, and ejection fraction, respectively, which indicate preserved left ventricular systolic function (Table 2). Interestingly, the heart rate was significantly decreased in the settings of hypercholesterolemia. The early (E) and late (A) ventricular filling velocities showed a trend toward a decrease; however, the E/A ratio was significantly elevated in the hearts of hypercholesterolemic animals, suggesting impaired diastolic function (Table 2). The presence of diastolic dysfunction was further supported by the significantly decreased values of the mitral annulus velocity (e') and mitral valve deceleration time in the hypercholesterolemic rats. Nevertheless, the E/e' ratio was not affected significantly (Table 2).

Table 2. Diet-induced hypercholesterolemia leads to cardiac dysfunction. Left ventricular morphological and functional parameters examined by echocardiography after the 8-week diet period in both normocholesterolemic (Normochol) and hypercholesterolemic (Hyperchol) rats. Values are the mean ± SEM (n = 6), * $p < 0.05$. AWT: anterior wall thickness, d: diastolic, MV A: late (atrial) ventricular filling velocity measured at the mitral valve, MV E: early ventricular filling velocity measured at the mitral valve, e': septal mitral annular velocity, EF: ejection fraction, FS: fractional shortening, IWT: inferior wall thickness, LVEDD: left ventricular end-diastolic diameter, LVESD: left ventricular end-systolic diameter, PWT: posterior wall thickness, s: systolic, and SWT: septal wall thickness.

	Normochol	**Hyperchol**	***p*-Value**
AWTs (mm)	3.86 ± 0.01	3.74 ± 0.13	0.471
AWTd (mm)	2.03 ± 0.10	2.17 ± 0.13	0.420
IWTs (mm)	3.88 ± 0.12	3.62 ± 0.13	0.154
IWTd (mm)	2.39 ± 0.13	2.30 ± 0.14	0.660
PWTs (mm)	3.71 ± 0.09	3.70 ± 0.22	0.938
PWTd (mm)	2.46 ± 0.20	2.43 ± 0.13	0.902
SWTs (mm)	3.81 ± 0.05	3.69 ± 0.13	0.442
SWTd (mm)	2.18 ± 0.06	2.27 ± 0.13	0.548
LVESD (mm)	2.39 ± 0.10	2.85 ± 0.28	0.155
LVEDD (mm)	6.32 ± 0.30	6.72 ± 0.25	0.343
FS (%)	62.06 ± 1.43	63.89 ± 4.06	0.679
EF (%)	93.61 ± 0.63	90.56 ± 2.18	0.209
MV E velocity (m/s)	1.28 ± 0.19	0.80 ± 0.14	0.067
MV A velocity (m/s)	0.95 ± 0.16	0.50 ± 0.16	0.076
E/A	1.39 ± 0.06	1.81 ± 0.17 *	0.043
e' (m/s)	0.06 ± 0.00	0.04 ± 0.00 *	0.005
E/e'	20.78 ± 3.38	20.08 ± 3.80	0.894
E deceleration time	79.00 ± 9.08	51.56 ± 6.12 *	0.031
Heart rate (1/min)	350.33 ± 10.89	323.50 ± 5.00 *	0.049

2.3. General Proteomic Characterization of the Left Ventricle of Hypercholesterolemic Rats

Altogether, 901 proteins were reliably identified from left ventricular samples by means of mass spectrometry. Statistical analysis (Welch's *t*-test) performed on the identified proteins revealed altered levels ($p < 0.05$) of 75 proteins due to hypercholesterolemia. Proteins showing $p < 0.05$ and >1.2 or <0.83-fold changes in response to hypercholesterolemia were considered as significant alterations and used for further network analysis. Based on these criteria, we observed the upregulation of 23 proteins and downregulation of 22 in the left ventricle of hypercholesterolemic animals compared with the normocholesterolemic controls (Figure 1; Table 3).

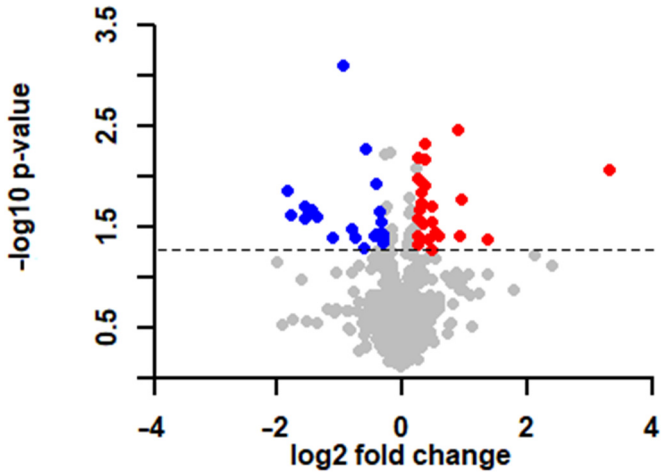

Figure 1. Diet-induced hypercholesterolemia leads to alterations in the myocardial proteome. Volcano plot showing the significantly ($p < 0.05$ of Welch's *t*-test, 1.2< and <0.83-fold changes) altered proteins induced by hypercholesterolemia in the left ventricles of rats. Each dot represents one distinct protein. The downregulated (blue) and upregulated (red) proteins are highlighted in the plot. The dashed line indicates the threshold value of significance ($-\log_{10}$ 1.3<) The differentially expressed proteins are listed in Table 3.

Table 3. List of hypercholesterolemia-induced significant alterations in the left ventricular proteins. Proteins with fold changes of >1.2 or <0.83 were considered as significant. The fold change values are shown as ratio pairs.

UniProt ID	Gene Symbol	Protein Name	Fold Change
P09895	*Rpl5*	60S ribosomal protein L5	2.60
Q03626	*Mug1*	Murinoglobulin-1	1.96
O35814	*Stip1*	Stress-induced-phosphoprotein 1	1.91
P09006	*Serpina3n*	Serine protease inhibitor A3N	1.90
P52873	*Pc*	Pyruvate carboxylase	1.54
P02680	*Fgg*	Fibrinogen gamma chain	1.45
P02564	*Myh7*	Myosin-7	1.42
P06399	*Fga*	Fibrinogen alpha chain	1.42
P01026	*C3*	Complement C3	1.35
D3ZWC6	*Sntb1*	Syntrophin, basic 1	1.31
P25113	*Pgam1*	Phosphoglycerate mutase 1	1.30
P29147	*Bdh1*	D-beta-hydroxybutyrate dehydrogenase	1.30
Q68FP1	*Gsn*	Gelsolin	1.29
P05545	*Serpina3k*	Serine protease inhibitor A3K	1.27
Q5RKI0	*Wdr1*	WD repeat-containing protein 1	1.27
P07335	*Ckb*	Creatine kinase B-type	1.25
A0A0G2K542	*Ugp2*	UTP--glucose-1-phosphate uridylyltransferase	1.22
Q99PD4	*Arpc1a*	Actin-related protein 2/3 complex subunit 1A	1.22
P50137	*Tkt*	Transketolase	1.22
D4A5W5	*Recql4*	RecQ-like helicase 4	1.22
P63102	*Ywhaz*	14-3-3 protein zeta/delta	1.21
P61589	*Rhoa*	Transforming protein RhoA	1.21
Q08163	*Cap1*	Adenylyl cyclase-associated protein 1	1.21
G3V885	*Myh6*	Myosin-6	0.83
Q925Q9	*Sh3kbp1*	SH3 domain-containing kinase-binding protein 1	0.83

F1LNF0	*Myh14*	Myosin heavy chain 14	0.83
F1M7L9		Uncharacterized protein	0.82
P38650	*Dync1h1*	Cytoplasmic dynein 1 heavy chain 1	0.81
Q925F0	*Smpx*	Small muscular protein	0.78
O35115	*Fhl2*	Four and a half LIM domains protein 2	0.77
P02401	*Rplp2*	60S acidic ribosomal protein P2	0.77
Q6PCU8	*Ndufv3*	NADH dehydrogenase [ubiquinone] flavoprotein 3	0.76
P41123	*Rpl13*	60S ribosomal protein L13	0.76
Q5XIG9	*Mtfp1*	Mitochondrial fission process 1	0.74
P02650	*Apoe*	Apolipoprotein E	0.68
P62902	*Rpl31*	60S ribosomal protein L31	0.66
C0KUC6	*Lims1*	LIM and senescent cell antigen-like-containing domain protein	0.61
Q924S5	*Lonp1*	Lon protease homolog	0.58
P02466	*Col1a2*	Collagen alpha-2(I) chain	0.52
P60711	*Actb*	Beta-actin	0.47
A0A0G2K1W9	*Ldhd*	Lactate dehydrogenase D	0.37
M0RB63	*LOC684509*	NADH-ubiquinone oxidoreductase B9 subunit	0.34
A0A0G2KAA3	*Ndufa3*	NADH:ubiquinone oxidoreductase subunit A3	0.34
P13697	*Me1*	NADP-dependent malic enzyme	0.34
Q9QZA6	*Cd151*	CD151 antigen	0.28

2.4. Pathway Enrichment Analysis of the Significantly Altered Proteins Revealed Changes in the Contractile and Cytoskeletal Systems

In order to assign biological functions and reveal potential networks for the significantly changed proteins, Gene Ontology (GO) and subsequent pathway enrichment analyses were carried out. The GO analysis covered all three independent ontology categories, including molecular function (MF), biological process (BP), and cellular component (CC). We observed the enrichment of 31 GO terms at FDR < 0.1, altogether (Figure 2). Interestingly, according to the GO terminology, a substantial number of the enriched nodes were in the CC category, possibly indicating hypercholesterolemia-induced rearrangements of subcellular structures and macromolecular complexes in the left ventricle. Based on the GO analysis, the enriched ontology terms involved proteins associated with contractile function and cytoskeletal organization (Figure 2). Additionally, a minor enrichment of mitochondrial proteins was also observed (Figure 2). Overall, the involvement of the observed processes might contribute to the initiation of the subcellular structural remodeling and subsequent contractile impairment of the myocardium in hypercholesterolemic animals.

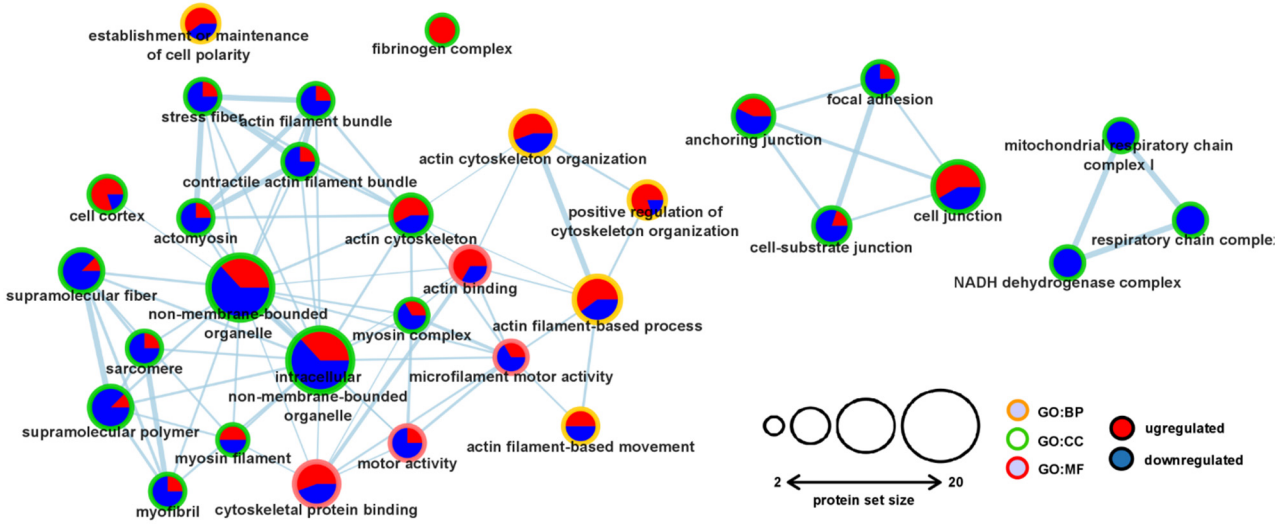

Figure 2. Pathway enrichment analysis revealed changes in the contractile and cytoskeletal systems. Significantly changed proteins were subjected to gene ontology (GO) and pathway enrichment analysis and visualized with Cytoscape v. 3.8.2. (Institute of Systems Biology, Seattle, WA, USA). The size of the nodes corresponds to the number of proteins falling into the respective category, while the GO terminologies are marked as differently colored borders (MF: molecular function, BP: biological process, CC: cellular component). Edges (lines) represent overlaps and functional interactions among the nodes. The width of each edge corresponds to the similarity score between the nodes. The numbers of up (red) and downregulated (blue) proteins were incorporated into the nodes as pie charts.

2.5. Functional Interaction Analysis of the Differentially Expressed Proteins

As the next step, we assessed the functional interactions and conducted subsequent cluster analysis within the significantly altered proteins. Our analyses revealed a modest number of connections among the identified proteins (Figure 3). Interestingly, beta-actin (ACTB) was downregulated in the hypercholesterolemic myocardium and ACTB established a prominent hub of the revealed network (Figure 3). ACTB turned out to be connected to both structural and accessory proteins. Among these interactions, many proteins were upregulated, such as Actin-related protein 2/3 complex subunit 1A (ARPC1A), Adenylyl cyclase-associated protein 1 (CAP1), WD repeat-containing protein 1 (WDR1), Myosin-7 (MYH7), Gelsolin (GSN), and Ras homolog family member A (RHOA). At the same time, the levels of Myosin-6 (MYH6), Myosin heavy chain 14 (MYH14), Collagen type 1 alpha 2 chain (COL1A2), and Cytoplasmic dynein heavy chain 1 (DYNC1H1) were downregulated (Figure 3).

Additionally, the cluster analysis also revealed other minor subnetworks among the resulting interactions (Figure 3), which might implicate disturbed metabolic functions and subsequent energy production. For instance, the resulting functional interaction network contained metabolic enzymes with altered expressions, including Pyruvate carboxylase (PC), Phosphoglycerate mutase 1 (PGAM1), Transketolase (TKT), Creatine kinase (CKB), Malic enzyme 1 (ME1), and Lactate dehydrogenase (Figure 3). Moreover, three subunits of the mitochondrial NADH dehydrogenase complex (NDUFV3, NDUFA3, and LOC684509) showed significantly downregulated expression and formed one of the loops in the network (Figure 3). These subnetworks may suggest impaired mitochondrial function and imbalance in the energy production of the hypercholesterolemic myocardium.

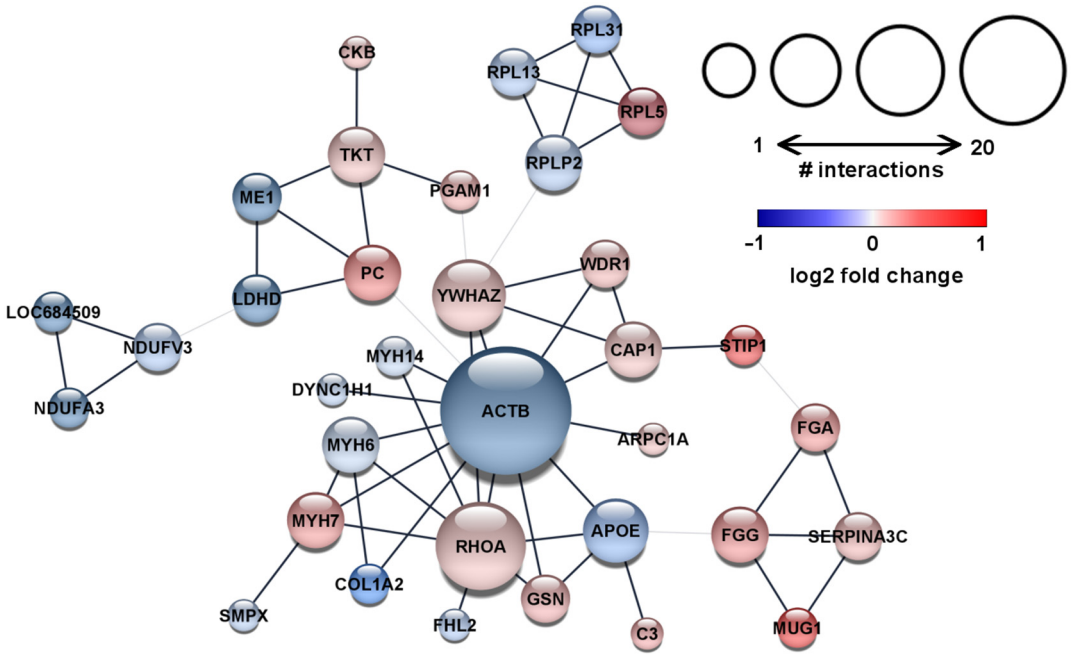

Figure 3. Downregulated beta-actin was established as a prominent hub of the protein interaction network in the hypercholesterolemic myocardium. Functional protein–protein interaction network and subsequent cluster analysis according to Markov Clustering Algorithm using the STRING database and the in-built plugin of Cytoscape. Each node (circle) represents one protein and is labeled according to gene IDs. The node size corresponds with the number of interactions of the respective protein. The color of each node indicates the fold change values (red for upregulated and blue for downregulated expression). Edges (grey lines) represent the interactions between nodes, with their thickness indicating interactions within the clusters (wide edges) or among the proteins in different clusters (narrow edges).

2.6. Protein-Specific Gene Set Enrichment Analysis Revealed Downregulated Expression Patterns of Mitochondrial and Contractile Proteins in the Unfiltered, Whole Left Ventricular Proteome

To reveal the potential associations between hypercholesterolemia-induced cardiac phenotype and classes of similarly changed proteins in the heart, gene set enrichment analysis (GSEA) was performed on the unfiltered, whole proteomic dataset. The GSEA identified similar downregulated expression patterns among the proteins related to specific pathways. The most prominent enrichment was observed in the GO terms associated with mitochondrial complexes, with particular emphasis on the elements of the respiratory chain complexes (Figure 4A). Additionally, our analysis revealed downregulated expression patterns of proteins previously assigned to heart development processes in the GO terminology (Figure 4A). Then, subsequent leading-edge analysis was carried out to determine which subsets of proteins contributed the most to the enriched GO terms. As expected, proteins of the respiratory chain complexes, i.e., subunits of the NADH:Ubiquinone Oxidoreductase complex (NDFU), were among the leading enrichment set (Figure 4B). Furthermore, another set of leading-edge proteins could be identified with important roles in normal cardiac contractile function (Figure 4B). For instance, downregulated expression patterns were observed in the case of cardiac-specific isoforms of the troponin complex, such as Troponin T2 (TNNT2), Troponin C1 (TNNC1), Troponin I3 (TNNI3), and Tropomyosin 1 (TPM1). Furthermore, hypercholesterolemia seemed to negatively affect the protein expression pattern of the ventricular isoform of myosin light chain (MYL3), as well as myosin heavy chain 6 (MYH6), which is preferably expressed in the ventricles of smaller mammals with rapid heart rates.

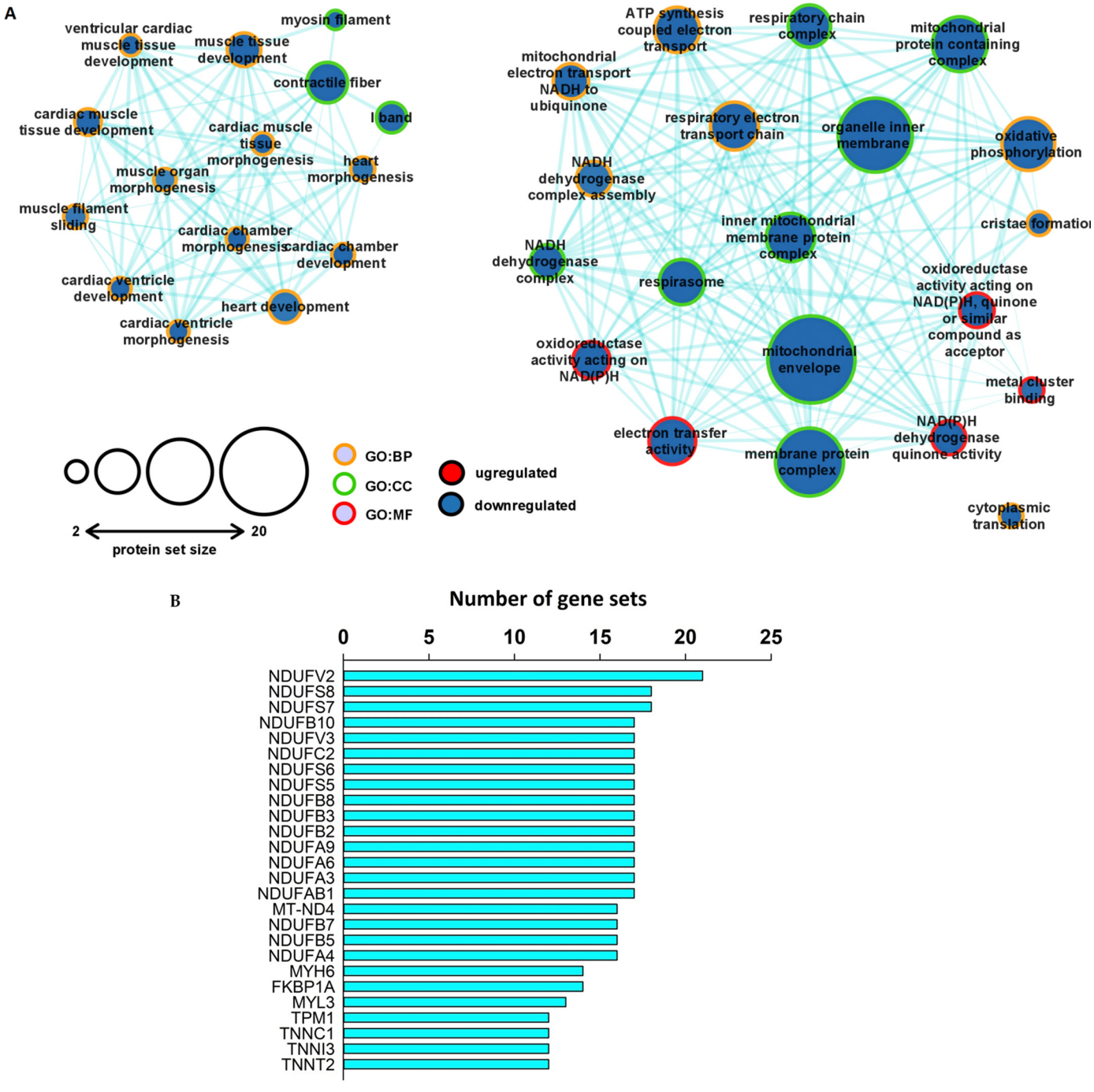

Figure 4. GSEA analysis of the unfiltered proteomic dataset revealed concordant downregulated expression patterns of proteins associated with the arrangement of the contractile and cytoskeletal system, as well as with the mitochondrial respiratory chain. (**A**) Enrichment map of the major GO sets influenced by hypercholesterolemia at the whole proteome level. Pathway enrichment analysis was performed with protein-specific GSEA. Circles represent enriched gene sets (nodes). The node size corresponds to the size of the number of proteins falling into a respective gene set category. The two node colors represent the trend of the quantitative change in the hypercholesterolemic left ventricle, while the color of the nodes' border indicates the respective GO category. Edges represent similarity among the gene sets, as the thickness of each edge corresponds to the overlap between the nodes. The enriched gene sets were visualized with Cytoscape v3.8.2. (**B**) Output of the leading-edge analysis of the enriched GO terms at FDR < 0.1 performed with GSEA. The numbers on the horizontal axis indicate the number of appearances of the respective protein in the significantly enriched subsets. The graph was created with SigmaPlot v.12.0.

2.7. KEGG Analysis of the Output of GSEA

In order to categorize the output protein list of the previous GSEA analysis, the core enrichment proteins from the significantly enriched gene sets were further analyzed according to the in-built Kyoto Encyclopedia of Genes and Genomes (KEGG) of the Pathview package. Proteins related to cardiac muscle contraction were affected, as shown by the concordant downregulated expression patterns of cardiac-specific troponins and myosin complex in the left ventricle of hypercholesterolemic animals (Figure 5). Additionally, the results of the KEGG-based analysis of our protein sets further support the possible deterioration of the mitochondrial function in the hypercholesterolemic left ventricle, affecting the expression of components of all the five major complexes of the respiratory chain system responsible for oxidative phosphorylation (Figure 6).

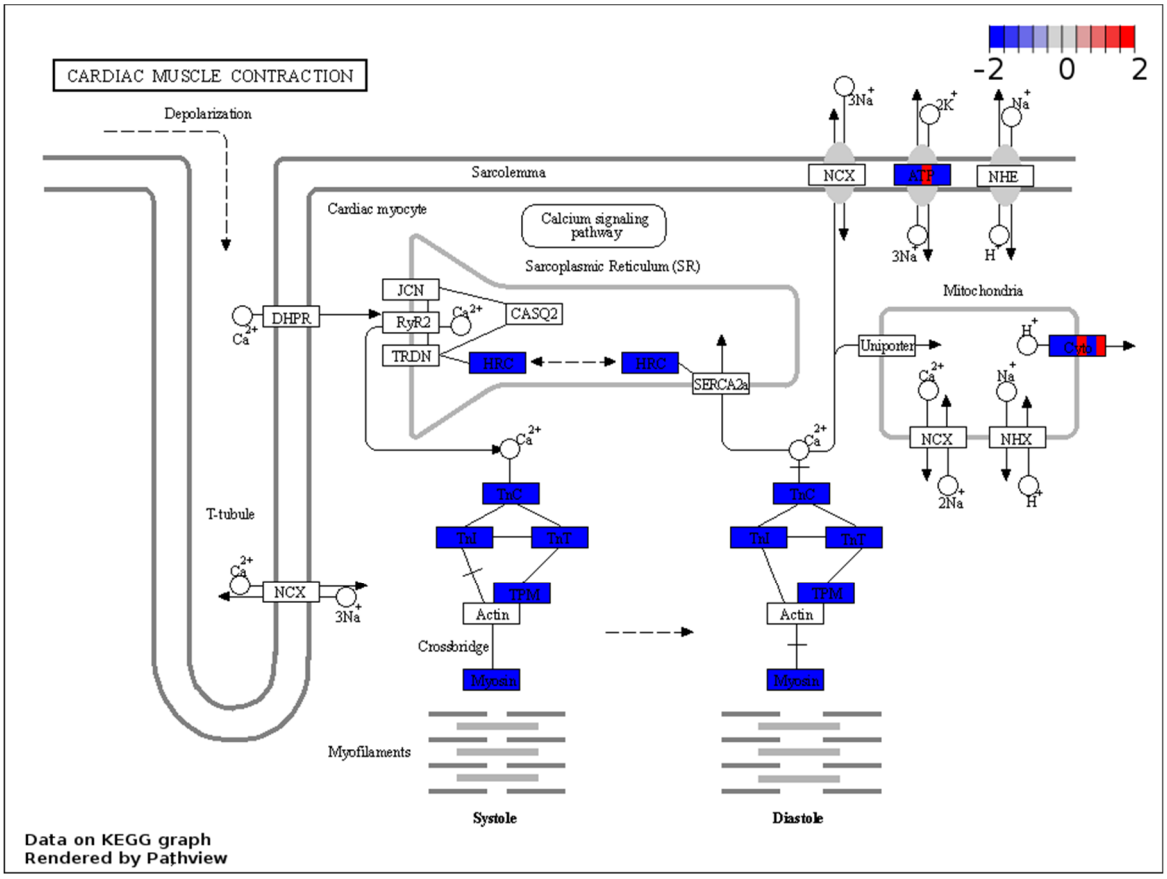

Figure 5. KEGG analysis showed concordant downregulated expression patterns of cardiac-specific troponins and the myosin complex. Visual representation of leading-edge protein subsets based on the Kyoto Encyclopedia of Genes and Genomes database. Each protein was divided into six sections and was colored based on the relative expression count compared with the normocholesterolemic group. Pathway graphs were created with Pathview Web (https://pathview.uncc.edu/home accessed on 17 January 2022).

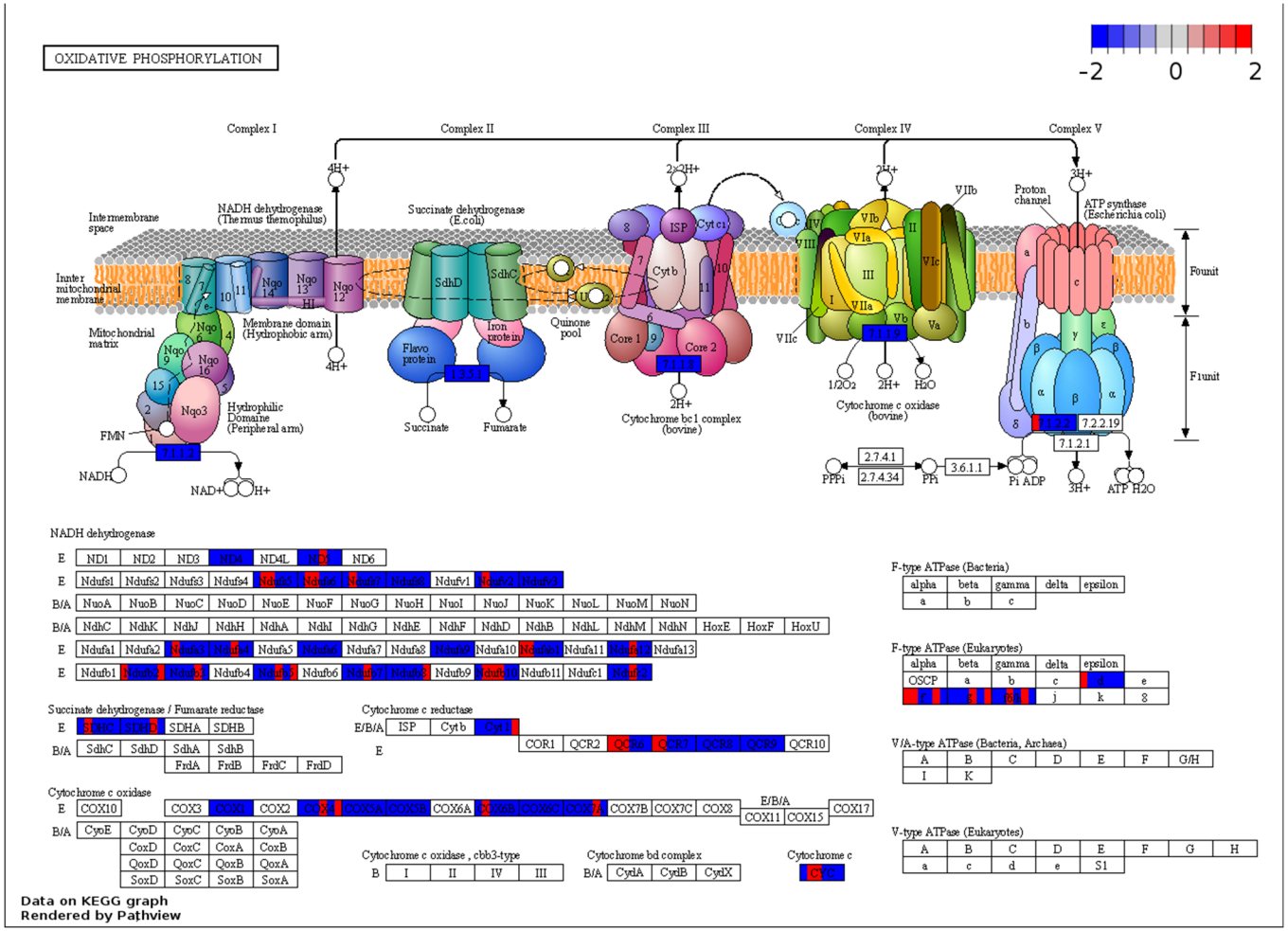

Figure 6. KEGG analysis showed concordant downregulated expression changes in protein components of the respiratory chain in the hypercholesterolemic left ventricle. Visual representation of leading-edge protein subsets based on the Kyoto Encyclopedia of Genes and Genomes database. Each protein was divided into six sections and was colored based on the relative expression count compared with the normocholesterolemic group. Pathway graphs were created with Pathview Web (https://pathview.uncc.edu/home accessed on 17 January 2022).

3. Discussion

In the present study, we investigated the effect of diet-induced hypercholesterolemia on the left ventricular proteome. To the best of our knowledge, this is the first proteomic study focusing on the myocardium of hypercholesterolemic animals. Our results show that chronic hypercholesterolemia alters the level of cardiac proteins related to the maintenance of cytoskeletal structure and energy-generation processes. Moreover, our enrichment and functional interaction analyses revealed solid networks among the identified proteins, thereby providing new aspects and deeper insights into the potential underlying subcellular mechanisms of the direct myocardial effects of hypercholesterolemia leading to cardiac dysfunction.

The general characterization and echocardiographic parameters demonstrating diastolic dysfunction in our experimental model are in accordance with previous reports from our laboratory and others using rodent models of diet-induced hypercholesterolemia [3,4,10,14,15]. In the present study, eight-week excess cholesterol uptake elevated the circulating cholesterol and resulted in diastolic cardiac dysfunction without any significant morphological changes in the heart. Previous studies suggested that hyperlipidemia, especially hypercholesterolemia, leads to the augmentation of oxidative and nitrosative stress and enhanced proinflammatory cytokine production (e.g., TNF-α and IL-6), consequently contributing to cardiac and endothelial dysfunction [3,4,16]. The related oxidative damage possibly involves contractile and cytoskeletal proteins and, hence, likely contributes to contractile impairment. The direct impact of increased plasma cholesterol on cardiac function is supported by both human and experimental animal investigations [8]. Echocardiographic characterization of patients with primary hypercholesterolemia or familial hypercholesterolemia without a history of cardiovascular disease disclosed subclinical myocardial abnormalities and contractility impairment [17,18]. Likewise, diminished cardiac function was also observed in hypercholesterolemic animals in vivo [19,20]. In accordance with the literature, our measured echocardiographic parameters suggest impaired diastolic function [21], while the ventricular wall thicknesses remained unaffected in the hypercholesterolemic myocardium, similar to previous studies [4,22].

Proteomic characterization of the hypercholesterolemic myocardium in the current study revealed modest quantitative changes in a substantial number of proteins, which is in accordance with other proteomics-based studies of the left ventricle with impaired contractile function [23,24]. One of the most notable changes in the level of an individual protein was observed in the case of the downregulated expression of ACTB, an essential component of the non-contractile cytoskeleton system. Similar to our results, metabolic perturbations, such as hyperglycemia and hyperlipidemia, reduced ACTB in both ventricles, which was associated with the further impairment of cellular elasticity and disorganized myocardial actin cytoskeleton [25–27]. Furthermore, in our study, MYH6 decreased, and MYH7 increased in the heart as a result of cholesterol feeding. The MYH6/MYH7 ratio is considered as a descriptive indicator of cardiac function, and the shift from MYH6 to MYH7 resulting in a decreased ratio indicated a maladaptive change in cardiac diseases [28–31]. The actin-activated ATPase activity of MYH6 is higher than that of MYH7, so both the relative and absolute repression of MYH6 may lead to compromised heart function [32].

Based on our GO analysis of the differentially expressed proteins, the resulting network indicates alterations in the contractile apparatus and cytoskeletal system of the hypercholesterolemic left ventricle. To date, this study is the first to propose that quantitative changes in myofibrillar proteins might also be responsible for the direct cardiac effects of hypercholesterolemia. Additionally, the protein–protein interaction network analysis of the significantly altered proteins further affirmed the influence of high cholesterol levels on cytoskeletal organization and structural development in the left ventricle. Interaction analysis showed that ACTB formed the hub of the revealed network, being involved in many interactions with other accessory proteins (e.g., with upregulated CAP1, WDR1,

GSN, RHOA, and ARPC1A), suggesting myocardial cytoskeleton rearrangement in response to hypercholesterolemia. These findings are in accordance with studies indicating the crucial role of actin assembly and disassembly dynamics in heart diseases [33,34].

A deeper analysis of the whole, unfiltered left ventricular proteome demonstrated that many protein sets are downregulated in the hypercholesterolemic heart. In accordance with the GO analysis restricted to the list of significantly altered proteins, contractile proteins showed similarly downregulated expression patterns in the hypercholesterolemic heart. Moreover, our results showed that hypercholesterolemia negatively influenced many protein components of the respiratory chain system in the heart, potentially leading to disturbances in energy supply and consequent contractile impairment. Although the individual expression of the majority of proteins in the enriched protein sets failed to meet the criteria of a significant change, the coordinated downregulation of these proteins as a group was significant. These findings are in line with other reports where impaired mitochondrial function was implicated in metabolic diseases, such as diabetes, obesity, and hypertension, accompanied by heart failure and dysfunction [35,36]. Similarly, the impairment of mitochondrial function is also implicated in the adverse cardiac effects of hypercholesterolemia [37]. Mitochondrial cholesterol accumulation is suggested to be a decisive factor for mitochondrial dysfunction, as increased cholesterol levels interfere with the normal function of mitochondrial membrane proteins and transporters [38]. Additionally, disturbed myocardial ATP synthesis and bioenergetics impairment are documented outcomes of a high-cholesterol diet [10], which might be associated with the downregulation of the elements of the respiratory chain complex.

Similar to all experimental investigations, our study is not without limitations. First of all, since we have applied a rodent model of hypercholesterolemia in our present study, further confirmation of our results is urged in the future in humans due to potential species-dependent differences in the cardiac effects of hypercholesterolemia. Moreover, we applied a shotgun proteomic analysis in the present study, which may have higher limits of detection than targeted approaches; however, it provides the possibility to obtain quantitative information about as many proteins as possible. Our study and the applied protocols were focused on the detection of differences in the expression of proteins, and the identification of possible changes in posttranslational modifications of proteins was outside of the scope of the present study. Future proof-of-concept studies are recommended to further confirm the causal role of the proteins or network of proteins identified in our study in diastolic dysfunction in the heart using targeted proteomics or immunochemical methods.

4. Materials and Methods

4.1. Animals

Altogether, 12 adult male Wistar rats were used in this study. The animals were kept in pairs in individually ventilated cages in a temperature-controlled room with 12 h:12 h light/dark cycles. Laboratory chow and water were supplied ad libitum throughout the study. The experiment conformed to the Guide for the Care and Use of Laboratory Animals published by the US National Institutes of Health (NIH publication No. 85-23, revised 1996) and was approved by the Animal Research Ethics Committee of the University of Szeged (approval code: XV.1181/2013-2018).

4.2. Experimental Setup

Hypercholesterolemia was induced as described previously [10,39]. Male Wistar rats were fed with laboratory chow enriched with 2% (*w*/*w*) cholesterol (Hungaropharma Zrt., Budapest, Hungary) and 0.25% (w/w) sodium–cholate hydrate (Sigma, St. Louis, MO, USA) for 8 weeks (n = 6), while rats fed with standard laboratory chow were used as the control (n = 6). At the end of the diet period, the rats were anesthetized by the intraperitoneal injection of pentobarbital sodium (Euthasol; 50 mg/kg; Produlab Pharma b.v.,

Raamsdonksveer, The Netherlands). Blood samples were collected from the thoracic aorta for plasma lipid measurements, and then hearts were immediately excised and placed in ice-cold Krebs–Henseleit buffer. The isolated hearts were cannulated and perfused with oxygenated Krebs–Henseleit buffer at 37 °C, according to Langendorff, in order to eliminate blood from the coronary vessels [39,40]. After 5 min of perfusion, the left ventricular tissue was frozen and stored at −80 °C until proteomic analysis. The body weight and tibia length were also measured.

4.3. Plasma Lipid Measurement

Blood samples were collected in EDTA-containing blood collection tubes. The plasma was separated by centrifugation (3000× *g* for 15 min at 4 °C). The upper, cell-free phase was used to determine the total cholesterol and triglyceride concentrations using a colorimetric detection method (Diagnosticum, Budapest, Hungary) with a microplate reader (BMG Labtech, Ortenberg, Germany). The plasma total cholesterol and triglyceride measurements were performed as described previously [39].

4.4. Transthoracic Echocardiography

Cardiac morphology and function were assessed by transthoracic echocardiography at week 8, as described previously [22,24]. The rats were anesthetized with 2% isoflurane (Forane, AESICA, Queenborough Limited, Kent, UK). Two-dimensional, M-mode, Doppler, tissue Doppler, and four-chamber-view images were performed according to the criteria of the American Society of Echocardiography with a Vivid IQ ultrasound system (General Electric Medical Systems, New York, NY, USA) using a phased array 5.0–11 MHz transducer (GE 12S-RS probe, General Electric Medical Systems, New York, NY, USA). Data of three consecutive heart cycles were analyzed (EchoPac Dimension software v201, General Electric Medical Systems, New York, NY, USA) by an experienced investigator in a blinded manner. The mean values of the three measurements were calculated and used for statistical evaluation. Systolic and diastolic wall thicknesses were obtained from the parasternal short-axis view at the level of the papillary muscles (anterior and inferior walls) and the long-axis view at the level of the mitral valve (septal and posterior walls). The left ventricular diameters were measured by means of M-mode echocardiography from long-axis and short-axis views between the endocardial borders. Functional parameters, including the ejection fraction and fractional shortening, were calculated on M-mode images in the long-axis view. Diastolic function was assessed using pulse-wave Doppler across the mitral valve and tissue Doppler on the septal mitral annulus from the apical four-chamber view. The early (E) and atrial (A) flow velocities, as well as septal mitral annulus velocity (e'), indicated diastolic function.

4.5. Protein Extraction

Approximately 30 mg of powered left ventricular tissue samples were homogenized in lysate buffer (containing 2% Sodium dodecyl sulfate (SDS) and 0.1 M Dithiothreitol (DTT) in 0.1 M Tris solution). The homogenized samples were incubated at 98 °C for 5 min. Proteins were precipitated by the addition of a methanol/chloroform mixture (4:1) and were resuspended in 8 M urea. The total protein contents were determined using the BCA (Thermo Scientific, Waltham, MA, USA) protocol.

4.6. Protein Digestion

Homogenates of all individual pulverized tissue samples containing 20 µg protein were diluted to 30 µL with 0.1 M NH_4HCO_3 (pH = 8.0) buffer, and then 15 µL 0.1% RapiGest SF (Waters) and 2 µL 100 mM DTT solution were added and the mixture was stored at 60 °C for 30 min to unfold and reduce the proteins. A volume of 2 µL 200 mM iodo-acetamide (IAA) solution was added to alkylate the proteins, which were kept for an

additional 30 min in the dark at room temperature. The samples were digested with trypsin (Promega, enzyme/protein ratio: 0.4/1) for 3 h at 37 °C. The digestion was stopped by the addition of 1 μL of concentrated hydrochloric acid. Pooled samples were created by mixing equal amounts of all digested samples to build a spectral library for quantitative liquid chromatography–mass spectrometry (LC-MS) analysis of individual samples.

4.7. LC-MS Analysis

The separation of the digested samples was carried out on a nanoAcquity Ultra Performance Liquid Chromatograph (UPLC, Waters, Milford, MA, USA) using a Waters ACQUITY UPLC M-Class Peptide C18 (130 Å, 1.78 μm, 75 μm×250 mm) column with a 90 min gradient. The eluents were water (A) and acetonitrile (B) containing 0.1 v/v% formic acid, and the separation of the peptide mixture was performed at 45 °C with a 0.35 μL/min flow rate using an optimized nonlinear LC gradient (3%–40% B). The LC was coupled to a high-resolution Q Exactive Plus quadrupole-orbitrap hybrid mass spectrometer (Thermo Scientific, Waltham, MA, USA). The measurements of the digested samples were performed in the DIA (Data Independent Acquisition) mode. The survey scan for the DIA method operated with a 35,000 resolution. The full scan was performed between 380 and 1020 m/z. The AGC target was set to 5×10^6 or 120 ms maximum injection time. In the 400–1000 m/z region, 22 m/z-wide overlapping isolation windows were acquired at 17,500 resolution (AGC target: 3×10^6 or 100 ms injection time, normalized collision energy: 30 for charge 2). Gas-phase fractionated (GPF) DIA measurements of the pooled samples were used to build a spectral library using the same settings, except for the m/z range. Four GPF LC-MS analyses of the pooled samples were run, each of them covering a 150 Th-wide fraction of the total 400–1000 m/z range using 6 m/z-wide overlapping isolation windows.

4.8. Proteomic Data Analysis

The quantitative analysis was performed in Encyclopedia 0.9 [41] using default settings. For the building of the GPF chromatogram library, a spectral library predicted by Prosit [42] from the UniProt rat reference proteome was used as the input. The quantitative samples were then analyzed using the empirically corrected GPF chromatogram library in Encyclopedia. The statistical evaluations were carried out using Perseus [43] software on text reports exported from Encyclopedia software. A $p < 0.05$ of the Welch's *t*-test and 1.2< and <0.83-fold change values were used as the criteria for significant changes. Protein quantification data and annotations from the UniProt database can be found in Table 3.

4.9. Pathway Enrichment Analysis

Pathway enrichment analysis was performed with the web-based g:Profiler public server using the g:GOSt tool (https://biit.cs.ut.ee/gprofiler accessed on 10 January 2022) [44]. Functional enrichment profiling was carried out, defining *Rattus norvegicus* as the queried organism, using the g:SCS multiple testing correction method and $p = 0.05$ as a threshold value. For the visualization of the results, the output gem file of the over-represented Gene Ontology Biological Process and Cellular Component terms were loaded to Cytoscape v3.8.2 [45]. An enrichment map was created with the EnrichmentMap v3.3.2. application of Cytoscape based on the instructions of Reimand and colleagues with <0.1 adjusted *p*-value similarity score [46].

4.10. Functional Protein–Protein Interaction and Network Clustering Analysis

Protein–protein interaction analysis among the identified proteins was performed with the STRING v11.5 database (https://string-db.org ELIXIR, Cambridge, UK, accessed on 31 December 2021) [47] using the default 0.4 medium confidence and 5% false discovery rate (FDR) stringency values. Without any modification, the resulting protein–protein

interaction chart was incorporated into Cytoscape and modified using the STRINGApp v1.7.0 and STRING Enrichment applications [48]. Cluster analysis was performed with clusterMaker2 v1.3.1 using the Markov Clustering Algorithm in Cytoscape. The clustering was based on the combined score calculated from the experimental and computational interaction values assigned by the STRING database.

4.11. Gene Set Enrichment Analysis of the Proteomic Dataset

Enriched gene sets from the whole, unfiltered proteomics data were explored with GSEA software v4.1.0 (joint project of UC San Diego, CA, USA and Broad Institute, Cambridge, MA, USA) [49]. After preprocessing to the requested format and the addition of appropriate phenotypes labels, the raw data were ranked according to the calculated fold change values, and GSEA was performed with all of the annotated ontology sets from the Molecular Signatures Database collections [50]. Only gene sets with FDR value 0.1 > were considered as significantly enriched. Interaction analysis was performed on only gene sets falling into FDR 0.1 > criteria and were visualized with Cytoscape as described in the previous sections. Subsequent leading-edge analysis was performed from the core enrichment proteins of the significantly enriched gene sets with the in-built plugin of the GSEA software.

4.12. KEGG Analysis and Visualization of Core Enrichment Proteins with Pathview

All the proteins that contributed to the core enrichment of the previously described GSEA analysis were further analyzed and classified according to the Kyoto Encyclopedia of Genes and Genome resource using Pathview Web (https://pathview.uncc.edu/home accessed on 17 January 2022). [51,52]. Proteins from the input list were colored according to the relative fold change values compared with the normocholesterolemic control group and then integrated into graphical images of the respective processes.

4.13. Statistics

All values are expressed as the mean + SEM (n = 6 in each group). Student's *t*-test was used to evaluate the effect of the cholesterol-enriched diet on the plasma lipid levels and echocardiographic measurements. For proteomic data, a two-one-sided test was used for the equivalence test, and the statistical significance was tested using the unpaired Welch test. Multiple testing correction was applied in pathway enriched analysis. A p value < 0.05 was considered as an indicator of significant difference among the groups.

5. Conclusions

We conclude that hypercholesterolemia leads to alterations in the left ventricular proteome, affecting both the structural and metabolic protein networks. Cholesterol feeding seemed to modify the cardiac cytoskeleton arrangement and contractile apparatus, and also impaired mitochondrial function. These alterations in the proteome may provide a feasible explanation for the mild cardiac dysfunction observed in hypercholesterolemia. The results of our network and enrichment analyses might contribute to a better understanding of how alterations in the proteome may contribute to cardiac dysfunction in the presence of metabolic risk factors.

Author Contributions: Conceptualization, T.C. and Z.S.; methodology, M.R.S., M.S., B.B., and Z.S.; formal analysis, M.R.S. and M.P.; writing—original draft preparation, M.R.S. and M.P.; writing—review and editing, T.C.; visualization, M.R.S.; funding acquisition, T.C. All authors have read and agreed to the published version of the manuscript.

Funding: This research was funded by the projects NKFIH K115990 (to TC) EFOP 3.6.2-16-2017-00006 (to TC) and GINOP-2.3.2-15-2016-00006 (to TC) supported by the National Research, Development and Innovation Office, and by the TKP2021-EGA-32 project (to TC). Project TKP2021-EGA-32 has been implemented with the support provided by the Ministry of Innovation and Technology of Hungary from the National Research, Development and Innovation Fund, financed under the

TKP2021-EGA funding scheme. MRS was supported by the ÚNKP-19-3-SZTE-269 New National Excellence Program of the Ministry for Innovation and Technology.

Institutional Review Board Statement: This investigation conformed to the National Institutes of Health Guide for the Care and Use of Laboratory Animals (NIH Publication No. 85-23, Revised 1996) and was approved by the Animal Research Ethics Committee of University of Szeged (approval code: XV.1181/2013-2018).

Informed Consent Statement: Not applicable.

Data Availability Statement: All data reported in this paper will be shared by the lead contact upon request.

Conflicts of Interest: The authors declare no conflict of interest.

References

1. Timmis, A.; Townsend, N.; Gale, C.P.; Torbica, A.; Lettino, M.; Petersen, S.E.; Mossialos, E.A.; Maggioni, A.P.; Kazakiewicz, D.; May, H.T.; et al. European Society of Cardiology: Cardiovascular Disease Statistics 2019. *Eur. Heart J.* **2020**, *41*, 12–85.
2. Gidding, S.S.; Allen, N.B. Cholesterol and Atherosclerotic Cardiovascular Disease: A Lifelong Problem. *J. Am. Heart Assoc.* **2019**, *8*, e012924.
3. Csont, T.; Bereczki, E.; Bencsik, P.; Fodor, G.; Görbe, A.; Zvara, A.; Csonka, C.; Puskás, L.G.; Sántha, M.; Ferdinandy, P. Hypercholesterolemia increases myocardial oxidative and nitrosative stress thereby leading to cardiac dysfunction in apoB-100 transgenic mice. *Cardiovasc. Res.* **2007**, *76*, 100–109.
4. Varga, Z.V.; Kupai, K.; Szűcs, G.; Gáspár, R.; Pálóczi, J.; Faragó, N.; Zvara, A.; Puskás, L.G.; Rázga, Z.; Tiszlavicz, L.; et al. MicroRNA-25-dependent up-regulation of NADPH oxidase 4 (NOX4) mediates hypercholesterolemia-induced oxidative/nitrative stress and subsequent dysfunction in the heart. *J. Mol. Cell. Cardiol.* **2013**, *62*, 111–121.
5. Pluijmert, N.J.; den Haan, M.C.; van Zuylen, V.L.; Steendijk, P.; de Boer, H.C.; van Zonneveld, A.J.; Fibbe, W.E.; Schalij, M.J.; Quax, P.H.A.; Atsma, D.E. Hypercholesterolemia affects cardiac function, infarct size and inflammation in APOE*3-Leiden mice following myocardial ischemia-reperfusion injury. *PLoS ONE* **2019**, *14*, e0217582.
6. Yao, Y.S.; Li, T.D.; Zeng, Z.H. Mechanisms underlying direct actions of hyperlipidemia on myocardium: An updated review. *Lipids Health Dis.* **2020**, *19*, 1–6.
7. Csonka, C.; Sárközy, M.; Pipicz, M.; Dux, L.; Csont, T. Modulation of Hypercholesterolemia-Induced Oxidative/Nitrative Stress in the Heart. *Oxid. Med. Cell. Longev.* **2016**, *2016*, 3863726.
8. Csonka, C.; Murlasits, Z.; Ferdinandy, P.; Csont, T. Ischemic stress adaptation of the myocardium in the disease states: Role of hyperlipidemia. In *Advances in Cardiomyocyte Research*; Nánási, P., Ed.; Transworld Research Network: Kerala, India, 2009; pp 245–265.
9. McCommis, K.S.; McGee, A.M.; Laughlin, M.H.; Bowles, D.K.; Baines, C.P. Hypercholesterolemia increases mitochondrial oxidative stress and enhances the MPT response in the porcine myocardium: Beneficial effects of chronic exercise. *Am. J. Physiol. -Regul. Integr. Comp. Physiol.* **2011**, *301*, R1250–R1258.
10. Csonka, C.; Kupai, K.; Bencsik, P.; Görbe, A.; Pálóczi, J.; Zvara, A.; Puskás, L.G.; Csont, T.; Ferdinandy, P. Cholesterol-enriched diet inhibits cardioprotection by ATP-sensitive K+ channel activators cromakalim and diazoxide. *Am. J. Physiology. Heart Circ. Physiol.* **2014**, *306*, H405–H413.
11. Puskás, L.G.; Nagy, Z.B.; Giricz, Z.; Onody, A.; Csonka, C.; Kitajka, K.; Hackler, L., Jr.; Zvara, A.; Ferdinandy, P. Cholesterol diet-induced hyperlipidemia influences gene expression pattern of rat hearts: A DNA microarray study. *FEBS Lett.* **2004**, *562*, 99–104.
12. Kocsis, G.F.; Csont, T.; Varga-Orvos, Z.; Puskas, L.G.; Murlasits, Z.; Ferdinandy, P. Expression of genes related to oxidative/nitrosative stress in mouse hearts: Effect of preconditioning and cholesterol diet. *Med. Sci. Monit.* **2010**, *16*, BR32–BR39.
13. Sárközy, M.; Zvara, Á.; Gyémánt, N.; Fekete, V.; Kocsis, G.F.; Pipis, J.; Szűcs, G.; Csonka, C.; Puskás, L.G.; Ferdinandy, P.; Csont, T. Metabolic syndrome influences cardiac gene expression pattern at the transcript level in male ZDF rats. *Cardiovasc. Diabetol.* **2013**, *12*, 1–17.
14. Huang, Y.; Walker, K.E.; Hanley, F.; Narula, J.; Houser, S.R.; Tulenko, T.N. Cardiac systolic and diastolic dysfunction after a cholesterol-rich diet. *Circulation* **2004**, *109*, 97–102.
15. Liu, L.; Mu, Y.; Han, W.; Wang, C. Association of hypercholesterolemia and cardiac function evaluated by speckle tracking echocardiography in a rabbit model. *Lipids Health Dis.* **2014**, *13*, 1–8.
16. Esposito, K.; Ciotola, M.; Sasso, F.C.; Cozzolino, D.; Saccomanno, F.; Assaloni, R.; Ceriello, A.; Giugliano, D. Effect of a single high-fat meal on endothelial function in patients with the metabolic syndrome: Role of tumor necrosis factor-α. *Nutr. Metab. Cardiovasc. Dis.* **2007**, *17*, 274–279.
17. Talini, E.; Di Bello, V.; Bianchi, C.; Palagi, C.; Delle Donne, M.G.; Penno, G.; Nardi, C.; Canale, M.L.; Del Prato, S.; Mariani, M.; et al. Early impairment of left ventricular function in hypercholesterolemia and its reversibility after short term treatment with rosuvastatin A preliminary echocardiographic study. *Atherosclerosis* **2008**, *197*, 346–354.

18. Saracoglu, E.; Kılıç, S.; Vuruşkan, E.; Düzen, I.; Çekici, Y.; Kuzu, Z.; Yıldırım, A.; Küçükosmanoğlu, M.; Çetin, M. Prediction of subtle left ventricular systolic dysfunction in homozygous and heterozygous familial hypercholesterolemia: Genetic analyses and speckle tracking echocardiography study. *Echocardiography* **2018**, *35*, 1289–1299.
19. Muthuramu, I.; Mishra, M.; Aboumsallem, J.P.; Postnov, A.; Gheysens, O.; De Geest, B. Cholesterol lowering attenuates pressure overload-induced heart failure in mice with mild hypercholesterolemia. *Aging* **2019**, *11*, 6872–6891.
20. Rubinstein, J.; Pelosi, A.; Vedre, A.; Kotaru, P.; Abela, G.S. Hypercholesterolemia and myocardial function evaluated via tissue doppler imaging. *Cardiovasc. Ultrasound* **2009**, *7*, 1–7.
21. Nagueh, S.F.; Smiseth, O.A.; Appleton, C.P.; Byrd, B.F., 3rd; Dokainish, H.; Edvardsen, T.; Flachskampf, F.A.; Gillebert, T.C.; Klein, A.L.; Lancellotti, P.; et al. Recommendations for the Evaluation of Left Ventricular Diastolic Function by Echocardiography: An Update from the American Society of Echocardiography and the European Association of Cardiovascular Imaging. *J. Am. Soc. Echocardiogr. Off. Publ. Am. Soc. Echocardiogr.* **2016**, *29*, 277–314.
22. Demján, V.; Kiss, T.; Siska, A.; Szabó, M.R.; Sárközy, M.; Földesi, I.; Csupor, D.; Csont, T. Effect of Stellaria media Tea on Lipid Profile in Rats. *Evid. -Based Complementary Altern. Med. Ecam* **2020**, *2020*, 5109328.
23. Hołda, M.K.; Stachowicz, A.; Suski, M.; Wojtysiak, D.; Sowińska, N.; Arent, Z.; Palka, N.; Podolec, P.; Kopeć, G. Myocardial proteomic profile in pulmonary arterial hypertension. *Sci. Rep.* **2020**, *10*, 14351.
24. Szűcs, G.; Sója, A.; Péter, M.; Sárközy, M.; Bruszel, B.; Siska, A.; Földesi, I.; Szabó, Z.; Janáky, T.; Vígh, L.; et al. Prediabetes Induced by Fructose-Enriched Diet Influences Cardiac Lipidome and Proteome and Leads to Deterioration of Cardiac Function prior to the Development of Excessive Oxidative Stress and Cell Damage. *Oxid. Med. Cell. Longev.* **2019**, *2019*, 3218275.
25. Yang, M.; Yan, J.; Wu, A.; Zhao, W.; Qin, J.; Pogwizd, S.M.; Wu, X.; Yuan, S.; Ai, X. Alterations of housekeeping proteins in human aged and diseased hearts. *Pflügers Arch.-Eur. J. Physiol.* **2021**, *473*, 351–362.
26. Michaelson, J.; Hariharan, V.; Huang, H. Hyperglycemic and Hyperlipidemic Conditions Alter Cardiac Cell Biomechanical Properties. *Biophys. J.* **2014**, *106*, 2322–2329.
27. Varela, R.; Rauschert, I.; Romanelli, G.; Alberro, A.; Benech, J.C. Hyperglycemia and hyperlipidemia can induce morphophysiological changes in rat cardiac cell line. *Biochem. Biophys. Rep.* **2021**, *26*, 100983.
28. Ojamaa, K.; Kenessey, A.; Shenoy, R.; Klein, I. Thyroid hormone metabolism and cardiac gene expression after acute myocardial infarction in the rat. *Am. J. Physiol. -Endocrinol. Metab.* **2000**, *279*, E1319–E1324.
29. Razeghi, P.; Young, M.E.; Alcorn, J.L.; Moravec, C.S.; Frazier, O.H.; Taegtmeyer, H. Metabolic gene expression in fetal and failing human heart. *Circulation* **2001**, *104*, 2923–2931.
30. Nakao, K.; Minobe, W.; Roden, R.; Bristow, M.R.; Leinwand, L.A. Myosin heavy chain gene expression in human heart failure. *J. Clin. Investig.* **1997**, *100*, 2362–2370.
31. Krenz, M.; Robbins, J. Impact of beta-myosin heavy chain expression on cardiac function during stress. *J. Am. Coll. Cardiol.* **2004**, *44*, 2390–2397.
32. Herron, T.J.; McDonald, K.S. Small amounts of alpha-myosin heavy chain isoform expression significantly increase power output of rat cardiac myocyte fragments. *Circ Res.* **2002**, *90*, 1150–1152.
33. Sequeira, V.; Nijenkamp, L.L.A.M.; Regan, J.A.; van der Velden, J. The physiological role of cardiac cytoskeleton and its alterations in heart failure. *Biochim. Biophys. Acta (BBA)-Biomembr.* **2014**, *1838*, 700–722.
34. Ehler, E. Actin-associated proteins and cardiomyopathy-the 'unknown' beyond troponin and tropomyosin. *Biophys. Rev.* **2018**, *10*, 1121–1128.
35. Zhou, B.; Tian, R. Mitochondrial dysfunction in pathophysiology of heart failure. *J. Clin. Investig.* **2018**, *128*, 3716–3726.
36. Bhatti, J.S.; Bhatti, G.K.; Reddy, P.H. Mitochondrial dysfunction and oxidative stress in metabolic disorders—A step towards mitochondria based therapeutic strategies. *Biochim. Biophys. Acta (BBA)-Mol. Basis Dis.* **2017**, *1863*, 1066–1077.
37. Castillo, R.L.; Herrera, E.A.; Gonzalez-Candia, A.; Reyes-Farias, M.; de la Jara, N.; Peña, J.P.; Carrasco-Pozo, C. Quercetin Prevents Diastolic Dysfunction Induced by a High-Cholesterol Diet: Role of Oxidative Stress and Bioenergetics in Hyperglycemic Rats. *Oxid. Med. Cell. Longev.* **2018**, *2018*, 7239123.
38. Elustondo, P.; Martin, L.A.; Karten, B. Mitochondrial cholesterol import. *Biochim. Et Biophys. Acta (BBA)-Mol. Cell Biol. Lipids* **2017**, *1862*, 90–101.
39. Szabó, M.R.; Gáspár, R.; Pipicz, M.; Zsindely, N.; Diószegi, P.; Sárközy, M.; Bodai, L.; Csont, T. Hypercholesterolemia Interferes with Induction of miR-125b-1-3p in Preconditioned Hearts. *Int. J. Mol. Sci.* **2020**, *21*, 3744.
40. Pipicz, M.; Varga, Z.V.; Kupai, K.; Gáspár, R.; Kocsis, G.F.; Csonka, C.; Csont, T. Rapid ventricular pacing-induced postconditioning attenuates reperfusion injury: Effects on peroxynitrite, RISK and SAFE pathways. *Br. J. Pharmacol.* **2015**, *172*, 3472–3483.
41. Searle, B.C.; Pino, L.K.; Egertson, J.D.; Ting, Y.S.; Lawrence, R.T.; MacLean, B.X.; Villén, J.; MacCoss, M.J. Chromatogram libraries improve peptide detection and quantification by data independent acquisition mass spectrometry. *Nat. Commun.* **2018**, *9*, 5128.
42. Gessulat, S.; Schmidt, T.; Zolg, D.P.; Samaras, P.; Schnatbaum, K.; Zerweck, J.; Knaute, T.; Rechenberger, J.; Delanghe, B.; Huhmer, A.; et al. Prosit: Proteome-wide prediction of peptide tandem mass spectra by deep learning. *Nat. Methods* **2019**, *16*, 509–518.
43. Tyanova, S.; Temu, T.; Sinitcyn, P.; Carlson, A.; Hein, M.Y.; Geiger, T.; Mann, M.; Cox, J. The Perseus computational platform for comprehensive analysis of (prote)omics data. *Nat. Methods* **2016**, *13*, 731–740.

44. Raudvere, U.; Kolberg, L.; Kuzmin, I.; Arak, T.; Adler, P.; Peterson, H.; Vilo, J. g:Profiler: A web server for functional enrichment analysis and conversions of gene lists (2019 update). *Nucleic Acids Res.* **2019**, *47*, W191–W198.
45. Shannon, P.; Markiel, A.; Ozier, O.; Baliga, N.S.; Wang, J.T.; Ramage, D.; Amin, N.; Schwikowski, B.; Ideker, T. Cytoscape: A software environment for integrated models of biomolecular interaction networks. *Genome Res.* **2003**, *13*, 2498–2504.
46. Reimand, J.; Isserlin, R.; Voisin, V.; Kucera, M.; Tannus-Lopes, C.; Rostamianfar, A.; Wadi, L.; Meyer, M.; Wong, J.; Xu, C.; et al. Pathway enrichment analysis and visualization of omics data using g:Profiler, GSEA, Cytoscape and EnrichmentMap. *Nat. Protoc.* **2019**, *14*, 482–517.
47. Szklarczyk, D.; Gable, A.L.; Nastou, K.C.; Lyon, D.; Kirsch, R.; Pyysalo, S.; Doncheva, N.T.; Legeay, M.; Fang, T.; Bork, P.; et al. The STRING database in 2021: Customizable protein-protein networks, and functional characterization of user-uploaded gene/measurement sets. *Nucleic Acids Res.* **2021**, *49*, D605–D612.
48. Doncheva, N.T.; Morris, J.H.; Gorodkin, J.; Jensen, L.J. Cytoscape StringApp: Network Analysis and Visualization of Proteomics Data. *J. Proteome Res.* **2019**, *18*, 623–632.
49. Subramanian, A.; Tamayo, P.; Mootha, V.K.; Mukherjee, S.; Ebert, B.L.; Gillette, M.A.; Paulovich, A.; Pomeroy, S.L.; Golub, T.R.; Lander, E.S.; et al. Gene set enrichment analysis: A knowledge-based approach for interpreting genome-wide expression profiles. *Proc. Natl. Acad. Sci. USA* **2005**, *102*, 15545–15550.
50. Liberzon, A.; Subramanian, A.; Pinchback, R.; Thorvaldsdóttir, H.; Tamayo, P.; Mesirov, J.P. Molecular signatures database (MSigDB) 3.0. *Bioinformatics* **2011**, *27*, 1739–1740.
51. Luo, W.; Brouwer, C. Pathview: An R/Bioconductor package for pathway-based data integration and visualization. *Bioinformatics* **2013**, *29*, 1830–1831.
52. Luo, W.; Pant, G.; Bhavnasi, Y.K.; Blanchard, S.G., Jr.; Brouwer, C. Pathview Web: User friendly pathway visualization and data integration. *Nucleic Acids Res.* **2017**, *45*, W501–W508.

III.

Physiology International 110 (2023) 2, 135–149
DOI: 10.1556/2060.2023.00198

AKADÉMIAI KIADÓ

The effect of electrical stimulation of skeletal muscle on cardioprotection and on muscle-derived myokine levels in rats: A pilot study

MÁRTON R. SZABÓ[1,2], TAMÁS CSONT[1,2] and CSABA CSONKA[1,2*]

[1] Department of Biochemistry, Albert Szent-Györgyi Medical School, University of Szeged, H-6720 Szeged, Hungary

[2] Centre of Excellence for Interdisciplinary Research, Development and Innovation of the University of Szeged, H-6720 Szeged, Hungary

Received: February 14, 2023 • Revised manuscript received: February 22, 2023 • Accepted: February 28, 2023
Published online: May 5, 2023

ABSTRACT

Electrical muscle stimulation (EMS) is a widely used method in sports and rehabilitation therapies to simulate physical exercise. EMS treatment via skeletal muscle activity improves the cardiovascular functions and the overall physical condition of the patients. However, the cardioprotective effect of EMS has not been proven so far, therefore, the aim of this study was to investigate the potential cardiac conditioning effect of EMS in an animal model. Low-frequency 35-min EMS was applied to the gastrocnemius muscle of male Wistar rats for three consecutive days. Their isolated hearts were then subjected to 30 min global ischemia and 120 min reperfusion. At the end of reperfusion cardiac specific creatine kinase (CK-MB) and lactate dehydrogenase (LDH) enzyme release and myocardial infarct size were determined. Additionally, skeletal muscle-driven myokine expression and release were also assessed. Phosphorylation of cardioprotective signaling pathway members AKT, ERK1/2, and STAT3 proteins were also measured. EMS significantly attenuated cardiac LDH and CK-MB enzyme activities in the coronary effluents at the end of the *ex vivo* reperfusion. EMS treatment considerably altered the myokine content of the stimulated gastrocnemius muscle without altering circulating myokine levels in the serum. Additionally, phosphorylation of cardiac AKT, ERK1/2, and STAT3 was not significantly different in the two groups. Despite the lack of significant infarct size reduction, the EMS treatment seems to influence the course of cellular damage due to ischemia/reperfusion and favorably modifies skeletal muscle myokine expressions. Our results suggest that EMS may have a protective effect on the myocardium, however, further optimization is required.

* Corresponding author. Department of Biochemistry, Albert Szent-Györgyi Medical School, University of Szeged, Hungary Dóm tér 9, H-6720 Szeged, Hungary. Tel.: +36 62 54 5755. E-mail: csonka.csaba@med.u-szeged.hu

KEYWORDS

electrical muscle stimulation, heart, cardioprotection, myokine, reperfusion injury

INTRODUCTION

Ischemic heart diseases including myocardial infarction are the leading cause of death worldwide [1]. It has been well established that there are remarkable endogenous adaptive responses of the heart to withstand the detrimental effects of ischemia/reperfusion (I/R) injury. Additionally, cardiac conditioning can be elicited through other organs termed as remote conditioning. Such interventions, which benefit multiple organs of the body at the same time, are of great clinical importance [2, 3].

The lack of physical exercise represents a global public health problem particularly because the human body rapidly adapts to insufficient physical activity [4]. The cardio-preventive and therapeutic potential of long-term exercise is manifested in lowering blood pressure, favorably modifying plasma lipoprotein profile, and enhancing cardiac contractile function. Apart from the advantageous outcome of exercise, the enormous adaptation capacity of the skeletal muscle might be transferred to the heart thereby inducing cardiac conditioning and subsequently protecting against the detrimental effects of I/R injury and having favorable outcomes in cardiac rehabilitation. However, performing regular exercise is often limited due to various health reasons. For those, electrical muscle stimulation (EMS), the rhythmical muscle activation triggered with electrical impulses, might provide an alternative way to partially gain the benefits of exercise [5, 6]. EMS is a widely used method in sport and rehabilitation therapy and is an attractive clinical application for subjects unable to perform regular exercise [7, 8]. Nevertheless, little is known whether the application of EMS can trigger cardiac preconditioning and protection against I/R injury.

Both humoral and neurological factors are implicated in the advantageous effects of skeletal muscle activity on the general health of the individual. Recently, skeletal muscle-derived myokines are emerged as important effectors of exercise-induced cardioprotection [9]. Myokines are a wide variety of molecules predominantly released by contracting skeletal muscles, supposed to regulate muscle mass and energy homeostasis [10]. Beyond the effect on the skeletal muscles, myokines are also considered as molecular mediators which link muscle exercise to the whole body physiology through endocrine signaling pathways [11, 12].

Taken together the promising therapeutic potential of EMS, the aim of the present study was to test (i) whether short-term EMS confers cardioprotection as a remote preconditioning intervention and (ii) whether EMS modulates myokine levels in the stimulated skeletal muscle.

MATERIALS AND METHODS

Animals

Altogether 20 male Wistar rats (300–350 g) were used in this study. The animals were kept in pairs in individually ventilated cages in a temperature-controlled room with 12 h:12 h light/dark cycles. Laboratory chow and water were available ad libitum throughout the study. The experiment conformed to the Guide for the Care and Use of Laboratory Animals published by the US National Institutes of Health (NIH publication No. 85-23, re-vised 1996) and was approved by the Animal Research Ethics Committee of the University of Szeged (approval number: XV./2153/2022).

Experimental setup

EMS treatment was performed in sedated animals with stimulating electrodes placed on the *gastrocnemius* muscles of the animals. EMS sessions were applied for three days; each session in each days includes 10-Hz frequency continuous stimulation for 35 min. Twenty-four hours after the last EMS treatment, rats were anesthetized with an intraperitoneal injection of sodium pentobarbital (50 mg/kg; Produlab Pharma b.v., Raamsdonksveer, The Netherlands), and blood and *gastrocnemius* muscle samples were collected for myokine level measurement. Hearts from EMS-treated and untreated animals were isolated and perfused according to Langendorff as described previously [13, 14]. A 15-min equilibration period was applied followed by 30 min global ischemia and 120 min reperfusion (I/R). Global ischemia was achieved via the complete closure of perfusion fluid toward the heart, therefore, the same degree of stress (i.e. ischemia) was applied to the entire myocardium. During reperfusion, coronary effluents were collected and used to measure cardiac lactate-dehydrogenase (LDH) and creatine kinase MB isoform (CK-MB) release. At the end of the reperfusion, infarct size was determined by TTC staining [15].

Electrical muscle stimulation

Rats were sedated with a 40 mg kg^{-1} sodium pentobarbital solution (Produlab Pharma b.v., Raamsdonksveer, The Netherlands), placed on a heating pad in a supine position, and hind limbs were fixed. EMS treatment was performed with a portable electrostimulator device (Sanitas SEM 44 digital EMS/TENS, Hans Dinslage GmbH, Germany) for three consecutive days. The stimulating pads of the EMS device were replaced with acupuncture needles to easily access the skeletal muscle with the electrodes. Bilateral EMS was applied targeting the gastrocnemius muscles with the stimulating electrodes once a day for three consecutive days with low frequency as reported in human studies [7, 16], respectively. The EMS treatment consisted of 35 min of continuous stimulation with bipolar rectangular pulses at 10 Hz frequency and 250 μs pulse width with minimal intensity to produce a visible muscle contraction. The control group underwent the same procedure, without switching on the EMS device.

Infarct size determination

Myocardial infarct size was measured after *ex vivo* global I/R in hearts isolated from both EMS-treated and untreated animals. After the end of reperfusion, atria were removed, and the total ventricles were used to determine the infarcted area. Briefly, frozen ventricles were cut into 7–8 equal slices and placed into triphenyl tetrazolium chloride (TTC) solution (Sigma, Saint Louis, MO, USA) for 10 min at 37 °C followed by a 10 min formaldehyde fixation and phosphate buffer washing steps [15]. As a result, survived area was stained red while the necrotic area remained pale. Digitalized images from the stained heart slices were evaluated with planimetry method and the amount of myocardial necrosis was expressed as infarct size/area at risk %.

LDH and CK-MB release measurement

Coronary effluents were collected 2, 5, 30, and 120 min after the beginning of reperfusion to measure the release of LDH and CK-MB enzymes. Enzyme activity was measured via kinetic enzyme activity assay using colorimetric LDH and CK-MB detecting kits (Diagnosticum, Hungary) and a microplate reader (Clariostar Plus, BMG Labtech). Enzyme activity was

normalized to the volume of coronary effluent and the total weight of the respective heart. Enzyme release was expressed as U min^{-1} g^{-1}wet weight.

Western blot

In a separate set of experiments, left ventricles of isolated hearts from EMS-treated and untreated animals were homogenized with an ultrasonicator in Radio Immunoprecipitation Assay (RIPA) buffer (Cell Signaling, Danvers, MA, USA) supplemented with protease inhibitor cocktail and phosphatase inhibitors phenylmethane sulfonyl fluoride (PMSF) and sodium fluoride (NaF, Sigma, Saint Louis, MO, USA). Homogenates were centrifuged, and protein concentrations of the supernatants were determined using BCA Protein Assay Kit (Pierce, Rockford, IL, USA). Twenty μg of reduced and denatured protein was loaded in 10% polyacrylamide gel, and SDS gel electrophoresis was performed. Separated proteins were transferred to 0.22 μm pore size nitrocellulose membranes. After checking the transfer efficiency with Ponceau-staining, membranes were blocked for 1 h in 5% (w/v) bovine serum albumin (BSA) at room temperature. Blocked membranes were incubated with the following primary antibodies in the concentrations of 1:1000 phospho-AKT (Ser473, #4060), AKT (#9272), phospho-ERK1/2 (Thr202/Tyr204, #9101), ERK1/2 (#9102), phospho-STAT3 (Tyr705, #9145), STAT3 (#4904) and in 1:5000 concentration against GAPDH (#2118) at 4 °C overnight (Cell Signaling, Danvers, MA, USA). After incubation with horseradish peroxidase (HRP)-conjugated goat anti-rabbit secondary antibody membranes were developed with an enhanced chemiluminescence kit. After the development of phosphorylated signals of AKT, ERK1/2, and STAT3 membranes were stripped and reassessed for the amount of total proteins. Signals were analyzed and evaluated by Quantity One Software.

ELISA

Double-antibody sandwich ELISA kits specific for rat Irisin, Decorin, Myonectin, Myoglobin, IL6, IL15, and FSTL1 proteins, respectively, were used to measure protein content in gastrocnemius and serum samples (Fine Test, Wuhan, China) according to the manufacturer's instruction. Myokine content was determined with a colorimetric detection method using a microplate reader (Clariostar Plus, BMG Labtech, Germany).

RT-qPCR

RNA was isolated from the *gastrocnemius* muscles with the phenol:chloroform:isoamyl alcohol extraction method and total RNA concentrations were determined. Reverse transcription of 500 ng RNA was performed with iScript cDNA Synthesis Kit (BioRad) and the resulting cDNA was used as a template for qPCR measurement of myokine expression levels using SYBR Green PCR Super Mix (BioRad) and BioRad CFX96 Touch Real-Time PCR machine (BioRad). Relative expression levels were determined with the $2^{-\Delta\Delta Ct}$ method and GAPDH was used as a housekeeping gene. Primer sequences are listed in Table 1, while primers used for the measurement of *Dcn, Fndc5,* and *Il15* are designed by BioRad (#10025636), and their relative expression was normalized for *Gapdh* provided by the same manufacturer.

Statistics

All values are expressed as mean ± SEM. The Shapiro-Wilk normality test was used to test the normal distribution of the data. Student's *t*-test was used to evaluate the effect of EMS on infarct

size. Repeated measures ANOVA was applied for changes in mean scores over different time points of reperfusion for the evaluation of LDH and CK-MB releases. Relative expression levels of myokines at the transcript level were determined with the $2^{-\Delta\Delta Ct}$ method. For all statistical evaluation P value <0.05 was considered as an indicator of significant difference among the groups.

RESULTS

Testing the cardioprotective effect of skeletal muscle EMS treatment on *ex vivo* perfused hearts

To assess the cardioprotective effect of EMS, *ex vivo* heart perfusion was performed on isolated hearts from EMS-treated and untreated control rats. LDH and CK-MB enzyme release, cardiac markers of the myocardial infarction, were measured from the coronary effluents collected at different time points of the reperfusion (Fig. 1A and B). Based on our results both cardiac LDH and CK-MB release were significantly lower upon EMS at the end of reperfusion. Furthermore, myocardial infarct size was also determined at the end of reperfusion, and although the mean value of infarct size tended to be lower in the EMS group compared to the nonstimulated control group, the applied EMS treatment failed to attenuate infarct size significantly (Fig. 1C).

Altered myokine expression in the gastrocnemius muscle in response to EMS

To determine the possible mediators of EMS-associated cardioprotection, myokine expression was measured in the stimulated gastrocnemius muscles. Among the investigated myokines the applied EMS treatment upregulated *Fstl1*, *Il6,* and *Igf1* mRNA levels in the gastrocnemius muscle (Table 2). Additionally, *Il15* mRNA content was downregulated in response to EMS.

Table 1. **Primer sequences used for the determination of myokine expression levels in the gastrocnemius muscle**. Fwd: forward, Rev: reverse primer

Fstl1 Fwd	GGCCTGTGTGTGGCAGTAAT	Follistatin-like 1
Fstl1 Rev	CAGCTCATCACGGTTAGCCT	
Fgf21 Fwd	CTCCAGTTTGGGGGTCAAGT	Fibroblast growth factor 21
Fgf21 Rev	GGAGACTTTCTGGACTGCGG	
Lif Fwd	AGTTGGTCGAGCTGTATCGG	Leukemia inhibitory factor
Lif Rev	GCCCACATGGTACTTGTTGC	
Il6 Fwd	GAGTTCCGTTTCTACCTGGAGT	Interleukin-6
Il6 Rev	TTGGTCCTTAGCCACTCCTTC	
Erfe Fwd	TCAAGCAGAGTGACAAGGGC	Erythroferrone/myonectin
Erfe Rev	CGTACCGCACCTTTCAACAA	
Bdnf Fwd	TCCCGGTATCAAAAGGCCAA	Brain-derived neurotrophic factor
Bdnf Rev	ATGAACCGCCAGCCAATTCT	
Igf1 Fwd	CTGGTGGACGCTCTTCAGTT	Insulin-like growth factor 1
Igf1 Rev	CGGATGGAACGAGCTGACTT	
Gapdh Fwd	GGTCATCAACGGGAAACCCA	Glyceraldehyde-3-phosphate dehydrogenase
Gapdh Rev	GAAGGGGCGGAGATGATGAC	

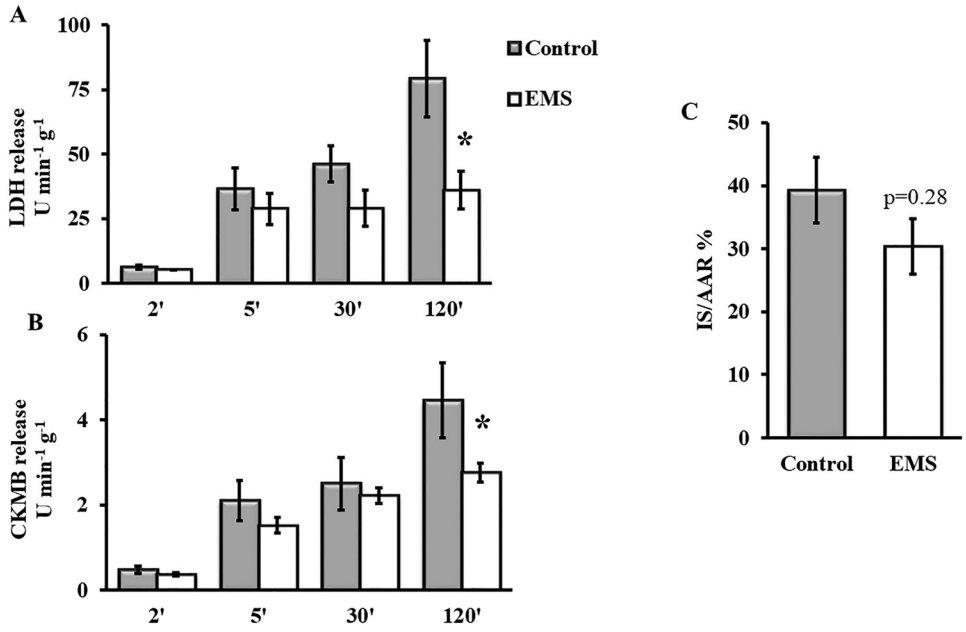

Fig. 1. Testing the potential preconditioning effect of EMS treatment against I/R in *ex vivo* perfused hearts. LDH (A) and CK-MB (B) enzyme release measurement. Coronary effluents were collected at different time points of the reperfusion and used for colorimetric CK-MB and LDH enzyme activity measurement. Infarct size values at the end of *ex vivo* heart perfusion (C). Hearts isolated from EMS-treated and untreated rats were subjected to 30 min global ischemia and 120 min reperfusion (I/R). Data are expressed as mean ± SEM; $n = 6$ in each group. $^{*}P < 0.05$

Table 2. **Myokine mRNA expression in the gastrocnemius muscle after EMS treatment**. *Fstl1*: Follistatin-like 1, *Fgf21*: Fibroblast growth factor 21, *Il6*: Interleukin-6, *Bdnf*: Brain-derived neurotrophic factor, *Erfe*: Erythroferrone/myonectin, *Igf1*: Insulin-like growth factor 1, *Lif*: Leukemia inhibitory factor, *Dcn*: Decorin, *Fndc5*: Fibronectin type III domain-containing protein 5/Irisin precursor, *Il15*: Interleukin-15, respectively. Data are expressed as mean ± SEM; $n = 10$, $^{*}P < 0.05$

Myokine mRNA	relative mRNA expression levels	
	Control	EMS
Fstl1	1.02 ± 0.08	2.80 ± 0.59 *
Fgf21	1.55 ± 0.47	1.44 ± 0.38
Il6	1.11 ± 0.17	3.90 ± 1.10 *
Bdnf	1.10 ± 0.15	0.93 ± 0.19
Erfe	1.07 ± 0.16	0.98 ± 0.11
Igf1	0.93 ± 0.07	1.42 ± 0.19 *
Lif	1.91 ± 0.70	1.50 ± 0.61
Dcn	1.08 ± 0.11	1.31 ± 0.21
Fndc5	1.06 ± 0.12	0.92 ± 0.15
Il15	1.04 ± 0.09	0.56 ± 0.07 *

Next, we assessed the protein content of some selected myokines in the stimulated gastrocnemius muscle. Based on our results Irisin, Decorin, Myonectin, FSTL1, and Myoglobin proteins were upregulated as a consequence of EMS (Table 3). Nevertheless, IL-6 and IL-15 protein levels remained unaffected upon EMS treatment, despite the increased level of their mRNA transcripts.

Serum myokine levels remained unaffected upon EMS treatment

To elucidate whether skeletal muscle-derived myokines may contribute to the cardioprotective effects of EMS, serum myokine levels were measured by ELISA. However, at the time of serum sampling none of the measured myokines showed significant differences in the blood compared to the untreated control animals (Table 4).

Investigation of the possible involvement of cardiac conditioning-associated pathways upon EMS of the gastrocnemius muscle

To further clarify the possible cardioprotective effect of the skeletal muscle EMS, the key protein elements of the Reperfusion Injury Salvage Kinase (RISK) and the Survivor Activating Factor

Table 3. **Myokine protein levels in the stimulated gastrocnemius muscle determined with ELISA**. Protein concentration values are expressed as ng mg^{-1} tissue protein. FSTL1: Follistatin-like 1, IL-6: Interleukin 6, IL-15: Interleukin-15. All data are mean ± SEM; $n = 8$, $^{*}P < 0.05$

Myokine	Tissue protein content ng mg^{-1}	
	Control	EMS
Irisin	22.14 ± 3.52	39.59 ± 5.26*
Decorin	0.24 ± 0.05	0.55 ± 0.09*
Myonectin	2.13 ± 0.32	4.84 ± 0.94*
FSTL1	25.46 ± 2.52	33.00 ± 1.87*
IL-6	9.28 ± 0.89	10.61 ± 1.12
IL-15	0.97 ± 0.08	0.94 ± 0.08
Myoglobin	0.57 ± 0.10	1.31 ± 0.34*

Table 4. **Serum myokine levels after one day of the last EMS treatment**. Protein concentration values expressed as ng mg^{-1} serum protein FSTL1: Follistatin-like 1, Data are mean ± SEM; $n = 8$, $^{*}P < 0.05$

Myokine	Serum protein content	
	Control	EMS
Irisin	0.61 ± 0.06	0.62 ± 0.10
Decorin	0.011 ± 0.006	0.012 ± 0.013
Myonectin	2.22 ± 0.21	2.55 ± 0.31
FSTL1	0.25 ± 0.02	0.26 ± 0.03
Myoglobin	6.64 ± 0.80	6.95 ± 0.84

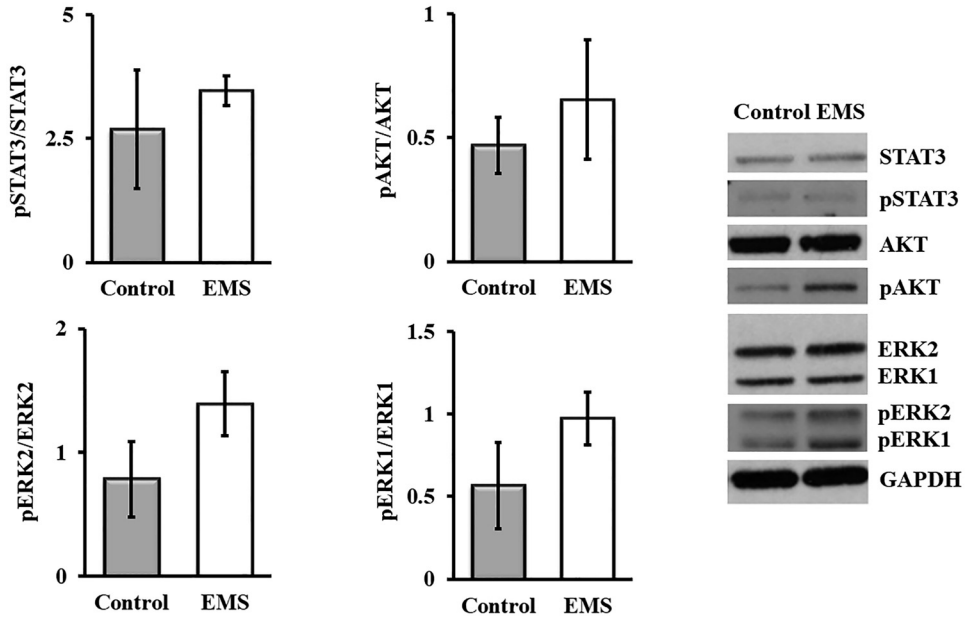

Fig. 2. Effect of skeletal muscle EMS training on the phosphorylation of STAT3, AKT and ERK1/2 proteins assessed by Western blots. Data are expressed as mean ± SEM; $n = 4$, $^{*}P < 0.05$

Enhancement (SAFE) pathways were investigated in ventricular samples at the end of the reperfusion. In regard to the RISK pathway, phosphorylation of AKT kinase was not affected significantly upon EMS, while phosphorylation of ERK1 and ERK2 showed a trend toward an increase ($P = 0.18$ and $P = 0.21$, respectively) in the hearts of EMS-treated animals compared to the untreated controls (Fig. 2). Additionally, phosphorylation of STAT3, the key transcription factor of the SAFE pathway, was not affected in the left ventricles either.

DISCUSSION

In the present study, we investigated whether EMS of the skeletal muscle confers cardioprotection in a remote preconditioning-like manner as well as if skeletal muscle myokine production and secretion is modified upon EMS treatment. Despite the lack of significant infarct size reduction, the EMS treatment seems to influence the course of cellular damage due to I/R shown by the decreased cardiac markers LDH and CK-MB release. Additionally, EMS altered the expression levels of several myokines in the skeletal muscle, which might be potential mediators of the beneficial effects of EMS in the cardiovascular system.

EMS has been long utilized to either supplement or substitute muscle strengthening in several rehabilitation settings [17, 18]. Although inferior to conventional training, nevertheless, improvements in exercise capacity and quality of life are established outcomes of EMS treatment in patients unable to perform regular exercise [7, 16, 19, 20]. The aim of the present study was to

test whether a short duration of EMS treatment of rats protects their heart against *ex vivo* I/R injury. In our perfusion model LDH and CK-MB release during the reperfusion were significantly decreased in the *ex vivo* perfused hearts of animals that received EMS. However, EMS prior to global I/R failed to significantly decrease the infarcted area. Our results suggest that despite the lack of significant infarct size reduction EMS treatment might initiate different cardioprotective mechanisms which were partially retained during the *ex vivo* heart perfusion. The effect of electrical stimulation as a cardiac remote preconditioning maneuver was tested in previous studies with different experimental setups. In an early study, Birnbaum and colleagues [21] reported that in combination with remote ischemic preconditioning electrical stimulation of the gastrocnemius muscle conferred cardioprotection in a rabbit model of *in vivo* I/R, however, the same approach failed to enhance the efficiency of preconditioning of human patients underwent coronary angioplasty [22]. Nevertheless, previous research mainly focused on the direct electrical stimulation of peripheral nerves rather than the muscle contraction-mediated preconditioning effects. Targeted electrical stimulation of the medial nerve [23], the femoral nerve [24–26], or electroacupuncture pretreatment [27, 28] straight before I/R mitigated myocardial infarct size and improved the post-ischemic cardiac performance in rodents. These observations implicated the immediate release of small molecular weight blood-borne humoral factors upon electrical stimuli and subsequent cardiac opioid receptor agonism.

Several hundred cytokines, other small proteins, proteoglycans, and oligopeptides are produced and released by muscle in response to muscle contractions [29]. These molecules, termed myokines or exerkines, exert their effects on other organs through inflammation modulation or metabolic control. The effect of EMS on skeletal muscle myokine levels was also addressed in our current study. Based on our results, the applied EMS protocol increased *Il6* mRNA, but not IL-6 protein levels in the gastrocnemius muscle. Similarly to our findings, electrical stimulation of rat myotube culture evoked an increase in *Il6* mRNA levels [30]. Additionally, a short duration of neuromuscular electrical stimulation led to markedly increased circulating IL-6 levels in healthy individuals [31, 32]. In the skeletal muscle, the exercise-induced release of IL-6 seems to exert anti-inflammatory actions [32] and could act as one of the major mediators of exercise-induced cardioprotection against myocardial I/R injury [33]. In contrast with observations of exercise-mediated IL-15 response, in our experimental settings, EMS decreased *Il15* mRNA expression in the stimulated gastrocnemius muscles, without any effect on muscle IL-15 protein content. During exercise, IL-15 is one of the expressed cytokines in the muscle, with essential roles in skeletal muscle anabolic processes. Moreover, these data suggest a possible link in the exercise-mediated muscle-fat crosstalk [34, 35] and indicate potential anti-inflammatory effects [36]. However, based on our results, the applied EMS seems to have no effect on IL-15 production.

Another myokine, FSTL1 was the only myokine upregulated both in mRNA and protein levels in the muscle, without any change in the bloodstream upon EMS. FSTL1 is a glycoprotein, secreted by skeletal muscle in a contraction-regulated manner [37, 38]. However, the effect of EMS on skeletal muscle FSTL1 production and secretion has not been clarified yet. Görgens and colleagues found that acute exercise-induced FSTL1 expression is possibly regulated by inflammatory cytokines rather than electrical pulse stimulation in myoblast culture [39]. However, opposite scenario was observed in mesenchymal stem cell culture after short-term electrostimulation and it might be associated with cardiomyogenic differentiation [40]. Furthermore, FSTL1 has been described as a cardioprotective myokine [41–43]. The related beneficial effects

on the myocardium are shown to involve improved endothelial cell function, mitigation of myocardial ischemic injury, and revascularization in ischemic tissue [44, 45].

In contrast to the observed myokine mRNA expression levels, EMS induced an increment in the protein levels of Decorin, Irisin, Myonectin and Myoglobin, respectively, after three days of the stimulation period. However, none of the selected myokines showed altered levels in the serum of EMS-treated animals. All of the selected myokines were previously implicated with exercise-mediated secretion and protection against various ischemic injury-related cell death [9, 46, 47]. To the best of our knowledge, Decorin, Irisin, and Myonectin levels were not yet investigated upon EMS treatment and the disclosure of their paracrine and endocrine functions might provide great value to the better understanding of the systemic effects of involuntary contractions of the skeletal muscles elicited by electrical stimulations. However, apart from the myokines of the scope of our research, previous studies highlighted the local and systemic effects of many other electrical stimulation-driven myokine production and secretion [48]. Altered circulating myokine levels upon neuromuscular electrical stimulation treatment, notably, brain-derived neurotrophic factor (BDNF), meteorin-like (METRNL), and IGF-1, respectively, possibly exert beneficial metabolic effects on glucose metabolism of the diabetic patient, skeletal muscle anabolic processes as well mitigation of sarcopenia in elderly people [49–52]. Previous studies suggested the importance of intact peripheral nerves for triggering electrical stimulation-driven cardioprotection. However, myokines might overcome the damaged peripheral sensory nerves which seem to be mandatory for remote conditioning, which further strengthens their prominent role in the potential protection of the myocardium during the application of EMS [53].

In the present study, the possible activation of the cytosolic protein components of the cardiac preconditioning-associated mechanisms were also investigated. Based on our results, EMS treatment failed to significantly modify the phosphorylation of ERK1, ERK2 and AKT kinases, respectively. Furthermore, the key protein component of the SAFE pathway was also unaffected upon EMS of the gastrocnemius muscles as shown in the phosphorylated state of STAT3 in the left ventricle. Upon phosphorylation, the activation of the STAT3, AKT and ERK1/2 kinases share a crucial role triggering cardiac conditioning accompanied by protection against ischemic injury. Similarly to the classical ischemic preconditioning maneuver, signal transduction of remote ischemic preconditioning through skeletal muscles or regular physical activity led the activation of the RISK and SAFE as well the endothelial nitric oxide synthase/protein kinase G (eNOS/PKG) pathways, respectively, as reviewed elsewhere [54, 55]. Interestingly, previous findings of Tsai and colleagues [56] revealed that electrical stimulation of the median nerve induced phosphorylation of myocardial AKT, GSK-3, and PKCε proteins, respectively, suggesting the potential remote preconditioning ability of EMS on the heart via a yet-to-be confirmed mechanisms.

LIMITATIONS

We are aware that the present study is not without limitations. In order to test the potential cardioprotective effect of EMS, we applied an *ex vivo* heart perfusion system, where global ischemia was induced. This approach is different from the stress during *in vivo* occurring ischemia and reperfusion. As known, the second window of preconditioning may be less robust than that of the first window, which requires further consideration of the exact time of testing the beneficial effects of EMS against I/R on the heart. However, the potential role of myokines on EMS-induced remote protection was also assessed, which molecules possibly contribute in a

later phase of the protection. Moreover, measuring secondary endpoints, like the incidence of myocardial arrhythmias might also be helpful to determine the preconditioning effect of EMS. Myokine levels were only measured one day after the third EMS session, which could also hide changes upon EMS due to the fast turnover of circulating proteins. Therefore, different sampling times for serum myokine measurements, as well as assessment of previously described myokine-evoked molecular changes in the heart, might elucidate the conditional role of several myokines in EMS-induced cardioprotection. Additionally, due to the anatomical characteristics of rats, EMS treatment was only applied to the gastrocnemius muscle, which is easily accessible for surface electrodes. Nevertheless, a more robust change in circulating myokine levels might happen with the involvement of greater muscle mass.

CONCLUSIONS

Despite the lack of significant infarct size reduction, the EMS treatment seems to influence the course of cellular damage due to ischemia/reperfusion. Our results suggest that EMS may have a protective effect on the myocardium, however, further optimization of the protocol is required. Similarly to voluntary exercise, myokines might be also involved in the cardioprotective effects of EMS, however, verification of their mechanistic role remains for the scope of future studies.

ACKNOWLEDGMENT

This research was funded by the projects TKP2021-EGA-32, GINOP-2.3.2-15-2016-00040 and K143889 by the National Research, Development and Innovation Office. We acknowledge the outstanding technical support of Andrea Apjok-Sója during the *ex vivo* heart perfusion experiments and Réka Somogyi for qPCR and ELISA measurements.

REFERENCES

1. Timmis A, Vardas P, Townsend N, Torbica A, Katus H, De Smedt D, et al. European Society of Cardiology: cardiovascular disease statistics 2021. Eur Heart J 2022: ehab892. https://doi.org/10.1093/eurheartj/ehab892.
2. Lang JA, Kim J. Remote ischaemic preconditioning – translating cardiovascular benefits to humans. J Physiol 2022; 600(13): 3053–67. https://doi.org/10.1113/JP282568.
3. Bell RM, Basalay M, Bøtker HE, Beikoghli Kalkhoran S, Carr RD, Cunningham J, et al. Remote ischaemic conditioning: defining critical criteria for success—report from the 11th Hatter Cardiovascular Workshop. Basic Res Cardiol 2022; 117(1): 39. https://doi.org/10.1007/s00395-022-00947-2.
4. Pedersen BK. The physiology of optimizing health with a focus on exercise as medicine. Annu Rev Physiol 2019; 81: 607–27. https://doi.org/10.1146/annurev-physiol-020518-114339.
5. Kern H, Carraro U. Home-based functional electrical stimulation for long-term denervated human muscle: history, basics, results and perspectives of the vienna rehabilitation strategy. Eur J Transl Myol 2014; 24(1): 3296. https://doi.org/10.4081/ejtm.2014.3296.

6. de Oliveira TMD, Felício DC, Filho JE, Durigan JLQ, Fonseca DS, José A, et al. Effects of whole-body electromyostimulation on function, muscle mass, strength, social participation, and falls-efficacy in older people: a randomized trial protocol. PLoS One 2021; 16(1): e0245809. https://doi.org/10.1371/journal.pone.0245809.
7. Palau P, Domínguez E, López L, Ramón JM, Heredia R, González J, et al. Inspiratory muscle training and functional electrical stimulation for treatment of heart failure with preserved ejection fraction: the TRAINING-HF trial. Revista espanola de cardiologia (English ed) 2019; 72(4): 288–97. https://doi.org/10.1016/j.rec.2018.01.010.
8. van Buuren F, Mellwig KP, Fründ A, Bogunovic N, Oldenburg O, Kottmann T, et al. Electrical myostimulation: improvement of quality of life, oxygen uptake and left ventricular function in chronic heart failure. Die Rehabil 2014; 53(5): 321–6. https://doi.org/10.1055/s-0033-1358734.
9. Szabó MR, Pipicz M, Csont T, Csonka C. Modulatory effect of myokines on reactive oxygen species in ischemia/reperfusion. Int J Mol Sci 2020; 21(24). https://doi.org/10.3390/ijms21249382.
10. Lee JH, Jun H-S. Role of myokines in regulating skeletal muscle mass and function. Front Physiol 2019; 10. https://doi.org/10.3389/fphys.2019.00042.
11. Pedersen BK, Febbraio MA. Muscles, exercise and obesity: skeletal muscle as a secretory organ. Nat Rev Endocrinol 2012; 8(8): 457–65. https://doi.org/10.1038/nrendo.2012.49.
12. Pedersen BK, Steensberg A, Fischer C, Keller C, Keller P, Plomgaard P, et al. Searching for the exercise factor: is IL-6 a candidate? J Muscle Res Cell Motil 2003; 24(2-3): 113–9. https://doi.org/10.1023/a:1026070911202.
13. Szabó MR, Gáspár R, Pipicz M, Zsindely N, Diószegi P, Sárközy M, et al. Hypercholesterolemia interferes with induction of miR-125b-1-3p in preconditioned hearts. Int J Mol Sci 2020; 21(11). https://doi.org/10.3390/ijms21113744.
14. Pipicz M, Varga ZV, Kupai K, Gáspár R, Kocsis GF, Csonka C, et al. Rapid ventricular pacing-induced postconditioning attenuates reperfusion injury: effects on peroxynitrite, RISK and SAFE pathways. Br J Pharmacol 2015; 172(14): 3472–83. https://doi.org/10.1111/bph.13154.
15. Csonka C, Kupai K, Kocsis GF, Novák G, Fekete V, Bencsik P, et al. Measurement of myocardial infarct size in preclinical studies. J Pharmacol Toxicol Methods 2010; 61(2): 163–70. https://doi.org/10.1016/j.vascn.2010.02.014.
16. McGregor G, Ennis S, Powell R, Hamborg T, Raymond NT, Owen W, et al. Feasibility and effects of intradialytic low-frequency electrical muscle stimulation and cycle training: a pilot randomized controlled trial. PLoS One 2018; 13(7): e0200354. https://doi.org/10.1371/journal.pone.0200354.
17. Sañudo B, Bartolomé D, Tejero S, Ponce-González JG, Loza JP, Figueroa A. Impact of active recovery and whole-body electromyostimulation on blood-flow and blood lactate removal in healthy people. Front Physiol 2020; 11: 310. https://doi.org/10.3389/fphys.2020.00310.
18. Smart NA, Dieberg G, Giallauria F. Functional electrical stimulation for chronic heart failure: a meta-analysis. Int J Cardiol 2013; 167(1): 80–6. https://doi.org/10.1016/j.ijcard.2011.12.019.
19. Banerjee P, Caulfield B, Crowe L, Clark AL. Prolonged electrical muscle stimulation exercise improves strength, peak VO2, and exercise capacity in patients with stable chronic heart failure. J Card Fail 2009; 15(4): 319–26. https://doi.org/10.1016/j.cardfail.2008.11.005.
20. Ploesteanu RL, Nechita AC, Turcu D, Manolescu BN, Stamate SC, Berteanu M. Effects of neuromuscular electrical stimulation in patients with heart failure - review. J Med Life 2018; 11(2): 107–18.
21. Birnbaum Y, Hale SL, Kloner RA. Ischemic preconditioning at a distance: reduction of myocardial infarct size by partial reduction of blood supply combined with rapid stimulation of the gastrocnemius muscle in the rabbit. Circulation 1997; 96(5): 1641–6. https://doi.org/10.1161/01.cir.96.5.1641.
22. Reinthaler M, Jung F, Empen K. Remote ischemic preconditioning of the heart: combining lower limb ischemia and electronic stimulation of the gastrocnemius muscle. Clin Hemorheol Microcirc 2018; 70(4): 381–9. https://doi.org/10.3233/ch-189303.

23. Tsou MT, Huang CH, Chiu JH. Electroacupuncture on PC6 (Neiguan) attenuates ischemia/reperfusion injury in rat hearts. The Am J Chin Med 2004; 32(6): 951–65. https://doi.org/10.1142/s0192415x04002557.
24. Dong JH, Liu YX, Zhao J, Ma HJ, Guo SM, He RR. High-frequency electrical stimulation of femoral nerve reduces infarct size following myocardial ischemia-reperfusion in rats. Sheng Li Xue Bao: [Acta Physiol Sinica] 2004; 56(5): 620–4.
25. Merlocco AC, Redington KL, Disenhouse T, Strantzas SC, Gladstone R, Wei C, et al. Transcutaneous electrical nerve stimulation as a novel method of remote preconditioning: in vitro validation in an animal model and first human observations. Basic Res Cardiol 2014; 109(3): 406. https://doi.org/10.1007/s00395-014-0406-0.
26. Redington KL, Disenhouse T, Strantzas SC, Gladstone R, Wei C, Tropak MB, et al. Remote cardioprotection by direct peripheral nerve stimulation and topical capsaicin is mediated by circulating humoral factors. Basic Res Cardiol 2012; 107(2): 241. https://doi.org/10.1007/s00395-011-0241-5.
27. Gao J, Fu W, Jin Z, Yu X. Acupuncture pretreatment protects heart from injury in rats with myocardial ischemia and reperfusion via inhibition of the beta(1)-adrenoceptor signaling pathway. Life Sci 2007; 80(16): 1484–9. https://doi.org/10.1016/j.lfs.2007.01.019.
28. Redington KL, Disenhouse T, Li J, Wei C, Dai X, Gladstone R, et al. Electroacupuncture reduces myocardial infarct size and improves post-ischemic recovery by invoking release of humoral, dialyzable, cardioprotective factors. The J Physiol Sci: JPS 2013; 63(3): 219–23. https://doi.org/10.1007/s12576-013-0259-6.
29. Feng L, Li B, Tian Z. Exerkines: opening the way to protecting ischemic heart. Curr Opin Physiol 2023; 31: 100615. https://doi.org/10.1016/j.cophys.2022.100615.
30. Bustamante M, Fernández-Verdejo R, Jaimovich E, Buvinic S. Electrical stimulation induces IL-6 in skeletal muscle through extracellular ATP by activating Ca(2+) signals and an IL-6 autocrine loop. Am J Physiol Endocrinol Metab 2014; 306(8): E869–82. https://doi.org/10.1152/ajpendo.00450.2013.
31. Wahl P, Hein M, Achtzehn S, Bloch W, Mester J. Acute effects of superimposed electromyostimulation during cycling on myokines and markers of muscle damage. J Musculoskelet Neuronal Interact 2015; 15(1): 53–9. https://doi.org/10.4081/ejtm.2018.7905.
32. Truong AD, Kho ME, Brower RG, Feldman DR, Colantuoni E, Needham DM. Effects of neuromuscular electrical stimulation on cytokines in peripheral blood for healthy participants: a prospective, single-blinded Study. Clin Physiol Funct Imaging 2017; 37(3): 255–62. https://doi.org/10.1111/cpf.12290.
33. McGinnis GR, Ballmann C, Peters B, Nanayakkara G, Roberts M, Amin R, et al. Interleukin-6 mediates exercise preconditioning against myocardial ischemia reperfusion injury. Am J Physiology-Heart Circulatory Physiol 2015; 308(11): H1423–33. https://doi.org/10.1152/ajpheart.00850.2014.
34. Quinn LS, Anderson BG, Strait-Bodey L, Stroud AM, Argilés JM. Oversecretion of interleukin-15 from skeletal muscle reduces adiposity. Am J Physiology-Endocrinology Metab 2009; 296(1): E191–202. https://doi.org/10.1152/ajpendo.90506.2008.
35. Tamura Y, Watanabe K, Kantani T, Hayashi J, Ishida N, Kaneki M. Upregulation of circulating IL-15 by treadmill running in healthy individuals: is IL-15 an endocrine mediator of the beneficial effects of endurance exercise? Endocr J 2011; 58(3): 211–5. https://doi.org/10.1507/endocrj.k10e-400.
36. Bazgir B, Salesi M, Koushki M, Amirghofran Z. Effects of eccentric and concentric emphasized resistance exercise on IL-15 serum levels and its relation to inflammatory markers in athletes and non-athletes. Asian J Sports Med 2015; 6(3): e27980-e. https://doi.org/10.5812/asjsm.27980.
37. Norheim F, Raastad T, Thiede B, Rustan AC, Drevon CA, Haugen F. Proteomic identification of secreted proteins from human skeletal muscle cells and expression in response to strength training. Am J Physiol Endocrinol Metab 2011; 301(5): E1013–21. https://doi.org/10.1152/ajpendo.00326.2011.
38. Kon M, Ebi Y, Nakagaki K. Effects of acute sprint interval exercise on follistatin-like 1 and apelin secretions. Arch Physiol Biochem 2019: 1–5. https://doi.org/10.1080/13813455.2019.1628067.

39. Görgens SW, Raschke S, Holven KB, Jensen J, Eckardt K, Eckel J. Regulation of follistatin-like protein 1 expression and secretion in primary human skeletal muscle cells. Arch Physiol Biochem 2013; 119(2): 75–80. https://doi.org/10.3109/13813455.2013.768270.
40. Genovese JA, Spadaccio C, Rivello HG, Toyoda Y, Patel AN. Electrostimulated bone marrow human mesenchymal stem cells produce follistatin. Cytotherapy 2009; 11(4): 448–56. https://doi.org/10.1080/14653240902960445.
41. Ogura Y, Ouchi N, Ohashi K, Shibata R, Kataoka Y, Kambara T, et al. Therapeutic impact of follistatin-like 1 on myocardial ischemic injury in preclinical models. Circulation 2012; 126(14): 1728–38. https://doi.org/10.1161/CIRCULATIONAHA.112.115089.
42. Ouchi N, Oshima Y, Ohashi K, Higuchi A, Ikegami C, Izumiya Y, et al. Follistatin-like 1, a secreted muscle protein, promotes endothelial cell function and revascularization in ischemic tissue through a nitric-oxide synthase-dependent mechanism. J Biol Chem 2008; 283(47): 32802–11. https://doi.org/10.1074/jbc.M803440200.
43. Yang W, Duan Q, Zhu X, Tao K, Dong A. Follistatin-like 1 attenuates ischemia/reperfusion injury in cardiomyocytes via regulation of autophagy. Biomed Res Int 2019; 2019: 9537382. https://doi.org/10.1155/2019/9537382.
44. Xi Y, Hao M, Liang Q, Li Y, Gong DW, Tian Z. Dynamic resistance exercise increases skeletal muscle-derived FSTL1 inducing cardiac angiogenesis via DIP2A-Smad2/3 in rats following myocardial infarction. J Sport Health Sci 2020. https://doi.org/10.1016/j.jshs.2020.11.010.
45. Xi Y, Hao M, Tian Z. Resistance exercise increases the regulation of skeletal muscle FSTL1 consequently improving cardiac angiogenesis in rats with myocardial infarctions. J Sci Sport Exercise 2019; 1(1): 78–87. https://doi.org/10.1007/s42978-019-0009-4.
46. Otaka N, Shibata R, Ohashi K, Uemura Y, Kambara T, Enomoto T, et al. Myonectin is an exercise-induced myokine that protects the heart from ischemia-reperfusion injury. Circ Res 2018; 123(12): 1326–38. https://doi.org/10.1161/CIRCRESAHA.118.313777.
47. Wang Z, Chen K, Han Y, Zhu H, Zhou X, Tan T, et al. Irisin protects heart against ischemia-reperfusion injury through a SOD2-dependent mitochondria mechanism. Sci Transl Med 2018; 72(6): 259–69. https://doi.org/10.1126/scitranslmed.aao629810.1097/fjc.0000000000000608.
48. Sanchis-Gomar F, Lopez-Lopez S, Romero-Morales C, Maffulli N, Lippi G, Pareja-Galeano H. Neuromuscular electrical stimulation: a new therapeutic option for chronic diseases based on contraction-induced myokine secretion. Front Physiol 2019; 10: 1463. https://doi.org/10.3389/fphys.2019.01463.
49. Kimura T, Kaneko F, Iwamoto E, Saitoh S, Yamada T. Neuromuscular electrical stimulation increases serum brain-derived neurotrophic factor in humans. Exp Brain Res 2019; 237(1): 47–56. https://doi.org/10.1007/s00221-018-5396-y.
50. Miyamoto T, Iwakura T, Matsuoka N, Iwamoto M, Takenaka M, Akamatsu Y, et al. Impact of prolonged neuromuscular electrical stimulation on metabolic profile and cognition-related blood parameters in type 2 diabetes: a randomized controlled cross-over trial. Diabetes Res Clin Pract 2018; 142: 37–45. https://doi.org/10.1016/j.diabres.2018.05.032.
51. Zampieri S, Pietrangelo L, Loefler S, Fruhmann H, Vogelauer M, Burggraf S, et al. Lifelong physical exercise delays age-associated skeletal muscle decline. J Gerontol A Biol Sci Med Sci 2015; 70(2): 163–73. https://doi.org/10.1093/gerona/glu006.
52. Amano Y, Nonaka Y, Takeda R, Kano Y, Hoshino D. Effects of electrical stimulation-induced resistance exercise training on white and brown adipose tissues and plasma meteorin-like concentration in rats. Physiol Rep 2020; 8(16): e14540. https://doi.org/10.14814/phy2.14540.
53. Sajer S, Guardiero GS, Scicchitano BM. Myokines in home-based functional electrical stimulation-induced recovery of skeletal muscle in elderly and permanent denervation. Eur J Transl Myol 2018; 28(4): 7905. https://doi.org/10.4081/ejtm.2018.7905.

54. Kleinbongard P, Skyschally A, Heusch G. Cardioprotection by remote ischemic conditioning and its signal transduction. Pflugers Archiv: Eur J Physiol 2017; 469(2): 159–81. https://doi.org/10.1007/s00424-016-1922-6.
55. Borges JP, da Silva Verdoorn K. Cardiac ischemia/reperfusion injury: the beneficial effects of exercise. Adv Exp Med Biol 2017; 999: 155–79. https://doi.org/10.1007/978-981-10-4307-9_10.
56. Tsai HJ, Huang SS, Tsou MT, Wang HT, Chiu JH. Role of opioid receptors signaling in remote electrostimulation–induced protection against ischemia/reperfusion injury in rat hearts. PLoS One 2015; 10(10): e0138108. https://doi.org/10.1371/journal.pone.0138108.